JSCSEN 79(1)1–113(2014)

ISSN 1820-7421(Online)

Journal of the Serbian Chemical Society

Electronic Version

VOLUME 79

No 1

BELGRADE 2014

Available on line at

www.shd.org.rs/JSCS/

The full search of JSCS is available through

DOAJ DIRECTORY OF OPEN ACCESS JOURNALS

www.doaj.org

Journal of the Serbian Chemical Society
JSCS-info@shd.org.rs • www.shd.org.rs/JSCS

J. Serb. Chem. Soc. Vol. 79, No. 1 (2014)

CONTENTS

Published by the Serbian Chemical Society
Karnegijeva 4/III, 11000 Belgrade, Serbia
Printed by the Faculty of Technology and Metallurgy
Karnegijeva 4, P.O. Box 35-03, 11120 Belgrade, Serbia

Journal of the Serbian Chemical Society
JSCS-info@shd.org.rs • www.shd.org.rs/JSCS
J. Serb. Chem. Soc. *79* (1) 1–10 (2014)
JSCS–4560
UDC 577.15+66.097.8+547.495.2:615.277
Original scientific paper

Synthesis, enzyme inhibition and anticancer investigations of unsymmetrical 1,3-disubstituted ureas

SANA MUSTAFA[1,2]*, SHAHNAZ PERVEEN[3] and AJMAL KHAN[4]

[1]Department of Chemistry, University of Karachi, Karachi-75270, Pakistan, [2]Department of Chemistry, Federal Urdu University for Arts, Science and Technology, Gulshan-e-Iqbal Campus, Karachi-75300, Pakistan, [3]PCSIR, Laboratories Complex, Karachi, Shahrah-e-Dr. Salimuzzaman Siddiqui, Karachi-75280, Pakistan and [4]HEJ Research Institute of Chemistry, International Center for Chemical and Biological Sciences, University of Karachi, Karachi-75270, Pakistan

(Received 12 December 2012, revised 11 July 2013)

Abstract: In this study, seventeen urea derivatives, including the five new derivatives *N*-mesityl-*N*′-(3-methylphenyl)urea (**2**), *N*-(3-methoxyphenyl)-*N*′--(3-methylphenyl)urea (**4**), *N*-mesityl-*N*′-(4-methylphenyl)urea (**6**), *N*-(1,3-benzothiazol-2-yl)-*N*′-(3-methylphenyl)urea (**9**) and *N*-(2-methylphenyl)-2-oxo-1--pyrrolidinecarboxamide (**15**), were synthesized by reacting *ortho*-, *meta*- and *para*-tolyl isocyanate with primary and secondary amines using a previously reported method. All the series **1**–**17** were subjected to urease, *β*-glucuronidase and snake venom phosphodiesterase enzyme inhibition assays. The ranges of inhibition of urease, *β*-glucuronidase and phosphodiesterase enzymes were 0.30–45.3, 4.9–44.9 and 1.2–46.4 %, respectively. Moreover, an effect of these compounds on a prostate cancer cell line was observed. The new compound *N*-(1,3-benzothiazol-2-yl)-*N*′-(3-methylphenyl)urea (**9**) showed *in vitro* anticancer activity with an IC_{50} value of 78.28±1.2 μM. All the compounds were characterized by state of art spectroscopic techniques.

Keywords: amine; *β*-glucuronidase; disubstituted ureas; isocyanate; phosphodiesterase; urease.

INTRODUCTION

Nitrogen-containing heterocyclic compounds play a significant role not only in the life science industry, but also in many other industrial fields related to special and fine chemistry. Among them, ureas represent an extensively used tremendous class of compounds with multi-focal applications in several fields.[1] A number of these compounds are reported to exhibit a wide spectrum of biological and pharmacological activities. In the last decade, much attention has been paid to the synthesis and application of such substituted urea derivatives.[2,3]

* Corresponding author. E-mail: sanachemana@yahoo.com
doi: 10.2298/JSC121212076M

Ureas have been synthesized by a number of methodologies basically employing substances such as phosgene. However, due to the harsh reaction conditions and the hazardous nature of phosgene, it has been promisingly substituted by safer compounds. Thus numerous substitutes of phosgene are well documented in the literature.[4] Additionally, their syntheses have been achieved by simpler and much more economical chemical substances such as carbon dioxide and carbon monoxide by the catalytic carbonation of amines.[5,6] Other methods involved the use of carbonates such as organic carbonate esters and ethylene carbonate for the mass scale production of *N*,*N*′-disubstituted ureas.[7,8]

Disubstituted ureas possess wide therapeutic activities, such as potent inhibitors of interleukin-8, anthelmintics, antimalarial, anti-HIV, diuretic, analgesic, antibacterial, antifungal, antimicrobial, algaecidal or antiperiphytic agents.[9–12] *N*,*N*′-Disubstituted ureas, amides and carbamates are reported as new powerful and stable inhibitors of soluble epoxide hydrolase, both *in vivo* and *in vitro*.[13] They were determined to be useful for the treatment of hypertension, Raynaud syndrome, respiratory distress syndrome, inflammation, diabetic complications, arthritis and renal diseases.[14]

A urease is an enzyme that decomposes urea to ammonia and carbonic acid and provides nitrogen to an organism.[15,16] On the other hand, bacterial ureases cause different pharmacological problems, ranging from the development of infectious stones, pathogenesis of encephalopathy, pyelonephritis, urinary catheter encrustation and hepatic coma to peptic ulceration.[15–20]

β-Glucuronidase is an exoglycosidase enzyme and its activity reflects liver enzyme loss during cell turnover in humans.[21,22] In the cell, it is present in lysosomes, although high levels are present in necrotic areas of large tumours. Sly syndrome is an inherited disease characterized by a deficiency of glucuronidase.[23] It was reported that in certain diseases, *e.g.*, cancer, hepatic diseases, inflammatory joint and AIDS, the activity of *β*-glucuronidase is increased.[21]

A phosphdiesterase (PDE) is an enzyme that participates in cell functions to maintain intracellular levels of cyclic adenosine and cyclic guanosine monophosphate by hydrolyzing cyclic nucleotides.[24] Nucleotide pyrophosphatase/phosphodiesterase (NPP) is a class of enzyme comprised of seven isoforms among them three are well known ectoenzymes as NPP-1 (PC-1), NPP-2 (autotaxin) and NPP-3 (B10; gp130 (RB13-6)) in mammalian. They are widely distributed in mammalian intestinal mucosa, liver cells and serum, snake venom and in various plants.[25] The calcification of bones and tissues is regulated by the NPP-1 enzyme. In humans, chondrocalcinosis and idiopathic infantile arterial calcification result from an over or under expression of NPP-1, respectively.[26,27] The potent phosphodiesterase (PDE) inhibitor drug sildenafil therapeutically obtained great world-wide success for the treatment of erectile dysfunction. Selective PDE inhibitors are highly beneficial in the treatment of various diseases, *e.g.*, PDE-II

inhibitors in sepsis; PDE-IV inhibitors in allergic rhinitis, asthma, psoriasis, multiple sclerosis, chronic obstructive pulmonary disease (COPD), Alzheimer disease, schizophrenia and depression and PDE-V inhibitors in cardiovascular disease, female sexual dysfunction and pulmonary hypertension.[24]

Therefore approaches based on inhibition of these enzymes always remain a need of world for the treatment of diseases arising from disturbed level of these enzymes.

The huge volume of research on the synthesis and anticancer activities of urea derivatives was previously reviewed. Many aromatic urea and thiourea derivatives, such as benzoylureas, *N*-(2-chloroethyl)-*N′*-phenylureas, primaquine derivatives, 3-(haloacylamino)benzoylurea and *N*-(benzothiazol-2-yl)-*N*-morpholinourea were synthesized and considered extensively for anticancer activity against murine leukaemia, colon carcinoma, haematoma, lymphoma, melanoma, breast cancer and prostate cancer cell lines of patients.[28–31]

In view of the large volume of literature, it is clear that the discovery of novel biologically active compounds for the treatment of malignancy is very important. A challenge still exists to design even better inhibitors with improved therapeutic effects. In continuation of ongoing studies on the discovery of new enzyme inhibitors and anticancer agents, the synthesis of 1,3-disubstituted ureas by a simple one pot reaction of tolyl isocyanates with selective amines is described herein. The resulting compounds were evaluated for their inhibitory activities on urease, β-glucuronidase and snake venom phosphodiesterase enzymes and their cytotoxicity against prostate cancer cell lines.

EXPERIMENTAL

Melting points were taken on Gallenkamp melting point apparatus. Thin layer chromatograpy was performed on pre-coated silica gel plates (Kieselgel 60 F_{254}, Merk, Germany) and the spots were visualized under UV radiation (Dual range, Merk Millipore, UK) at 254 and 365 nm. The IR spectra were taken on a Thermo Nicolet Avatar 370 DTGS FT-IR spectrometer. The EI-MS measurements were performed on a MAT-312 and a JEOLJMS-HX 110 instrument. The ^{1}H-NMR spectra were recorded on a Bruker Avance 400 MHz instrument, δ in ppm related to $SiMe_4$ (0 ppm) as internal standard. The ^{13}C-NMR spectra were taken on a Bruker Avance 125 MHz instrument. Elemental analyses were realized on a Perkin Elmer 2400 CHN elemental analyzer. All used solvents were of reagent grade. Yields, physical, analytical and spectral data for the prepared ureas are given in the Supplementary material to this paper.

General procedure for the synthesis of the 1,3-disubstituted ureas ***1*****–*****17***

The respective amine (3.18 mmol) was taken in 5–10 mL of 1,4-dioxane and then approximately 1.60 mmol of *ortho*-, *meta*- or *para*-tolyl isocyanate was added dropwise. The reactions are completed in 30–60 min. After completion of the reaction, the mixture was cooled with ice to afford white crystals of the title compound.[32]

Urease inhibition assay

Reaction mixtures containing 1 unit of urease enzyme isolated from jack-bean and 55 μL of buffers containing 100 mM urea were incubated with 5 μL of 1 mM test compound for 15 min in 96-well plates at 30 °C. The ammonia production, which in turn quantifies the urease activity, was measured by the indophenol method. For this purpose, 70 μL of alkali (0.5 % w/v NaOH and 0.1 % active chloride NaOCl) and 45 μL of phenol reagent (1 % w/v phenol and 0.005 % w/v sodium nitroprusside) were poured into each well. After 50 min, the increase in absorbance at a wavelength of 630 nm was measured by a microplate reader (Molecular Device, USA). All reactions were run in triplicate in a total volume of 200 μL and the change in absorbance per min were processed using Soft-Max Pro software (Molecular Device, USA).[33]

β-*Glucuronidase assay*

The *β*-glucuronidase activity was determined by a spectrophotometric method that involved the measurement of the absorbance of *p*-nitrophenol formed from the substrate at 405 nm. The reaction mixture consisting of 185 μL of 0.1 M acetate buffer (pH 7.00), 10 μL of enzyme solution and 5 μL of test compound (0.4 mM) solution was incubated for 30 min at 37 °C. The plates were read on a multiplate reader SpectraMax plus 384 (Molecular Devices, U.S.A.) after the addition of 50 μL of 0.4 mM *p*-nitrophenyl-*β*-D-glucuronide at 405 nm. All assays were performed in triplicate.[34]

Phosphodiesterase-I inhibition assay

Phosphodiesterase I inhibition assay was performed using snake venom according to a previously reported method with minute variations. Briefly, 33 mM Tris–HC1 buffer of pH 8.8 (97 μL), 30 mM Mg acetate with an enzyme concentration of 0.000742 U $well^{-1}$ and 0.33 mM bis-(*p*-nitrophenyl) phosphate (Sigma N-3002, 60 μL) as substrate were taken. EDTA with an IC_{50}±*SD* of 274±0.007 μM was used as the positive control.

After a pre-incubation period of 30 min, the enzyme with the test samples was observed spectrophotometrically for enzyme activity on a microtitre plate reader at 37 °C by following the rate of change in OD min^{-1} at 410 nm of the *p*-nitrophenol released from *p*-nitrophenyl phosphate. All assays were processed in triplicate.[35]

Anticancer assay

Anticancer activity of compounds was evaluated in 96-well flat-bottomed micro plates by using the standard reduction of MTT (3-(4,5-dimethylthiazol-2-yl)-2,5-diphenyltetrazolium bromide) colorimetric assay. For this purpose, PC3 cells (prostate cancer) were cultured in Dulbecco-modified Eagle medium, containing 5 % of foetal bovine serum (FBS), 100 μg mL^{-1} of streptomycin and 100 IU mL^{-1} of penicillin in 25 cm^3 flasks, in an incubator at 37 °C under a 5 % carbon dioxide atmosphere. The exponentially growing cells were counted with a haemocytometer and diluted to a concentration of 1×10^5 cells mL^{-1}. The diluted culture was then introduced into 96-well plates (100 μL $well^{-1}$) and incubated overnight. After incubation, medium was separated and 200 μL of fresh medium was added with various concentrations of the compounds in the range 1–100 μM. After 72 h, 50 μL MTT (2 mg mL^{-1}) was added to each well and incubated further for 4 h. Subsequently, 100 μL of DMSO was added to each well. The MTT was reduced to formazan within viable cells and its absorbance was measured at 570 nm using a microplate ELISA reader (Spectra Max plus, Molecular Devices, CA, USA).[36]

RESULTS AND DISCUSSION

Chemistry

In a typical reaction *ortho*-, *meta*- or *para*-tolyl isocyanate was treated with a primary or secondary amine in 1,4-dioxane at room temperature (Scheme 1). The product formation and progress of reaction was observed by TLC. The difference in retardation factor (R_f) values of the reaction mixture and the starting pure reactants indicated completion of the reaction. After completion of reaction, the mixture was cooled by the addition of a few cubes of crushed ice. As a result, the solid product precipitated. The obtained solid was filtered and washed several times with cold distilled water to remove excess amine and to obtain the pure product[34] (Table I).

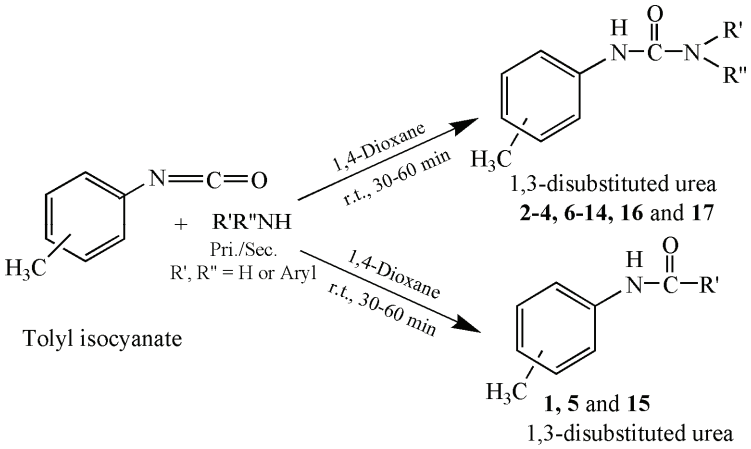

Scheme 1. Synthetic route for 1,3-disubstituted ureas.

TABLE I. Synthesis of 1,3-disubstituted urea derivatives (**1**–**17**)

Cmpd.	–R	–R′	–R″	Cmpd.	–R	–R′	–R″
1	*m*-CH_3	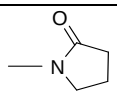	–	**10**	*m*-CH_3	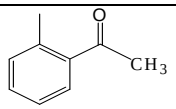	H
2	*m*-CH_3	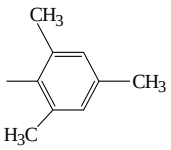	H	**11**	*p*-CH_3	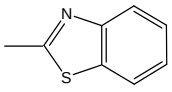	H
3	*m*-CH_3	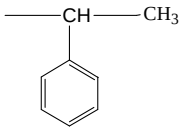	H	**12**	*o*-CH_3	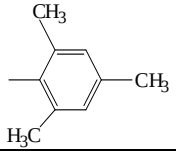	H

TABLE I. Continued

Cmpd.	–R	–R′	–R″	Cmpd.	–R	–R′	–R″
4	*m*-CH_3	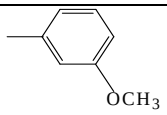	H	**13**	*o*-CH_3	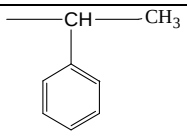	H
5	*p*-CH_3	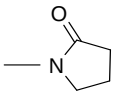	–	**14**	*o*-CH_3	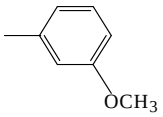	H
6	*p*-CH_3	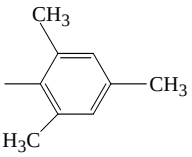	H	**15**	*o*-CH_3	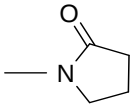	–
7	*p*-CH_3	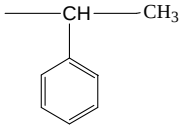	H	**16**	*o*-CH_3	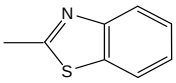	H
8	*p*-CH_3	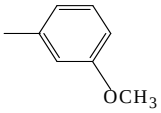	H	**17**	*p*-CH_3	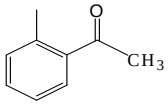	H
9	*m*-CH_3	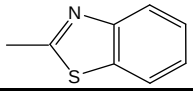	H				

The structures of the compounds were confirmed by mass, NMR and IR spectroscopy, and CHN elemental analysis. Their melting points were also recorded. The compounds were evaluated for their inhibition of different enzymes and anticancer activities.

Biology

Enzyme inhibition screening. In vitro screening is one of the initial phases in drug discovery and many drug molecules are enzyme inhibitors; hence, their discovery and improvement is an active area of research in biochemistry and pharmacology. Thus in this study, compounds **1**–**17** were synthesized and randomly checked in three enzyme-inhibition assays (urease, *β*-glucoranidase and phosphodiestrase-I). All compounds showed various range of % inhibition against these enzymes (Table II).

In the series, compounds **1**–**4**, **9** and **10** are *m*-tolyl urea derivatives having various R′ groups. It was found that compound **4** with an *m*-methoxy group in the phenyl ring of R′ exhibited 53.2 % urease inhibition and was the most potent of these compounds, which exhibited an activity of less than 50 %. For compounds

5–**8**, **11** and **17**, a similar result was observed, *i.e.*, that the *para* tolyl compound **8** having an *m*-methoxy group in phenyl ring of R′ was the most potent with a 59.1 % urease inhibition. Compound **6** with a 2,4,6-trimethylphenyl group was also active (45.3 % inhibition). Of the *o*-tolyl derivatives **12**–**16**, again compound **14** with an *m*-methoxy in the phenyl group of R′ exhibited the greatest inhibition (47.5 %). The other compounds had an activity in the range of 0.3 to 45.3 % inhibition. Comparing compounds **4**, **8** and **14** with same R′ group, compound **8**, which is a *p*-tolyl urea, exhibited the highest urease inhibition.

TABLE II. Enzyme inhibitions (±*SD*, %) and anticancer activities (IC_{50}±*SD*, μM) of synthesized urea derivatives (**1**–**17**); PC3 = prostate cancer cell lines; – = no inhibition; *SD* = = standard deviation; IC_{50} = concentration at 50 % inhibition

Cmpd.	Urease	*β*-Glucuronidase	Phosphodiesterase	Anticancer (PC3)
1	37.70±0.09	26.90±0.02	46.40±0.02	>100
2	21.70±0.04	4.90±0.01	–	>100
3	0.30±0.05	–	32.00±0.01	>100
4	53.20±0.03	40.30±0.01	4.80±0.01	>100
5	19.90±0.04	2.30±0.02	–	>100
6	45.30±0.02	20.40±0.01	–	>100
7	32.50±0.01	–	–	>100
8	59.10±0.01	37.80±0.01	–	>100
9	40.70±0.01	16.50±0.01	–	78.3±1.2
10	6.90±0.04	28.70±0.02	37.80±0.01	>100
11	12.20±0.02	20.60±0.01	–	>100
12	4.00±0.03	8.50±0.01	–	>100
13	30.20±0.02	6.00±0.03	–	>100
14	47.50±0.02	44.90±0.01	2.10±0.01	>100
15	23.70±0.01	19.60±0.01	1.20±0.01	>100
16	12.90±0.02	7.20±0.02	6.50±0.01	>100
17	–	24.50±0.02	9.800±0.003	>100
Standard	Thiourea 98.20±0.01	D-Sacchuric acid, 1,4-lactone, 97.1±1.2	EDTA 90.10±0.01	Doxorubicin 0.91±0.12

The high activity of the *m*-methoxyphenyl moiety-containing compounds may arise because of the mutual effect of the electronegative oxygen of the methoxy group and the nitrogens and oxygen of the carbamide residue, which may increase the ligand–chelator ability of the compounds to form octahedral complexes with the nickel ions of urease enzyme. Moreover, the presence of bulky groups around the active nitrogen in other compounds decreased the activity of enzyme and the *m*-methoxyphenyl was the least bulky group in this series, which makes it easier for the urease to enter the active substrate binding site. In contrast, certain urea derivatives with *m*-methyl- and *m*-methoxyphenyl groups were previously reported in the literature as potent inhibitor of urease.[37,38]

However, in the inhibition studies of *β*-glucuronidase, compounds **1**, **2**, **4**–**6** and **8**–**17** showed % inhibition in the range 4.9 to 44.9 %, *i.e.*, no significant activity, while the other compounds gave negative results towards *β*-glucuronidase in the enzyme inhibition assay.

In the phosphodiestrase enzyme inhibition studies, the range of % inhibition was 1.2 to 46.4 %, *i.e.*, none of the prepared urea derivatives showed significant activity, except compound **1**, *N*-(3-methylphenyl)-2-oxo-1-pyrrolidinecarboxamide, that exhibited low activity with a percentage inhibition value of 46.4 %, while its *ortho* and *meta* derivatives were nearly inactive towards phosphodiesterase-I (Table II).

Anticancer screening against PC3 cell lines. To explore further their biological activity against prostate cancer cell lines (PC3), all the compounds were tested. Unfortunately, only one urea derivative, *N*-(1,3-benzothiazol-2-yl)-*N*′-(3--methylphenyl)urea (**9**) showed better cytotoxicity activity with an IC_{50} value of 78.3, as compared to our standard doxorubicin having an IC_{50}±*SD* value of 0.91±0.12 μM (Table II).

CONCLUSIONS

In this study, attention was focused on the synthesis and biological activities of 1,3-disubstitued ureas. Thus, seventeen urea derivatives, including five new derivatives **2**, **4**, **6**, **9** and **15**, were synthesized. The % inhibition for urease, *β*-glucuronidase and phosphodiesterase enzymes were in the range 0.3–45.3, 4.9––44.9 and 1.2–46.4 %, respectively. In the *in vitro* anticancer study, the new compound *N*-(1,3-benzothiazol-2-yl)-*N*′-(3-methylphenyl)urea showed significant anticancer activity with an IC_{50} value of 78.28±1.2 μM against PC3 cell lines.

SUPPLEMENTARY MATERIAL

Yields, physical, analytical and spectral data for the prepared ureas are available electronically from http://www.shd.org.rs/JSCS/, or from the corresponding author on request.

Acknowledgement. This work was supported by the Higher Education Commission (HEC), Pakistan, under the Indigenous 5000 PhD Fellowship Program.

И З В О Д

СИНТЕЗА, ЕНЗИМСКА ИНХИБИЦИЈА И ИСПИТИВАЊЕ АНТИТУМОРСКЕ АКТИВНОСТИ НЕСИМЕТРИЧНИХ 1,3-ДИСУПСТИТУИСАНИХ УРЕА

SANA MUSTAFA[1,2], SHAHNAZ PERVEEN[3] и AJMAL KHAN[4]

[1]Department of Chemistry, University of Karachi, Karachi-75270, Pakistan, [2]Department of Chemistry, Federal Urdu University for Arts, Science and Technology, Gulshan-e-Iqbal Campus, Karachi-75300, Pakistan, [3]PCSIR, Laboratories Complex, Karachi, Shahrah-e-Dr. Salimuzzaman Siddiqui, Karachi-75280, Pakistan и [4]HEJ Research Institute of Chemistry, International Center for Chemical and Biological Sciences, University of Karachi, Karachi-75270, Pakistan

Током истраживања синтетисано је седамнаест деривата, укључујући и нова једињења: *N*-мезитил-*N*′-(3-метилфенил)уреа (**2**), *N*-(3-метилфенил)-*N*′-(3-метоксифенил)-

уреа (**4**), *N*-мезитил-*N*′-(4-метилфенил)уреа (**6**), *N*-(1,3-бензотиазол-2-ил)-*N*′-(3-метил -фенил)уреа (**9**) и *N*-(2-метилфенил)-2-оксо-1-пиролидинкарбоксамид (**15**) реакцијом *орто*-, *мета*- и *пара*-толил-изоцијаната са примарним и секундарним аминима. Испитана је инхибиторна активност добијених деривати према уреази, *β*-глукуронидази и фосфодиестерази змијског отрова. Утврђено је да је опсег инхибиције према уреази, *β*-глукуронидази и фосфодиестерази змијског отрова. 0,3–45,3, 4,9–44,9 и 1,2–46,4 %, редом. Осим тога, испатан је и ефекат синтетисаних једињења према ћелијској линији рака простате. Нов дериват *N*-(1,3-бензотиазол-2-ил)-*N*′-(3-метилфенил)уреа (***9***) показује *in vitro* активност IC_{50} од 78,3±1,2 μM. Сва синтетисана једињења окаратактерисана су стандардним спектроскопским техникама.

(Примљено 12. децембра 2012, ревидирано 11. јула 2013)

REFERENCES

1. I. L. Finar, *Organic Chemistry*, Vol. 1, 6th ed., Pearson Education Asia Ltd., Hong Kong, 2003, p. 460
2. P. Y. S. Lam, P. K. Jadhav, C. J. Eyermann, C. N. Hodge, Y. Ru, L. T. Bacheler, J. L. Meek, M. J. Otto, M. M. Rayner, Y. N. Wong, C. H. Chang, P. C. Weber, D. A. Jackson, T. R. Sharpe, S. Erickson-Viitanen, *Science* **263** (1994) 380
3. J. L. Castro, R. G. Ball, H. B. Broughton, M. G. N. Russell, D. Rathbone, A. P. Watt, R. Baker, K. L. Chapman, A. E. Fletcher, S. Patel, A. J. Smith, G. R. Marshall, W. Ryecroft, V. G. Matassa, *J. Med. Chem.* **39** (1996) 842
4. F. Bigi, R. Maggi, G. Sartori, *Green Chem.* **2** (2000) 140
5. N. Sonoda, T. Yasuhara, K. Konodo, T. Ikeda, S. Tsutsumi, *J. Am. Chem. Soc.* **93** (1971) 691
6. J. D. Diaz, K. A. Darko, L. McElwee-White, *Eur. J. Org. Chem.* **27** (2007) 4453
7. S. Fujita, B. M. Bhanage, H. Kanamaru, M. Arai, *J. Mol. Catal. A: Chem.* **230** (2005) 43
8. S. Franceso, R. Bruno, *Tetrahedron Lett.* **51** (2010) 6301
9. B. Olga, B. Chiara, F. Bondavalli, S. Schenone, A. Ranise, N. Arduino, M. B. Bertolotto, F. Montecucco, L. Ottonello, F. Dallegri, M. Tognolini, V. Ballabeni, S. Bertoni, E. Barocelli, *J. Med. Chem.* **50** (2007) 3618
10. J. N. Dominguez, C. Leon, J. Rodrigues, N. G. Dominguez, J. Gut, P. J. Rosenthal, *J. Med. Chem.* **48** (2005) 3654
11. C. Sahlberg, R. Norren, P. Engelhardt, M. Hogberg, J. Kangasmetsa, L. Vrang, H. Zang, *Bioorg. Med. Chem. Lett.* **8** (1998) 1511
12. S. Igarashi, M. Futagawa, N. Tanaka, Y. Kawamura, K. Morimoto, W. O. Patent No. 039289 (1998)
13. I. H. Kim, C. Morisseau, T. Watanabe, B. D. Hammock, *J. Med. Chem.* **47** (2004) 2110
14. B. D. Hammock, P. D. Jones, C. Morisseau, H. Huang, H. Tsai, R. J. Gless, W. O. Patent No. 106525 (2007)
15. H. L. Mobley, M. D. Island, R. P. Hausinger, *Microbiol. Rev.* **59** (1995) 451
16. H. L. Mobley, R. P. Hausinger, *Microbiol. Rev.* **53** (1989) 85
17. S. Perveen, K. M. Khan, M. A. Lodhi, M. I. Choudhary, Atta-ur-Rahman, W. Voelter, *Lett. Drug Des. Discov.* **5** (2008) 401
18. J. C. Polacco, M. A. Holland, *Int. Rev. Cytol.* **145** (1993) 65
19. S. Perveen, UK Patent Publication No. GB 2443892 A (2008)
20. J. M. Bremner, *Nutr. Cycl. Agroecosys.* **42** (1995) 321
21. B. Sperker, J. T. Backman, H. K. Kroemer, *Clin. Pharmacokinet.* **33** (1997) 18
22. W. L. Johanna, S. S. Li, J. D. Potter, I. B. King, *J. Nutr.* **132** (2002) 1341

23. M. Graaf, E. Boven, H. W. Scheeren, H. J. Haisma, H. M. Pinedo, *Curr. Pharm. Desig*. **8** (2002) 1391
24. V. Boswell-Smith, D. Spina, C. P. Page, *Br J. Pharmacol*. **147** (2006) S252
25. J. W. Goding, R. Terkeltaub, M. Maurice, P. Deterre, A. Sali, S. A. Belli, *Immunol. Rev*. **161** (1998) 11
26. K. Johnson, S. Hashimoto, M. Lotz, K. Pritzker, J. Goding, R. Terkeltaub, *Arthr. Rheum*. **44** (2001) 1071
27. F. Rutsch, S. Vaingankar, K. Johnson, I. Goldfine, B. Maddux, P. Schauerte, H. Kalhoff, K. Sano, W. A. Boisvert, A. Superti-Furga, R. Terkeltaub, *Am. J. Pathol.* **158** (2001) 543
28. H. Q. Li, P. C. Lv, T. Yan, H. L. Zhu, *Anticancer Agents Med. Chem.* **9** (2009) 471
29. G. Dzimbeg, B. Zorc, M. Kralj, K. Ester, K. Pavelic, G. Andrei, R. Snoeck, J. Balzarini, E. D. Clercq, M. Mintas, *Eur. J. Med. Chem.* **43** (2008) 1180
30. D. Q. Song, Y. Wang, L. Z. Wu, P. Yang, Y. M. Wang, L. M. Gao, Y. Li, J. R. Qu, Y. H. Wang, Y. H. Li, N. N. Du, Y. X. Han, Z. P. Zhang, J. D. Jiang, *J. Med. Chem.* **51** (2008) 3094
31. M. A. R. Hamdy, M. A. Morsy, *J. Enzyme Inhib. Med. Chem.* **22** (2007) 57
32. S. Perveen, S. Mustafa, M. A. Khan, A. Dar, K. M. Khan, W. Voelter, *Med. Chem*. **8** (2012) 330
33. K. M. Khan, S. Iqbal, M. A. Lodhi, G. M. Maharvi, Zia-Ullah, M. I. Choudhary, Atta-ur-Rahman, S. Perveen, *Bioorg. Med. Chem.* **12** (2004) 1963
34. N. Riaz, I. Anis, Aziz-ur-Rahman, A. Malik, Z. Ahmad, P. Muhammad, S. Shujaat, Atta--ur-Rahman, *Nat. Prod. Res.* **17** (2003) 247
35. V. U. Ahmad, M. A. Abbasi, H. Hussain, M. N. Akhtar, U. Farooq, N. Fatima, M. I. Choudhary, *Phytochemistry* **63** (2003) 217
36. T. Mosmann, *J. Immunol. Meth.* **65** (1983) 55
37. S. Uesato, Y. Hashimoto, M. Nishino, Y. Nagaoka, H. Kuwajima, *Chem. Pharm. Bull.* **50** (2002) 1280
38. Z. Amtul, A. U. Rahman, R. A. Siddiqui, M. I. Choudhary, *Curr. Med. Chem.* **9** (2002) 1323.

Journal of the Serbian Chemical Society
JSCS@tmf.bg.ac.rs • www.shd.org.rs/JSCS
J. Serb. Chem. Soc. 79 (1) S1–S5 (2014) *Supplementary material*

SUPPLEMENTARY MATERIAL TO

Synthesis, enzyme inhibition and anticancer investigations of unsymmetrical 1,3-disubstituted ureas

SANA MUSTAFA[1,2]*, SHAHNAZ PERVEEN[3] and AJMAL KHAN[4]

[1]Department of Chemistry, University of Karachi, Karachi-75270, Pakistan, [2]Department of Chemistry, Federal Urdu University for Arts, Science and Technology, Gulshan-e-Iqbal Campus, Karachi-75300, Pakistan, [3]PCSIR, Laboratories Complex, Karachi, Shahrah-e-Dr. Salimuzzaman Siddiqui, Karachi-75280, Pakistan and [4]HEJ Research Institute of Chemistry, International Center for Chemical and Biological Sciences, University of Karachi, Karachi-75270, Pakistan

J. Serb. Chem. Soc. 79 (1) (2014) 1–10

YIELDS, PHYSICAL, ANALYTICAL AND SPECTRAL DATA FOR THE PREPARED UREAS

N-*(3-Methylphenyl)-2-oxo-1-pyrrolidinecarboxamide (**1**)*. Yield: 70 %; m.p.: 229 °C; Anal. Calcd. for $C_{12}H_{14}N_2O_2$: C, 66.11; H, 6.47; N, 12.85 %. Found: C, 66.10; H, 6.43; N, 12.81 %; IR (KBr, cm^{-1}): 3233 (NH), 1638 (C=O); ^{1}H-NMR (400 MHz, DMSO-d_6, δ / ppm): 8.56 (1H, *br.s*, NH), 7.28 (1H, *br.s*, Ar-H), 7.19 (1H, *d*, *J* = 8.0 Hz, Ar-H), 7.13 (1H, *t*, *J* = 7.2, Ar-H), 6.76 (1H, *d*, *J* = 7.2 Hz, Ar-H), 3.28 (2H, *br.s*, CH_2), 2.49 (4H, *br.s*, $2CH_2$), 2.26 (3H, *s*, CH_3); ^{13}C-NMR (125 MHz, $CDCl_3$, δ / ppm): 173.55, 145.48, 138.78, 135.55, 131.61, 121.16, 119.73, 116.48, 43.70, 31.84, 21.00, 20.95; EI MS (*m*/*z* (relative abundance, %)): 218 (M^+, 2) 161 (4), 133 (8), 134 (4), 107 (BP, 100).

N-*Mesityl*-N′-*(3-methylphenyl)urea (**2**)*. Yield: 71 %; m.p.: 271 °C; Anal. Calcd. for $C_{17}H_{20}N_2O$: C, 76.18; H, 7.52; N, 10.45 %. Found: C, 76.15; H, 7.51; N, 10.47 %; IR (KBr, cm^{-1}): 3293 (NH), 1646 (C=O); ^{1}H-NMR (400 MHz, DMSO-d_6, δ / ppm): 8.26 (2H, *br.s*, NH), 7.31 (2H, *d*, *J* = 4.8 Hz, Ar-H,), 7.19 (1H, *s*, Ar-H), 7.07 (1H, *t*, *J* = 7.2 Hz, Ar-H), 6.68 (1H, *d*, *J* = 7.2 Hz, Ar-H), 6.56 (1H, *d*, *J* = 7.2 Hz, Ar-H), 3.31 (6H, *s*, $2CH_3$), 3.28 (3H, *s*, CH_3), 2.21 (3H, *s*, CH_3); ^{13}C-NMR (125 MHz, $CDCl_3$, δ / ppm): 155.42, 143.30, 140.28, 137.12, 136.61, 136.04, 132.10, 129.95, 120.76, 120.71, 117.51, 20.95, 20.50, 18.89; EI MS (*m*/*z* (relative abundance, %)): 268 (M^+, 21) 161 (6), 135 (85), 107 (BP, 100).

* Corresponding author. E-mail: sanachemana@yahoo.com

N-*(3-Methylphenyl)*-N′-*(1-phenylethyl)urea* (***3***). Yield: 72 %; m.p.: 123 °C; Anal. Calcd. for $C_{16}H_{18}N_2O$: C, 75.65; H, 7.14; N, 11.02 %. Found: C, 75.67; H, 7.13; N, 11.04 %; IR (KBr, cm^{-1}): 3317 (NH), 1634 (C=O); ^{1}H-NMR (400 MHz, DMSO-d_6, δ / ppm): 7.56 (2H, *br.s*, NH), 7.26 (1H, *br.s*, Ar-H), 7.19 (1H, *br.d*, *J* = 8.0 Hz, Ar-H), 7.10 (1H, *t*, *J* = 8.0 Hz, H-5), 6.86 (5H, *br.s*, Ar-H), 6.72 (1H, *br.d*, *J* = 8.0 Hz, Ar-H), 2.23 (1H, *br.s*, C**H**–CH_3), 2.21 (3H, *br.s*, CH–C**H**$_3$), 2.14 (3H, *s*, CH_3); ^{13}C-NMR (125 MHz, $CDCl_3$, δ / ppm): 156.82, 140.71, 138.98, 135.68, 131.70, 127.62, 126.64, 126.63, 120.46, 120.37, 117.12, 47.73, 20.95; EI MS (*m*/*z* (relative abundance, %)): 254 (M^+, 10) 196 (2), 120 (3), 107 (BP, 100).

N-*(3-Methoxyphenyl)*-N′-*(3-methylphenyl)urea* (***4***). Yield: 90 %; m.p.: 202 °C; Anal. Calcd. for $C_{15}H_{16}N_2O_2$: C, 70.37; H, 6.30; N, 10.94 %. Found: C, 70.35; H, 6.31; N, 10.95 %; IR (KBr, cm^{-1}): 3284 (NH), 1629 (C=O); ^{1}H-NMR (400 MHz, DMSO-d_6, δ / ppm): 8.63 (1H, *br.s*, NH), 8.54 (1H, *br.s*, NH), 7.28 (1H, *br.s*, Ar-H), 7.18 (2H, *m*, Ar-H), 7.15 (2H, *t*, *J* = 8.0 Hz, Ar-H), 6.90 (1H, *dd*, *J* = 8.0, 1.6 Hz, Ar-H), 6.77 (1H, *d*, *J* = 8.0 Hz, , Ar-H), 6.53 (1H, *dd*, *J* = 8.0, 2.4 Hz, Ar-H), 3.71 (3H, *s*, OCH_3), 2.26 (3H, *s*, CH_3); ^{13}C-NMR (125 MHz, $CDCl_3$, δ / ppm): 160.62, 155.57, 140.01, 136.04, 135.86, 132.10, 129.82, 120.76, 120.71, 118.27, 113.39, 112.41, 109.13, 55.22, 20.95; EI MS (*m*/*z* (relative abundance, %)): 256 (M^+, 22) 149 (4), 123 (65), 107 (BP, 100).

N-*(4-Methylphenyl)-2-oxo-1-pyrrolidinecarboxamide* (***5***). Yield: 70 %; m.p: 263 °C; Anal. Calcd. for $C_{12}H_{14}N_2O_2$: C, 66.11; H, 6.47; N, 12.85 %. Found: C, 66.10; H, 6.43; N, 12.81 %; IR (KBr, cm^{-1}): 3309 (NH), 1634 (C=O); ^{1}H-NMR (400 MHz, $CDCl_3$, δ / ppm): 7.18 (2H, *d*, *J* = 8.1 Hz, Ar-H), 7.08 (2H, *d*, *J* = 8.1 Hz, Ar-H), 6.32 (1H, *br.s*, NH), 4.19 (2H, *br.s*, CH_2), 2.29 (2H, *d*, *J* = 7.8 Hz, CH_2), 1.77 (2H, *br.s*, CH_2), 1.52 (3H, *s*, CH_3); ^{13}C-NMR (125 MHz, $CDCl_3$, δ / ppm): 173.55, 145.48, 136.44, 129.24, 126.86, 116.19, 43.70, 31.84, 21.00, 20.45; EI MS (*m*/*z* (relative abundance, %)): 218 (M^+, 21) 167 (1), 149 (10), 133 (BP, 100).

N-*Mesityl*-N′-*(4-methylphenyl)urea* (***6***). Yield: 71 %; m.p.: 270 °C; Anal. Calcd. for $C_{17}H_{20}N_2O$: C, 76.18; H, 7.52; N, 10.45 %. Found: C, 76.15; H, 7.51; N, 10.47 %; IR (KBr, cm^{-1}): 3293 (NH), 1646 (C=O); ^{1}H-NMR (400 MHz, DMSO-d_6, δ / ppm): 7.57 (1H, *br.s*, NH), 7.30 (2H, *d*, *J* = 8.0 Hz, Ar-H), 7.03 (2H, *d*, *J* = 8.0 Hz, Ar-H), 6.85 (2H, *br.s*, Ar-H), 4.76 (1H, *br.s*, NH), 2.28 (6H, *s*, $2CH_3$), 2.21 (3H, *s*, CH_3), 2.14 (3H, *s*, CH_3); ^{13}C-NMR (125 MHz, $CDCl_3$, δ / ppm): 155.42, 143.30, 139.72, 137.12, 136.61, 129.95, 129.73, 126.42, 117.23, 20.50, 20.45, 18.89; EI MS (*m*/*z* (relative abundance, %)): 268 (M^+, 12) 146 (1), 135 (55), 107 (BP, 100).

N-*(4-Methylphenyl)*-N′-*(1-phenylethyl)urea* (***7***). Yield: 72 %; m.p.: 164 °C; Anal. Calcd. for $C_{16}H_{18}N_2O$: C, 75.65; H, 7.14; N, 11.02 %. Found: C, 75.67; H, 7.13; N, 11.04 %; IR (KBr, cm^{-1}): 3293 (NH), 1629 (C=O); ^{1}H-NMR (400 MHz,

DMSO-d_6, δ / ppm): 8.23 (2H, *br.s*, NH), 7.30 (4H, *s*, Ar-H), 7.22 (2H, *d*, *J* = 8.0 Hz, Ar-H), 6.99 (2H, *d*, *J* = 8.0 Hz, Ar-H), 6.53 (1H, *d*, *J* = 7.6 Hz, Ar-H), 4.78 (1H, *q*, *J* = 7.2 Hz, C**H**–CH_3), 2.19 (3H, *s*, CH_3), 1.36 (3H, *d*, *J* = 7.2 Hz, CH–C**H**$_3$); ^{13}C-NMR (125 MHz, $CDCl_3$, δ / ppm): 156.82, 140.71, 138.43, 129.32, 127.62, 126.64, 126.36, 126.17, 116.83, 47.73, 20.95, 20.45; EI MS (*m*/*z* (relative abundance, %)): 254 (M^+, 8) 149 (1), 132 (2), 107 (BP, 100).

N-(3-Methoxyphenyl)-N-*(4-methylphenyl)urea* (***8***). Yield: 90 %; m.p.: 183 °C; Anal. Calcd. for $C_{15}H_{16}N_2O_2$: C, 70.37; H, 6.30; N, 10.94 %. Found: C, 70.35; H, 6.31; N, 10.95 %; IR (KBr, cm^{-1}): 3293 (NH), 1638 (C=O); ^{1}H-NMR (400 MHz, DMSO-d_6, δ / ppm): 8.60 (1H, *br.s*, NH), 8.51 (1H, *br.s*, NH), 7.31 (2H, *d*, *J* = 8.0 Hz, Ar-H), 7.16 (1H, *br.s*, Ar-H), 7.14 (1H, *m*, Ar-H), 7.06 (1H, *d*, *J* = 8.0 Hz, Ar-H), 6.89 (1H, *d*, *J* = 8.0 Hz, Ar-H), 6.52 (1H, *d*, *J* = 8.0 Hz, Ar-H), 3.71 (3H, *s*, OCH_3), 2.23 (3H, *s*, CH_3); ^{13}C-NMR (125 MHz, $CDCl_3$, δ / ppm): 160.62, 155.57, 138.73, 135.86, 129.82, 129.73, 126.42, 119.96, 113.39, 112.41, 109.13, 55.22, 20.45; EI MS (*m*/*z* (relative abundance, %)): 256 (M^+, 15) 149 (5), 123 (44), 107 (BP, 100).

N-*(1,3-Benzothiazol-2-yl)*-N′-*(3-methylphenyl)urea* (***9***). Yield: 90 %; m.p.: 319 °C; Anal. Calcd. for $C_{15}H_{13}N_3OS$: C, 63.65; H, 4.63; N, 14.84 %. Found: C, 63.67; H, 4.61; N, 14.86 %; IR (KBr, cm^{-1}): 3396 (NH), 1695 (C=O); ^{1}H-NMR (400 MHz, DMSO-d_6, δ / ppm): 9.07 (1H, *br.s*, NH), 8.81 (1H, *br.s*, NH), 8.13 (1H, *d*, *J* = 8.0 Hz, Ar-H), 7.90 (1H, *br.s*, Ar-H), 7.81 (1H, *d*, *J* = 8.0 Hz, Ar-H), 7.65 (1H, br.*s*, Ar-H), 7.38 (1H, *d*, *J* = 7.6 Hz, Ar-H), 7.25 (1H, *t*, *J* = 7.6 Hz, Ar-H), 7.20 (1H, *t*, *J* = 7.6 Hz, Ar-H), 6.85 (1H, *t*, *J* = 8.0 Hz, Ar-H), 2.29 (3H, *s*, CH_3); ^{13}C-NMR (125 MHz, $CDCl_3$, δ / ppm): 161.12, 150.43, 148.77, 139.76, 135.63, 131.70, 127.30, 126.07, 122.99, 121.37, 120.46, 119.74, 118.84, 116.63, 20.95; EI MS (*m*/*z* (relative abundance, %)): 283 (M^+, 4) 240 (1), 176 (20), 150 (BP, 100).

N-*(2-Acetylphenyl)*-N′-*(3-methylphenyl)urea* (***10***). Yield: 90 %; m.p.: 182 °C; Anal. Calcd. for $C_{16}H_{16}N_2O_2$: C, 71.70; H, 6.01; N, 10.45 %. Found: C, 71.68; H, 6.02; N, 10.42 %; IR (KBr, cm^{-1}): 3297 (NH), 1683 (C=O); ^{1}H-NMR (400 MHz, DMSO-d_6, δ / ppm): 8.87 (1H, *br.s*, NH), 8.62 (1H, *br.s*, NH), 8.06 (1H, *br.s*, Ar-H), 7.65 (1H, *d*, *J* = 8.0 Hz, Ar-H), 7.57 (1H, *d*, *J* = 7.6 Hz, Ar-H), 7.43 (1H, *t*, *J* = 8.0 Hz, Ar-H), 7.31 (1H, *br.s*, Ar-H), 7.21 (1H, *d*, *J* = 8.0 Hz, Ar--H), 7.16 (1H, *t*, *J* = 7.6 Hz, Ar-H), 6.79 (1H, *d*, *J* = 7.6 Hz, Ar-H), 2.56 (3H, *s*, $OCCH_3$) 2.27 (3H, *s*, CH_3); ^{13}C-NMR (125 MHz, $CDCl_3$, δ / ppm): 200.60, 152.74, 140.27, 140.03, 138.70, 136.04, 132.64, 132.10, 121.91, 120.76, 120.71, 119.34, 117.51, 117.07, 26.80, 20.95; EI MS (*m*/*z* (relative abundance, %)): 268 (M^+, 16) 146 (9), 135 (44), 120 (59), 107 (BP, 100).

N-*(1,3-Benzothiazol-2-yl)*-N′-*(4-methylphenyl)urea* (***11***). Yield: 90 %; m.p.: 328 °C; Anal. Calcd. for $C_{15}H_{13}N_3OS$: C, 63.65; H, 4.63; N, 14.84 %. Found: C, 63.67; H, 4.61; N, 14.86 %; IR (KBr, cm^{-1}): 3440 (NH), 1691 (C=O); ^{1}H-NMR

(400 MHz, DMSO-d_6, δ / ppm): 9.04 (1H, *br.s*, NH), 8.46 (1H, *br.s*, NH), 7.89 (1H, *br.s*, Ar-H), 7.65 (1H, *br.s*, Ar-H), 7.38 (1H, *t*, *J* = 7.8 Hz, Ar-H), 7.30 (1H, *d*, *J* = 7.8 Hz, Ar-H), 7.24 (1H, *t*, *J* = 7.8 Hz, Ar-H), 7.13 (2H, *d*, *J* = 7.2 Hz, Ar-H), 7.06 (1H, *d*, *J* = 7.8 Hz, Ar-H), 2.23 (3H, *s*, CH_3); ^{13}C-NMR (125 MHz, $CDCl_3$, δ / ppm): 161.12, 150.43, 148.77, 139.21, 129.32, 127.30, 126.17, 126.07, 121.37, 119.46, 118.84, 116.63, 20.99; EI MS (*m*/*z* (relative abundance, %)): 283 (M^+, 4) 176 (25), 150 (BP, 100).

N-*Mesityl*-N′-*(2-methylphenyl)urea* ***(12)***. Yield: 90 %; m.p.: 279 °C; Anal. Calcd. for $C_{17}H_{20}N_2O$: C, 76.18; H, 7.52; N, 10.45 %. Found: C, 76.15; H, 7.51; N, 10.47 %; IR (KBr, cm^{-1}): 3297 (NH), 1642 (C=O); ^{1}H-NMR (400 MHz, DMSO-d_6, δ / ppm): 7.95 (2H, *br.s*, NH), 7.77 (1H, *d*, *J* = 7.6 Hz, Ar-H), 7.14 (1H, *d*, *J* = 7.6 Hz, Ar-H), 7.09 (1H, *t*, *J* = 7.6 Hz, Ar-H), 6.90 (1H, *t*, *J* = 7.6 Hz, Ar-H), 6.87 (2H, *s*, Ar-H), 2.23 (3H, *s*, CH_3), 2.22 (3H, *s*, CH_3), 2.16 (6H, *s*, CH_3); ^{13}C-NMR (125 MHz, $CDCl_3$, δ / ppm): 156.88, 143.30, 137.63, 137.12, 136.61, 132.58, 129.95, 127.43, 125.94, 122.88, 119.96, 20.95, 18.89, 17.49; EI MS (*m*/*z* (relative abundance, %)): 268 (M^+, 23) 161 (1), 135 (69), 107 (BP, 100).

N-*(2-Methylphenyl)*-N′-*(1-phenylethyl)urea* ***(13)***. Yield: 90 %; m.p.: 179 °C; Anal. Calcd. for $C_{16}H_{18}N_2O$: C, 75.65; H, 7.14; N, 11.02 %. Found: C, 75.67; H, 7.13; N, 11.04 %; IR (KBr, cm^{-1}): 3374 (NH), 1646 (C=O); ^{1}H-NMR (400 MHz, DMSO-d_6, δ / ppm): 7.82 (1H, *d*, *J* = 8.0 Hz, Ar-H), 7.60 (2H, *br.s*, NH), 7.34 (5H, *s*, Ar-H), 7.09 (1H, *t*, *J* = 7.6 Hz, Ar-H), 7.04 (1H, *d*, *J* = 7.6 Hz, Ar-H), 6.83 (1H, *t*, *J* = 7.6 Hz, Ar-H), 4.80 (1H, *q*, *J* = 7.2 Hz, C**H**–CH_3), 2.16 (3H, *s*, CH_3), 1.38 (3H, *d*, *J* = 7.2 Hz, CH–C**H**$_3$); ^{13}C-NMR (125 MHz, $CDCl_3$, δ / ppm): 156.28, 140.71, 136.33, 132.17, 127.62, 127.03, 126.64, 126.63, 125.54, 122.62, 119.56, 47.73, 20.95, 17.49; EI MS (*m*/*z* (relative abundance, %)): 254 (M^+, 11) 196 (1), 120 (3), 107 (BP, 100).

N-*(3-Methoxyphenyl)*-N′-*(2-methylphenyl)urea* ***(14)***. Yield: 90 %; m.p.: 163 °C; Anal. Calcd. for $C_{15}H_{16}N_2O_2$: C, 70.37; H, 6.30; N, 10.94 %. Found: C, 70.35; H, 6.31; N, 10.95 %; IR (KBr, cm^{-1}): 3301 (NH), 1638 (C=O); ^{1}H-NMR (400 MHz, DMSO-d_6, δ / ppm): 9.00 (2H, *br.s*, NH), 7.88 (1H, *s*, Ar-H), 7.81 (1H, *d*, *J* = 8.0 Hz, Ar-H), 7.17 (1H, *br.s*, Ar-H), 7.15 (1H, *t*, *J* = 8.0 Hz, Ar-H), 7.10 (1H, *d*, *J* = 7.6 Hz, Ar-H), 6.93 (2H, *t*, *J* = 7.6 Hz, Ar-H), 6.53 (1H, *d*, *J* = = 7.6 Hz, Ar-H), 3.72 (3H, *s*, OCH_3), 2.22 (3H, *s*, CH_3); ^{13}C-NMR (125 MHz, $CDCl_3$, δ / ppm): 160.62, 157.03, 137.23, 135.87, 132.58, 130.00, 129.82, 125.94, 122.88, 119.96, 113.39, 112.41, 109.13, 55.20, 20.93; EI MS (*m*/*z* (relative abundance, %)): 256 (M^+, 42) 149 (7), 123 (84), 107 (BP, 100).

N-*(2-Methylphenyl)-2-oxo-1-pyrrolidinecarboxamide* ***(15)***. Yield: 70 %; m.p.: 263 °C; Anal. Calcd. for $C_{12}H_{14}N_2O_2$: C, 66.11; H, 6.47; N, 12.85 %. Found: C, 66.10; H, 6.43; N, 12.81 %; IR (KBr, cm^{-1}): 3313 (NH), 1646 (C=O); ^{1}H-NMR (400 MHz, DMSO-d_6, δ / ppm): 8.22 (1H, br.*s*, NH), 7.78 (1H, *d*, *J* =

= 7.6 Hz, Ar-H), 7.16 (1H, *d*, *J* = 7.6 Hz, Ar-H), 7.11 (1H, *t*, *J* = 7.6 Hz, Ar-H), 6.93 (1H, *t*, *J* = 7.6 Hz, Ar-H), 3.28 (2H, *br.s*, CH_2), 2.49 (4H, *br.s*, $2CH_2$), 2.26 (3H, *s*, CH_3); ^{13}C-NMR (125 MHz, $CDCl_3$, δ / ppm): 173.55, 146.93, 136.14, 132.08, 126.39, 125.45, 123.32, 118.92, 43.70, 31.84, 21.00, 17.49; EI MS (*m*/*z* (relative abundance, %)): 218 (M^+, 1) 161 (1), 133 (2), 107 (BP, 100).

N-*(1,3-Benzothiazol-2-yl)*-N′-*(2-methylphenyl)urea* ***(16)***. Yield: 90 %; m.p.: 329 °C; Anal. Calcd. for $C_{15}H_{13}N_3OS$: C, 63.65; H, 4.63; N, 14.84 %. Found: C, 63.67; H, 4.61; N, 14.86 %; IR (KBr, cm^{-1}): 3472 (NH), 1695 (C=O); ^{1}H-NMR (400 MHz, DMSO-d_6, δ / ppm): 11.11 (1H, *br.s*, NH), 8.65 (1H, *br.s*, NH), 7.91 (1H, *d*, *J* = 7.6 Hz, Ar-H), 7.84 (1H, *d*, *J* = 7.6 Hz, Ar-H), 7.65 (2H, *d*, *J* = 8.0 Hz, Ar-H), 7.38 (1H, *t*, *J* = 7.6 Hz, Ar-H), 7.22 (2H, *m*, Ar-H), 7.02 (1H, *t*, *J* = = 7.6 Hz, Ar-H), 2.27 (3H, *s*, CH_3); ^{13}C-NMR (125 MHz, $CDCl_3$, δ / ppm): 161.12, 151.88, 148.77, 137.12, 132.17, 129.65, 127.30, 126.07, 122.62, 122.54, 122.19, 121.37, 118.84, 116.63, 20.88; EI MS (*m*/*z* (relative abundance, %)): 283 (M^+, 6) 176 (12), 150 (BP, 100).

N-*(2-Acetylphenyl)*-N′-*(4-methylphenyl)urea* ***(17)***. Yield: 90 %; m.p.: 235 °C; Anal. Calcd. for $C_{16}H_{16}N_2O_2$: C, 71.70; H, 6.01; N, 10.45 %. Found: C, 71.68; H, 6.02; N, 10.40 %; IR (KBr, cm^{-1}): 3378 (NH), 1674 (C=O); ^{1}H-NMR (400 MHz, DMSO-d_6, δ / ppm): 8.84 (1H, *br.s*, NH), 8.58 (1H, *br.s*, NH), 8.04 (1H, *br.s*, Ar-H), 7.65 (1H, *d*, *J* = 8.0 Hz, Ar-H), 7.56 (1H, *d*, *J* = 8.0 Hz, Ar-H), 7.42 (1H, *t*, *J* = 8.0 Hz, Ar-H), 7.33 (2H, *d*, *J* = 8.0 Hz, Ar-H), 7.08 (1H, *d*, *J* = = 8.0 Hz, Ar-H), 2.55 (3H, *s*, $OCCH_3$), 2.24 (3H, *s*, CH_3); ^{13}C-NMR (125 MHz, $CDCl_3$, δ / ppm): 200.60, 152.73, 140.03, 139.72, 138.70, 132.64, 129.76, 126.42, 121.91, 119.34, 117.23, 117.07, 26.80, 20.45; EI MS (*m*/*z* (relative abundance, %)): 268 (M^+, 21) 146 (7), 135 (33), 120 (46), 107 (100).

Journal of the Serbian Chemical Society
JSCS-info@shd.org.rs • www.shd.org.rs/JSCS
J. Serb. Chem. Soc. *79* (1) 11–24 (2014)
JSCS–4561
UDC 547.56–32:541.515:663.222+547.973(497.11)
Original scientific paper

Phenolic composition and free radical scavenging activity of wine produced from the Serbian autochthonous grape variety Prokupac – A model approach

NEBOJŠA MENKOVIĆ[1], JELENA ŽIVKOVIĆ[1]*, KATARINA ŠAVIKIN[1], DEJAN GOĐEVAC[2] and GORDANA ZDUNIĆ[1]

[1]*Institute for Medicinal Plant Research "Dr. Josif Pančić", Tadeuša Košćuška 1, 11000 Belgrade, Serbia and* [2]*Institute for Chemistry, Technology and Metallurgy, Njegoševa 12, 11000 Belgrade, Serbia*

(Received 11 May, revised 6 July 2013)

Abstract: Phenolic compounds are very important quality parameters of wine because of their impact on colour, taste and health properties. The present study was aimed at evaluating the general phenolic composition and free radical scavenging activity of aqueous and organic fractions obtained using liquid–liquid extraction of red wine produced from the Serbian autochthonous grape variety Prokupac. The total phenolic contents in the different fractions ranged from 48.22 to 289.12 mg GAE per g dry fraction. Phenolic acids (mainly hydroxycinnamic acids) and quercetin 3-*O*-glucuronide were the main components in the EtOAc fraction at pH 2.0; catechins, phenolic acids (mainly hydroxybenzoic acids) and quercetin were found in the EtOAc fraction at pH 7.0, while anthocyanins were identified in the aqueous residue after EtOAc extraction. The major anthocyanin extracted into the aqueous fraction was malvidin-3-glucoside, while the most abundant non-anthocyanin phenolic compounds in the organic fractions were ethyl gallate and *trans*-caftaric acid. The radical scavenging activities of the fraction differed significantly and the IC_{50} values were 138.58 μg mL^{-1} for the aqueous fraction, 17.83 and 3.47 μg mL^{-1} for the EtOAc fractions at pH 2.0 and 7.0, respectively. As the EtOAc fractions were found to be more potent radical scavengers, it could be assumed that non-anthocyanin phenolic compounds were responsible for such activity in Prokupac wine.

Keywords: anthocyanins; flavonoids; phenolic acids.

INTRODUCTION

The southern region of Serbia has a long-standing tradition of viticulture and winemaking since the dominant soil types and climatic conditions of the region

* Corresponding author. E-mail: jelenazivkovic1@yahoo.com
doi: 10.2298/JSC130511089M

are very favourable for the cultivation of vines. The vineyards of southern Serbia are focused on the old autochthonous vine varieties such as Prokupac.[1] According to the literature, there is only limited information about the chemical composition of wines produced from the Prokupac variety cultured in southern Serbia.

Based on their carbon ring structure, wine polyphenols are divided into flavonoids (anthocyanins, flavan-3-ols, flavonols, dihydroflavonols) and non-flavonoids (hydroxybenzoic and hydroxycinnamic acids and derivatives, stilbenes and volatile phenols).[2] The quantities of these phenolic compounds vary considerably in different types of wines depending on the grape variety, environmental factors in the vineyard, the wine processing techniques, soil and atmospheric conditions during ripening and fruit maturation.[3] The ageing of the wine could also modify the phenolic composition because phenolic compounds undergo different transformations, such as oxidation processes, condensation and polymerisation reactions, and extraction from wood.[4] Therefore, each type of grape presents a distinct sensory appeal, chemical composition and biological activity.

The anti-oxidant activity of wines has been related to their polyphenolic constituents and is mainly based on their free radical scavenging capacity.[5] Wine phenolics show beneficial physiological properties, *e.g.*, cardioprotective, anticarcinogenic and anti-inflammatory activities, due to their ideal chemical structure for free radical scavenging activities.[6] As oxidative stress arises from an imbalance in the human antioxidant status, it contributes to the pathology of chronic diseases.[7] Reactive oxygen species (ROS), naturally formed during normal metabolism, can damage biological structures, such as proteins, lipids or DNA. Human metabolism counts on an antioxidant defensive system involving enzymes and proteins to prevent these effects.[8] Since these protective mechanisms can be disrupted by various pathological phenomena, antioxidant supplements are essential to counter oxidative damage.[9] It is recognised that besides a role in endogenous defence in plants, the consumption of dietary polyphenols plays an important role in protecting against some pathological events.[10]

In addition to the importance of wine polyphenols as antioxidants, their study may also contribute to wine grape taxonomic characterisation and for certification of wine quality and origin.[11] In fact, both antioxidant activity and sensory properties depend on not only the amount, but also the type and structural features of polyphenols.[12]

The aim of this work was to determine the phenolic composition and free radical-scavenging activity in different fractions of red wine produced from the Serbian autochthonous grape variety Prokupac. For this purpose, three fractions of Prokupac wine containing different classes of phenolics were obtained by liquid–liquid extractions. Chemical analyses were realized using HPLC and LC-MS, while antiradical activity was tested using the DPPH (2,2-diphenyl-1-(2,4,6--trinitrophenyl)hydazinyl) method.

EXPERIMENTAL

Wine sample

The wine produced from the autochthonous grape variety Prokupac (2010 vintage) was obtained from the Braća Rajković vinery in the southwest region of Serbia. Prokupac grape was cultivated in Gornje Zleginje (altitude 359 m, 43°26′15″N, 21°10′01″E).

Standards

Standard compounds: delphinidin 3-*O*-*β*-glucoside chloride, malvidin 3-*O*-*β*-glucoside chloride, gentisic acid, caffeic acid, ellagic acid, catechin, proanthocyanidin B1 and B2, epicatechin, protocatechuic acid and quercetin were obtained from Extrasynthese (France).

Fractionation of Prokupac wine

Liquid–liquid extraction methods according to Ghiselli *et al.*[13] were performed to obtain several fractions containing different classes of polyphenolic compounds. In brief, ethanol removal was realized by vacuum evaporation. Special attention was paid to control the evaporation process, monitoring the pH and the volume of the solution to avoid complexation and precipitation processes. The de-alcoholised wine (100 mL) was first extracted with ethyl acetate (three times with 100 mL of EtOAc each), whereby an aqueous residue and an organic phase were obtained. The organic phase was evaporated, re-dissolved in water at pH 7.0 and further extracted with EtOAc (three times with 100 mL of EtOAc each) The aqueous residue from this extraction was adjusted at pH 2.0 and extracted again with EtOAc (three times with 100 mL of EtOAc each). The obtained fractions were then evaporated under reduced pressure.

Determination of the total phenolics

The concentration of total phenolic compounds in the fractions was determined spectrophotometrically using the Folin–Ciocalteu method with slight modifications.[14] Two hundred microlitres of the fractions (5 mg mL^{-1} 50 % EtOH) were added to 1 mL of 1:10 diluted Folin–Ciocalteu reagent. After 4 min, 800 µl of sodium carbonate (75 g L^{-1}) were added. After 2 h of incubation at room temperature, the absorbance at 765 nm was measured. Gallic acid (0–100 mg L^{-1}) was used for the construction of a calibration curve. The results were expressed as milligrams of gallic acid equivalents per gram of dry weight of fraction (mg GAE g^{-1} DW). Triplicate measurements were taken and the mean values were calculated.

Fingerprint HPLC-DAD analysis

Analyses of phenolic compounds from the aqueous and organic fractions were performed using HPLC Agilent 1200 Series with UV–Vis diode-array detector (DAD) for multi-wavelength detection. The aqueous fraction was separated on a Zorbax SB-Aq column (250 mm×4.6 mm, 5µm) according to the Compendium of International Methods OIV.[15] A gradient consisting of solvent A (H_2O/HCOOH/CH_3CN, 87:10:3, v/v/v) and solvent B (H_2O/ /HCOOH/CH_3CN, 40:10:50, v/v/v) was applied at a flow rate 0.8 mL min^{-1} as follows: 6 to 30 % B linear in 0 to15 min, 30 to 50 % B linear in 15 to 30 min, 50 to 60 % B linear in 30 to 35 min, and 60 to 6 % B linear in 35 to 41 min. The column was thermostated at 40 °C. Fifty microlitres of wine, previously filtered through a 0.45-µm membrane, was injected onto the column. Identification was possible by monitoring the anthocyanins at 520 nm and by comparing their spectra and retention times with those of commercial standards.

Analysis of the EtOAc wine fractions obtained at pH 7.0 and 2.0 was performed on a reversed-phase Zorbax SB-Aq column (250 mm×4.6 mm, 5µm) at 40 °C. A gradient consisting of solvent A (H_2O/CH_3COOH, 95:5, v/v) and solvent B (CH_3CN) was applied at a flow rate of 0.5 mL min^{-1} as follows: 0 to 60 % B linear from 0 to 35 min. Fifty microlitres of

wine, previously filtered through a 0.45 μm membrane, was injected onto the column. Chromatograms were acquired at 280–330 nm. The content of an individual phenolic compound was determined by comparing the area of the appropriate peak against the total peak area of the phenolics and the data are expressed in percentages.

LC–MS analysis

LC–MS analysis was performed on an Agilent MSD TOF coupled to an Agilent 1200 series HPLC. For the analysis of the EtOAc wine fractions, the same column and gradient program was used as for the HPLC-DAD analysis. For the analysis of anthocyanins, mobile phase A was 10 % formic acid in water and mobile phase B was acetonitrile. The injection volume was 10 μL, and elution was at 1 mL min^{-1} with gradient program (0–1 min, 1–7 % B; 1–4 min, 7 % B; 4–7.5 min, 7–10 % B; 7.5–11.5 min, 10–14 % B; 11.5–15.5 min, 14–25 % B; 15.5–18.5 min, 25–40 % B; 18.5–22 min 40–75 % B; 22–25 min 75% B; 25–26 min 75–99 % B; 26–27 min, 99–1 % B) using the same column as that employed for the HPLC-DAD analysis. Mass spectra were acquired using an Agilent ESI-MSD TOF. The drying gas (N_2) flow was 12 L min^{-1}; the nebulizer pressure was 45 psig; the drying gas temperature was 350 °C. For ESI analysis, the parameters were: capillary voltage, 4000 V; fragmentor, 140 V; skimmer, 60 V; Oct RF V 250 V, for the negative (EtOAc wine fractions) and positive modes (anthocyanins). The mass range was from 100 to 2000 *m*/*z*. Processing of data was realized with the software Molecular Feature Extractor.

Free radical scavenging activity

The free radical scavenging activity of the fractions were analysed using the DPPH assay.[16] This antioxidant assay is based on the measurement of the DPPH colour loss at 517 nm caused by the reaction of DPPH with the test sample. Fractions diluted in appropriate solvents (10–100 μL) were dispensed into a set of test tubes and the final volume was adjusted to 5 mL. Finally, 0.5 ml of a 0.5 mM methanolic DPPH solution was transferred into each test tube. The absorbances were recorded at 517 nm after 30 min incubation at room temperature in the dark, against methanol as the blank. The percent inhibition was calculated against the control solution, containing methanol instead of a test solution.

Statistical analysis

All data are expressed as the mean values ± standard deviation from three replicates (n = 3). For statistical analysis, one-way analysis of variance (ANOVA) was applied, followed by the Student's t test. The correlation coefficient between antioxidant activity values and the content of total phenolic compounds were measured using the Pearson correlation coefficient (r) and the Origin 8.0 software program. Correlations were considered statistically significant, if the p-value was less than 0.05.

RESULTS AND DISCUSSION

Total phenolics

In this study, the total amount of polyphenols was measured using the Folin–Ciocalteu method, referred to gallic acid. Total phenolic contents in different fractions ranged from 48.22±2.03 to 289.12±5.05 mg GAE g^{-1} dry fraction (Table I). The highest level was observed in the EtOAc fraction obtained at pH 7.0, while the aqueous fraction showed the lowest amount of total polyphenols. Although Ghiselli *et al.*[13] also showed that the EtOAc fraction obtained at pH 7.0

of the wine produced from the Sangiovese R10 grape clone from Italy was more abundant in phenolics than the EtOAc fraction obtained at 2.0, they found significantly bigger amounts of polyphenolics in the aqueous residue.

TABLE I. Total phenolic content and free radical-scavenging activity of different fractions obtained from Prokupac wine

Fraction	Total phenolic content mg GAE g^{-1} dry fraction[a]	DPPH-IC_{50}[a] µg mL^{-1}
Aqueous	48.22±2.03	138.58±3.33
EtOAc at pH 2.0	118.36±3.12	17.83±0.97
EtOAc at pH 7.0	289.12±5.05	3.47±0.34

[a]Values are significantly different, $p < 0.05$

According to Atanacković *et al.*,[17] of the wines produced from the cultivars Prokupac, Merlot, Cabernet Sauvignon and Pinot noir, the lowest phenolic content was found in the wine from the native cultivar Prokupac.

Phenolic compounds of Prokupac wine

Phenolic compounds are very important quality parameters of wine because of their impact on colour, taste and health properties,[18] as well as from chemotaxonomic point of view. The application of the liquid–liquid extraction method allowed the separation of the phenolics of Prokupac wine into fractions containing compounds with similar characteristics. This method made the identification of individual compounds easier and allowed an estimation of which classes of compounds were mainly responsible for the radical scavenging activity of the wine.

HPLC-DAD and LC–MS were applied to analyze the compounds in the obtained fractions and the results are presented in Tables II–IV and Figs. 1–3. The exact mass measurements of the pseudo-molecular ions of analytes performed by the time-of-flight (TOF) mass spectrometer in the negative polarity mode enabled the determination of the molecular formula of the phenolic acids, flavonoids, and procyanidins. Molecular formula determinations were performed by Molecular Feature Extractor program, taking into account *m*/*z* values and isotopic abundance patterns for all ion species noticed for respective compound. Molecular formulas of anthocyanins were determined using MS spectra in positive polarity mode, from corresponding molecular ions.

Complete identification of the compounds was achieved by comparing the UV spectra and molecular formula obtained from accurate mass measurements, with those from the literature, together with comparison of the HPLC retention times with those of authentic standards.

Generally, phenolic acids (mainly hydroxycinnamic acids) and quercetin 3--*O*-glucuronide were the main components of the EtOAc fraction at pH 2.0. Some procyanidins, catechin, epicatechin, phenolic acids (mainly hydroxyben-

zoic acids) and quercetin were found in the EtOAc extract at pH 7.0. Several anthocyanins were identified in the aqueous residue after EtOAc extraction.

TABLE II. Anthocyanin compounds detected in the aqueous fraction of Prokupac wine

Peak	*Rt* min	Compound	DAD λ_{max} / nm	Accurate mass g mol^{-1}	Total phenolics content in the fraction, %
1	12.6	Delphinidin 3-*O*-glucoside	524	465.1022	5.1
2	15.4	Petunidin 3-*O*-hexoside	526	479.1191	7.4
3	16.5	Peonidin 3-*O*-hexoside	520	463.1276	8.6
4	17.1	Malvidin 3-*O*-glucoside	528	493.1371	49.1
5	17.6	Vitisin A	510	561.1259	6.0
6	19.5	Peonidin 3-*O*-(6-*O*-acetyl)hexoside	520	505.1401	1.0
7	19.6	Malvidin 3-*O*-(6-*O*-acetyl)hexoside	520	535.1423	2.6
8	20.3	Malvidin 3-*O*-(6-*O*-coumaroyl)-hexoside	534	639.1719	1.2
9	20.6	Pionitin A	510	625.1588	2.1
10	21.2	(*p*-Hydroxyphenyl)pyranomalvidin glucoside	504	625.1588	3.0

TABLE III. Phenolic compounds detected in EtOAc fraction at pH 2.0

Peak	*Rt* min	Compound	DAD λ_{max} / nm	MS species	Accurate mass g mol^{-1}	Total phenolics content in the fraction, %
1	6.0	*cis*-Caftaric acid	302*sh*, 324	M–H, M+HCOOH, M+Cl, 2M–H	312.0525	4.3
2	6.2	Gentisic acid	260, 296	M–H, M+HCOOH, M+Cl, 2M–H	154.0283	11.8
3	6.8	*trans*-Caftaric acid	302*sh*, 330	M–H, M+HCOOH, M+Cl, 2M–H	312.0528	13.2
4	8.4	*trans*-Fertaric acid	302*sh*, 330	M–H, M+HCOO, M+Cl	326.0671	3.4
5	8.9	Coutaric acid	302*sh*, 314	M–H, M+HCOO, M+Cl	296.0564	5.4
6	10.0	Caffeic acid	302*sh*, 322	M–H, M+HCOO, M+Cl	180.0437	6.4
7	10.5	*cis*-Fertaric acid	302*sh*, 330	M–H, M+HCOO, M+Cl	326.0670	5.5
8	16.3	Quercetin 3-*O*-glucuronide	256, 264*sh*, 296*sh*, 346	M–H, M+HCOO, M+Cl	478.0790	4.3
9	17.0	Ellagic acid	254, 366	M–H, M+HCOO, M+Cl	302.0097	6.2

The principal source of the red colour in wine comes from its anthocyanin content. Nevertheless, free anthocyanins are not particularly stable.[19] Their extraction and stability are affected by vinery production practices. Monomeric anthocyanins are subject to hydrolysis, oxidation, and polymerization in wines. Their concentration usually decreases during the fermentation and maceration but this process may continue throughout the life of a wine.[1] Wine anthocyanins are the 3-*O*-monoglucosides of delphinidin, cyanidin, petunidin, peonidin and malvidin. Glucosylated derivatives of these anthocyanins esterified at the C6 of the glucose with acetyl or cumaroyl groups are also usually found in wine samples, generally in low concentrations.[20]

TABLE IV. Phenolic compounds detected in the EtOAc fraction at pH 7.0

Peak	*Rt* min	Compound	DAD λ_{max} / nm	MS species	Accurate mass g mol^{-1}	Total phenolics content in the fraction, %
1	7.5	Catechin	280	M–H, M+HCOO, M+Cl	290.0821	6.8
2	7.9	Proanthocyanidin dimer	280	M–H, M+HCOO, M+Cl, 2M–H	578.1462	9.7
3	8.4	Epicatechin	280	M–H, M+HCOO, M+Cl	290.0824	7.3
4	9.7	Proanthocyanidin dimer	280	M–H, M+HCOO, M+Cl, 2M–H	578.1462	2.8
5	10.4	Protocatechuic acid	290	M–H, M+HCOO, M+Cl	154.0273	6.4
6	11.6	Ethyl gallate	272	M–H, M+HCOO, M+Cl, 2M–H, 2M–Cl	198.0549	19.7
7	13.7	Proanthocyanidin dimer	280	M–H, M+HCOO, M+Cl, 2M–H	578.1462	1.5
8	24.6	Ethyl caffeate	300, 324	M–H, M+HCOO, M+Cl	208.0737	3.0
9	31.8	Quercetin	254, 264, 292*sh*, 370	M–H, M+HCOO, M+Cl	302.0457	2.4

In the present work, the analysis of the aqueous fraction by HPLC-DAD and LC–MS allowed the identification of 10 anthocyanin compounds (Table II). Malvidin glucoside was the predominant anthocyanin (49.1 % of the total), as it is usual for *Vitis vinifera* wines,[21] followed by peonidin hexoside (8.6 % of the total) and petunidin hexoside (7.4 % of the total). Mitić *et al*.[22] showed that malvidin glucoside was the most abundant among anthocyanins detected in Prokupac grapes. Furthermore, they detected some flavan-3-ols and hydroxycinnamic acids in grapes, which were also found in the Prokupac wine fractions investigated in the present study. The pattern of the anthocyanins showed that the sugar substi-

tuents were hexose (about 70 % of the total) followed by acetyl hexose (3.6 % of the total) and coumaroyl hexose (1.2 % of the total). The presence of pyrano-anthocyanins vitisin A, pinotin A and (*p*-hydroxyphenyl)pyranomalvidin 3-*O*--glucoside were also evidenced. These compounds are produced during alcoholic fermentation and wine aging. Although cyanidin derivatives have been detected in red wines of different grape varieties,[18,23,24] cyanidin compounds were not found in the present fractions of Prokupac wine.

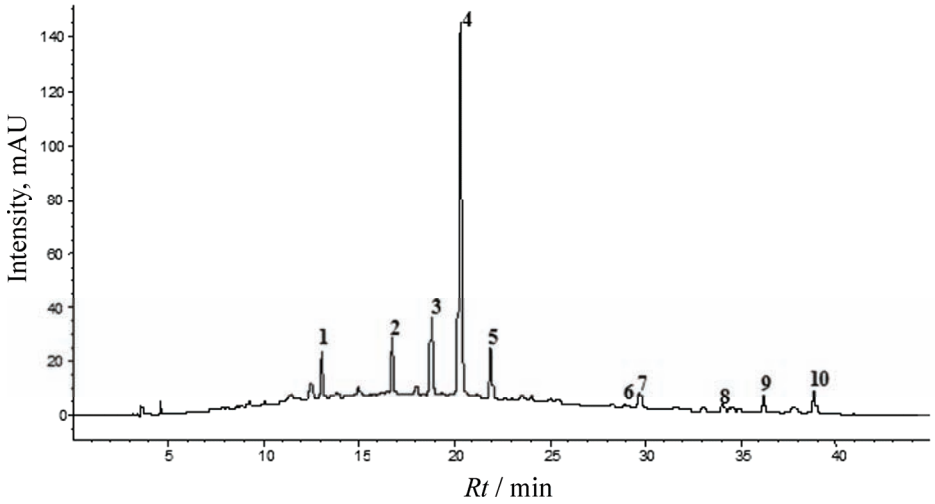

Fig. 1. HPLC profile of the aqueous fraction of Prokupac wine: delphinidin 3-*O*-glucoside (1), petunidin hexoside (2), peonidin hexoside (3), malvidin 3-*O*-glucoside (4), vitisin A (5), peonidin acetyl-hexoside (6), malvidin acetyl-hexoside (**7**), malvidin coumaroyl-hexoside (8), pinotin A (9), and (*p*-hydroxyphenyl)pyranomalvidin glucoside (10).

Non-anthocyanin phenolic compounds, including 4 benzoic acids, 7 cinnamic acids, 5 flavan-3-ols and 2 flavonols were detected in the organic fractions (Tables III and IV). Benzoic acids are minor components in wines, whereas hydroxycinnamates are the most important class of non-flavonoid phenolics.[25] The EtOAc fraction obtained at pH 2.0 was found to be rich in hydroxycinnamic acids and their derivatives. The main phenolic acids found in this fraction were *trans*-caftaric acid (13.2 % of the total) and gentisic acid (11.8 % of the total). *cis*-Caftaric acid, coutaric acid, fertaric acid (*cis* and *trans* isomers), ellagic acid and caffeic acid (the hydrolysis product of caftaric acid) were also detected.

Phenolic acids and their derivatives identified in the EtOAc fraction at pH 7.0 were protocatechuic acid, ethyl gallate and ethyl caffeate. Flavan-3-ols, which are mainly responsible for the astringency, bitterness, and structure of the wines, were also detected and among them catechin, epicatechin and three proanthocyanidin dimers were identified in the EtOAc fraction at pH 7.0.

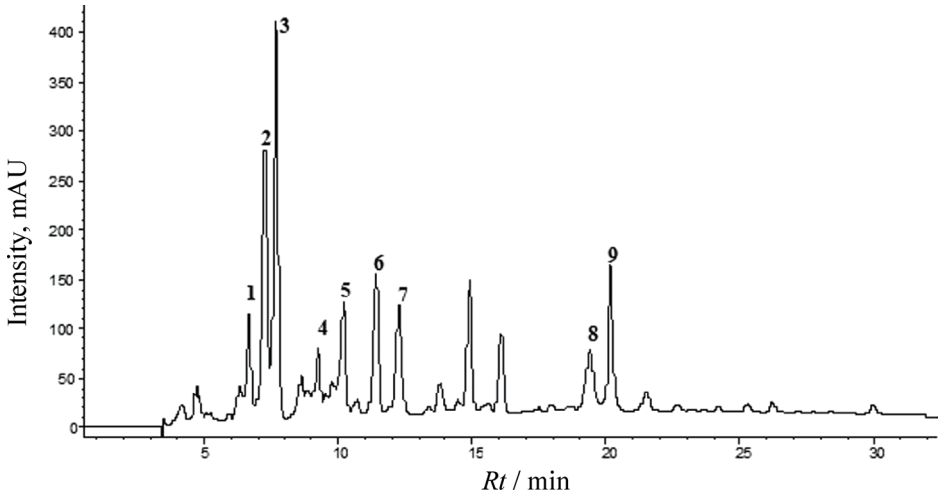

Fig. 2. HPLC profile of the EtOAc fraction at pH 2.0: *cis*-caftaric acid (1), gentisic acid (2), *trans*-caftaric acid (3), *trans*-fertaric acid (4), coutaric acid (5), caffeic acid (6), *cis*-fertaric acid (**7**), quercetin 3-*O*-glucuronide (8) and ellagic acid (9).

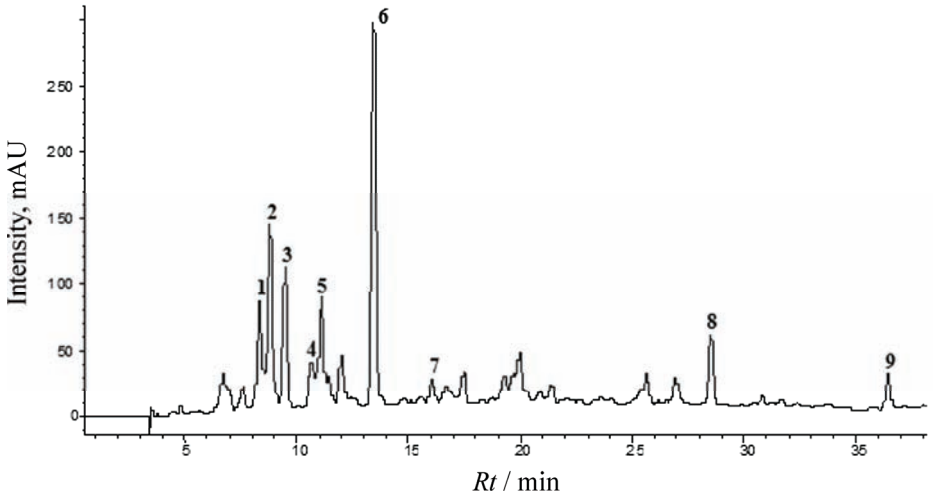

Fig. 3. HPLC profile of the EtOAc fraction at pH 7.0: catechin (1), proanthocyanidin dimer (2), epicatechin (3), proanthocyanidin dimer (4), protocatechuic acid (5), ethyl gallate (6), proanthocyanidin dimer (7), ethyl caffeate (8) and quercetin (9).

Radical scavenging activity of the Prokupac wine fractions

Although wines contain various phenolics, and their antioxidant activities could be connected with a synergy of these compounds, it is important to determine which group of phenolic compounds has most influence on the radical scavenging properties of wines. The fractions obtained in the present study were

subjected to a radical scavenging activity assay employing the stable DPPH radical widely used to characterize the radical scavenging activity of a variety of natural polyphenols. The measurement of the consumption of the DPPH radical allowed the exclusive determination of the intrinsic ability of a substance to donate hydrogen atoms or electrons to this reactive species in a homogeneous system. The method is based on the reduction of an alcoholic DPPH· solution in the presence of a hydrogen-donating antioxidant due to the formation of the non-radical form DPPH–H.[26] In this study, both organic fractions demonstrated effective scavenging activity against DPPH radicals (Table I). The order of scavenging activity was: EtOAc fraction at pH 7.0 > EtOAc fraction at pH 2.0 > aqueous fraction. The fractions that contained higher levels of total phenolics showed better radical scavenging activity. A negative, but insignificant, correlation between the total polyphenol content in the examined fractions and the DPPH IC_{50} values was found. Radovanović *et al.*[27] analyzed wines produced from three autochthonous grape cultivars, *i.e.*, Vranac, Kratošija and Prokupac, and showed that all samples possessed antioxidant activity. Atanacković *et al.*[17] also showed that the Prokupac wine they analyzed exhibited antioxidant potential. The present results and those previously published showed that Serbian red wines produced from the indigenous variety Prokupac may serve as a good source of potential antioxidant agents.

Several authors have described significant and positive correlations between the total polyphenol levels of wines and their antioxidant activities evaluated by DPPH.[5,28,29] In contrast, other studies have shown a lack of the aforementioned correlation and even some negative correlation was found, thus indicating that wines having the highest contents of total polyphenols did not always show the highest values for antioxidant activity.[30] It was suggested that the antioxidant activity of wine is more related to the type of the phenolic compounds present than to their total content.[31] There are disagreements regarding the main compounds that act as antioxidants. Di Majo *et al.*[32] showed high correlation between antioxidant activity and the flavonoid fraction as did Radovanović *et al.*,[1] who confirmed high correlation between the total anthocyanin content and DPPH scavenging activity of the 5 vines they tested. On the other hand, Sánchez-Moreno *et al.*[33] found poor correlations between the ability of wines to block free radicals and their anthocyanin levels (whether total or monomeric). Regarding flavonols, Brenna and Pagliarini[34] obtained good correlations between antioxidant activity and the quercetin and myricetin contents. On the contrary, Arnous *et al.*[35] found quercetin levels to be negatively correlated with antioxidant activity and suggested that quercetin might be a pro-oxidant. Fernández-Pachón *et al.*[29] studied the anti-radical ability of various polyphenol fractions in wines (phenolic acids, flavanols, anthocyanins and flavonols) and concluded that flavo-

nols play no prominent role as antioxidants. Other authors found positive correlations between the anti-radical ability of wines and their flavanol levels.[29,33–36]

The antioxidant activity of hydroxybenzoic acids basically depends on the number of hydroxyl groups in the molecule, whereas for hydroxycinnamic acids, the presence of methoxy groups seemed to positively influence their antioxidant activity.[37] Ethyl gallate as the major compound (19.7 % of total) of the most active fraction (EtOAc at pH 7.0) presents three available hydroxyl groups that could donate a hydrogen to stabilize free radicals. In contrast to anthocyanins, the content of which decreased during time, the concentration of the hydroxybenzoic acids and their derivatives increased with time.[3]

The antioxidant activity of proanthocyanidins is, in part, dictated by the oligomer chain length. Flavan-3-ol monomers and dimers were found to inhibit more efficiently LDL oxidation than trimers and tetramers.[38] In the EtOAc fraction at pH 7.0, the amounts of detected dimers and monomers were almost equal (14 and 14.1 % of the total, respectively). Several structures appear to be important for these antioxidant activities, including an 3′4′-dihydroxyl (catechol) group or 3′4′5′-trihydroxyl (gallate) group in the B ring, a gallate group esterified at the 3 position of the C ring, and hydroxyl groups at the 5 and 7 positions of the A ring.[31]

From the flavonol group, quercetin glucuronide and its corresponding aglycon, released by hydrolysis in wine, were detected in the EtOAc fraction at pH 2 and the EtOAc fraction at pH 7.0, respectively. Besides five hydroxyl groups, quercetin also contains a 2,3-double bond in its C ring and a 4-oxo function. This structure enhances the total antioxidant activity of quercetin towards free radicals by allowing electron delocalization across the molecule.[37]

According to the obtained results, non-anthocyanin polyphenols, mainly flavan-3-ols, ethyl gallate and quercetin that dominates in the most active fraction (EtOAc at pH 7.0), could be considered as the main phenolic compounds responsible for radical scavenging activity of Prokupac wine. This is consistent with a study of Rice-Evans *et al.*,[31] in which anthocyanins, such as malvidin 3-glucoside, were found to be less effective as antioxidants than non-anthocyanin components, such as gallic acid, catechin and quercetin. Moreover, Arnous *et al.*[40] affirmed that catechin, epicatechin and proanthocyanidins are the compounds that mostly contribute to the antioxidant activity of wines.

CONCLUSIONS

The phenolic composition of different fractions obtained from wine produced from the Serbian autochthonous grape variety Prokupac was reported for the first time. Twenty-eight phenolic compounds belonging to five different classes (anthocyanins, flavonols, flavan-3-ols, hydroxycinnamic acids and hydroxybenzoic acids) were characterized. Anthocyanins dominated in the aqueous frac-

tion while other classes of compounds were separated in the organic fractions. Non-anthocyanin phenolics were indicated as the key compounds responsible for the radical scavenging activity of Prokupac wine. It is important to bear in mind that the polyphenols identified in this study represent a proportion of the total polyphenols of Prokupac wine, indicating that other non-identified compounds could contribute in a significant manner to the antioxidant activity. In addition, besides polyphenols, many other bioactive compounds, such as vitamins and minerals.[40] could also be connected with the free radical scavenging capacity of red wines generally.

Acknowledgement. The authors acknowledge their gratitude to the Ministry of Education, Science and Technological Development of the Republic of Serbia for financial support, Project No. 46013.

И З В О Д

ФЕНОЛНИ САСТАВ И СПОСОБНОСТ ХВАТАЊА СЛОБОДНИХ РАДИКАЛА ФРАКЦИЈА РАЗДВОЈЕНИХ ИЗ ЦРНОГ ВИНА ПРОИЗВЕДЕНОГ ОД СРПСКЕ АУТОХТОНЕ СОРТЕ ГРОЖЂА ПРОКУПАЦ

НЕБОЈША МЕНКОВИЋ[1], ЈЕЛЕНА ЖИВКОВИЋ[1], КАТАРИНА ШАВИКИН[1], ДЕЈАН ГОЂЕВАЦ[2] и ГОРДАНА ЗДУНИЋ[1]

[1]*Институт за проучавање лековитог биља "Др Јосиф Панчић", Тадеуша Кошћушка 1, 11000 Београд, и* [2]*Институт за хемију, технологију и металургију, Његошева 12, 11000 Београд*

Садржај фенолних једињења је веома значајан параметар квалитета вина због утицаја ових једињења на боју, укус и лековита својства. Циљ овог рада је одређивање фенолног састава и способности хватања слободних радикала водене и органских фракција добијених применом течно–течне екстракције из црвеног вина произведеног од српске аутохтоне сорте грожђа Прокупац. Садржај укупних фенола у испитиваним фракцијама износио је од 48,22 до 289,12 mg GAE g^{-1} суве фракције. Фенолне киселине (углавном хидроксициметне киселине) и кверцетин-3-глукуронид главне су компоненте етилацетатне фракције при pH 2,0; катехини, фенолне киселине (углавном хидроксибензоеве) и кверцетин нађени су у етилацетатној фракцији при pH 7,0, док су антоцијани идентификовани у воденом остатку након екстракције етилацетатом. Главни антоцијан водене фракције је малвидин-3-глукозид, док су најзаступљенија неантоцијанска фенолна једињења органских фракција етил-галат и *trans*-кафтарна киселина. Способност хватања слободних радикала значајно се разликовала међу фракцијама па је IC_{50} вредност за водену фракцију износила је 138,58 μg mL^{-1}, док су за етилацетатне фракције при pH 2,0 и 7,0 ове вредности износиле 17,83 и 3,47 μg mL^{-1}, редом. Показано је да су етилацетатне фракције снажнији хватачи слободних радикала, па се може претпоставити да су неантоцијанска фенолна једињења одговорна за ову активност испитиваног вина.

(Примљено 11. маја, ревидирано 6. јула 2013)

REFERENCES

1. A. Radovanović, B. Radovanović, B. Jovančićević, *Food Chem.* **117** (2009) 326

2. V. Ivanova, A. Dörnyei, L. Márk, B. Vojnoski, T. Stafilov, M. Stefova, F. Kilár, *Food Chem*. **124** (2011) 316
3. D. Granato, F. C. U. Katayama, I. A: Castro, *LWT-Food Sci. Technol*. **43** (2010) 1542
4. S. Pérez-Magariño, M. L. González-San José, *Food Chem*. **96** (2006) 197
5. C. Sánchez-Moreno, J. A. Larrauri, F. Saura-Calixto, *J. Sci. Food Agric*. **79** (1999) 1301
6. M. V. Martínez-Ortega, M. C. García-Parrilla, A. M. Troncoso, *Food Chem*. **73** (2011) 11
7. O. I. Aroma, *J. Am. Oil Chem. Soc*. **75** (1998) 199
8. G. C. Tenore, J. Troisi, R. Di Fiore, M. Manfra, E. Novellino, *Food Chem*. **129** (2011) 792
9. S. Dragland, H. Senoo, K. Wake, K. Holte, R. Blomhoff, *J. Nutr*. **20** (2003) 1286
10. J. Yang, T. E. Martinson, R. H. Liu, *Food Chem*. **116** (2009) 332
11. M. De Nisco, M. Manfra, A. Bolognese, A. Sofo, A. Scopa, G. C. Tenore, F. Pagano, C. Millite, M. T. Russo, *Food Chem*. **140** (2013) 623
12. B. Sun, A. C. Neves, T. A. Fernandes, A. L. Fernandes, N. Mateus, V. De Freitas, C. Leandro, M. I. Spranger, *J. Agric. Food Chem*. **59** (2011) 6550
13. A. Ghiselli, M. Nardini, A. Baldi, C. Scaccini, *J. Agric. Food Chem.* **46** (1998) 361
14. P. Waterman, S. Mole, *Analysis of Phenolic Plant Metabolites*, Blackwell Scientific Publication, Oxford, 1994, p. 16
15. International Organisation of Vine and Wine, *OIV Compendium of International Methods of Analysis of Wine and Must*, Office International de la Vigne et du Vin, Paris, 2013
16. M. Cuendet, K. Hostettmann, O. Potterat, W. Dyatmiko, *Helv. Chim. Acta* **80** (1997) 1144
17. M. Atanacković, A. Petrović, S. Jović, L. G. Bukarica, M. Bursać, J. Cvejić, *Food Chem.* **131** (2012) 513
18. M. Fanzone, F. Zamora, V. Jofré, M. Assof, C. Gómez-Cordovés, A. Peña-Neira, *J. Sci. Food Agric*. **92** (2012) 704
19. F. He, N. N. Liang, L. Mu, Q. H. Pan, J. Wang, M. J. Reeves, C. Q. Duan, *Molecules* **17** (2012) 1571
20. R. Cristino, E. Costa, F. Cosme, A. M. Jordao, *J. Sci. Food Agric*. **93** (2013) 2486
21. V. Ivanova, V. Stefova, *Fruit and Cereal Bioactivities: Sources, Chemistry and Applications*, CRC Press, Boca Raton, FL, 2011, p. 172
22. M. Mitić, J. M. Souquet, M. Obradović, S. Mitić, *Food Sci. Biotechnol*. **21** (2012) 1619
23. I. Revilla, S. Pérez-Magariño, M. L. González-SanJosé, S. Beltrán, *J. Chromatogr., A* **847** (1999) 83
24. A. Soriano, P. M. Pérez-Juan, A. Vicario, J. M. González, M. S. Pérez-Coello, *Food Chem*. **104** (2007) 1295
25. A. Basli, S. Soulet, N. Chaher, J. M. Mérillon, M. Chibane, J. P. Monti, T. Richard, *Oxid. Med. Cell. Longev*. **2012** (2012) Article ID 805762
26. N. Paixão, R. Perestrelo, J. C. Marques, J. S. Câmara, *Food Chem*. **105** (2007) 204
27. B. Radovanović, A. Radovanović, V. Tomić, *Int. J. Food Prop*. **15** (2012) 725
28. N. Landrault, P. Poucheret, P. Ravel, F. Gasc, G. Cros, P. L. Teissedre, *J. Agric. Food Chem*. **49** (2001) 3341
29. M. S. Fernández-Pachón, D. Villaño, M. C. García-Parrilla, A. M. Troncoso, *Anal. Chim. Acta* **513** (2004) 113
30. M. D. Rivero-Pérez, P. Muñiz, M. L. González-SanJosé, *J. Agric. Food Chem*. **55** (2007) 5476
31. C. A. Rice-Evans, N. J. Miller, *Biochem. Soc. Trans*. **24** (1996) 790

32. D. Di Majo, M. La Guardia, S. Giammanco, L. La Neve, M. Giammanco, *Food Chem.* **111** (2008) 45
33. C. Sánchez-Moreno, G. Cao, B. Ou, R. Prior, *J. Agric. Food Chem.* **51** (2003) 4889
34. O. V. Brenna, E. Pagliarini, *J. Agric. Food Chem.* **49** (2001) 4841
35. A. Arnous, D. P. Makris, P. Kefalas, *J. Agric. Food Chem.* **49** (2001) 5736
36. F. Cimino, V. Sulfaro, D. Trombetta, A. Saija, A. Tomano, *Food Chem.* **103** (2007) 75
37. D. Granato, F. C. U. Katayama, I. A. De Castro, *Food Chem.* **129** (2011) 366
38. E. F. Gris, F. Mattivi, E. A. Ferreira, U. Vrhovsek, R. C. Pedrosa, M. T. Bordignon-Luiz, *Food Chem.* **126** (2011) 213
39. A. Arnous, D. P. Makris, P. Kefalas, *J. Food Comp. Anal.* **15** (2002) 655
40. P. Zafrilla, J. Marillas, J. Mulero, J. M. Cayuela, A. Martínez-Cachá, F. Parda, J. M. L. Nicolás, *J. Agric. Food Chem.* **51** (2003) 4694.

Journal of the Serbian Chemical Society
JSCS-info@shd.org.rs • www.shd.org.rs/JSCS
J. Serb. Chem. Soc. *79* (1) 25–38 (2014)
JSCS–4562
UDC 547.261+534–8:544.77.022.004.74
Original scientific paper

Application of ultrasound and methanol for the rapid removal of surfactant from MCM-41 molecular sieve

MOHAMMAD A. ZANJANCHI and SHAGHAYEGH JABARIYAN*

Department of Chemistry, Faculty of Science, University of Guilan, P. O. Box 1914, Rasht 41335, Iran

(Received 12 January 2013, revised 12 April 2013)

Abstract: Ultrasound waves were successfully applied for the removal of the template from mesoporous MCM-41 molecular sieve. The method uses 28 KHz ultrasound irradiation in a methanol solvent for disrupting the micellar aggregation of the surfactant molecules, cetyltrimethylammonium bromide, which fill the pores of as-synthesized MCM-41. After 15 min sonication at the moderate temperature of 40 °C, the majority of surfactant molecules had been removed from powder MCM-41. The template removal rate using ultrasound irradiation (15 min) is faster than the rate obtained *via* thermal calcination. In addition, a perfect hexagonal pore structure was obtained after template removal using ultrasound irradiation, according to characterization using X-ray diffraction (XRD) and nitrogen adsorption analyses, while high temperatures during calcination cause shrinkage that affected the surface properties of the materials. In the present procedure, the surfactant molecules are released into methanol and can be recovered for reuse. The effectiveness of the sonication-prepared MCM-41 as an adsorbent was confirmed by the adsorption of methylene blue (MB).

Keywords: ultrasound; methanol; mesoporous; MCM-41; template removal; micelle.

INTRODUCTION

During the past decade, the study of the physical and chemical effects of ultrasound irradiation is a rapidly growing area of research.[1–3] Ultrasound is the name given to sound waves having frequencies higher than those to which the human ear can respond (16 kHz). The use of ultrasound may be divided broadly into two areas: *i*) high frequency ultrasound (2–10 MHz), and *ii*) low frequency ultrasound (20–100 kHz). Over the last few years, the principal application of ultrasound was in synthesis (organic, organometallic and inorganic), polymer chemistry (degradation, initiation, and copolymerization) and some aspects of

* Corresponding author. E-mail: shaghayeghjabariyan@yahoo.com
doi: 10.2298/JSC130112056A

catalysis. This field of scientific research that uses ultrasound is called sono-chemistry.[4]

Ultrasound waves consist of a cyclic succession of expansion and compression phases imparted by mechanical vibration. The expansion cycles exert a negative pressure and pull the molecules apart, while the compression cycles exert a positive pressure and push the liquid molecules together. When cyclic stress through repeated implosion exceeds the tensile strength of a liquid in the rarefaction regions, small vapor-filled voids, called cavitation bubbles, are formed. The compression of the bubbles during cavitation is more rapid than thermal transport, which generates a short-lived localized hot-spot. Experimental results have shown that hot-spots with high local temperatures of around 5000 K, pressures of roughly 1000 atm*, and combined with heating and extraordinarily rapid cooling rates of above 10^{10} K s^{-1} provide a unique means for driving chemical reactions under extreme conditions.[5–8]

In sonochemical reactions, the ultrasonic energy influences the chemical reactions by providing huge heat (pyrolysis) or producing reactive free radicals. There are mainly three reaction sites (Fig. 1): a) cavity interior, b) gas–liquid interface and c) bulk liquid. Inside the cavitation bubble, water molecules are pyrolyzed forming •OH and •H in the gas phase. The substrate either reacts with

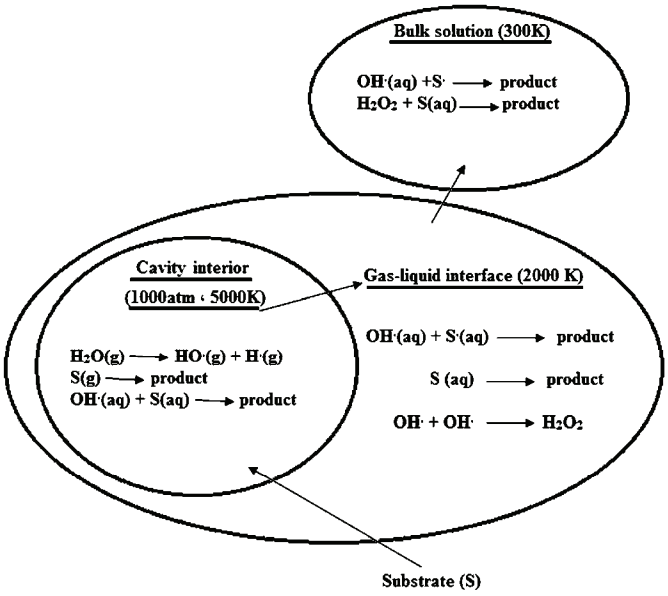

Fig. 1. Sonochemical reaction zones.[7]

the hydroxyl radical or undergoes pyrolysis. In the interfacial region, a similar

* 1 atm = 101325 Pa

reaction occurs but in an aqueous phase. The additional reaction is the recombination of the OH radicals to form H_2O_2. In the bulk phase, the reactions are between the substrate and the $^{\bullet}OH$ or H_2O_2. All these reactions are considered homogeneous in sonochemistry.[7]

MCM-41, one of the members of the extended family of mesoporous sieves, possesses a hexagonal array of uniform mesopores. MCM-41 was discovered in 1992 by researchers at Mobil. In addition, it has been synthesized with uniform channels varying from approximately 15 Å to greater than 100 Å in size. Thus, it has potential applications in the field of adsorption and catalysis.[9–11]

Although the synthesis of MCM-41 is possible *via* a number of methods, generally it is synthesized from the surfactant micellar template addition of an inorganic silica source, with cetyltrimethylammonium bromide (CTA^+Br^-) being the most commonly used template.[12,13]

In order to make the porous network accessible in such systems, the template has to be removed from the mesoporous channels inside the particles. The most common method used in laboratories to remove the template is calcination at high temperatures.[14–16] Although all organic templates are removed from the structure using this method, high temperatures cause shrinkage, which affects the surface and the catalytic and adsorption properties of the materials. For this reason, methods and other conditions should be used for template removal.

Extraction with conventional solvent is another method for template removal.[17,18] The efficiency of solvent extraction methods depends on the interaction between organic molecules and inorganic framework. For mesoporous materials that are synthesized by the S+X–I+ and S0I0 way, the interaction between the organic phase and the inorganic network is weak. Therefore, the surfactant molecules in the pores of mesoporous materials can be removed by extraction with ethanol.[19] Since solvent extraction methods due to the strong electrostatic interactions between the surfactant and a network of micelle cannot be applied to ordered mesoporous materials prepared in the alkaline environment (S+I-way), ion exchange is widely used under this condition. In recent years, many different solutions, such as HCl,[17,20] H_2SO_4[18] and NH_4NO_3[21] in ethanol solvent were used for the removal of surfactant. Although structural damage is minimized in the solvent extraction method, several extraction steps are required to remove the organic template completely and thus, large amounts of solvent and lots of extraction time are required.

Additionally, oxidation methods were used for template removal. In these methods, several oxidizing agents, such as $KMnO_4$,[22] UV–ozone or ozone,[23–25] perchlorates,[26] H_2O_2 and H_2O_2–UV/Fe[27,28] have been used. Although template removal by these methods is fast, the surfactant is oxidized and degraded, and hence cannot be recovered. Microwave,[29,30] plasma[31,32] and supercritical fluid

extraction[33,34] are other techniques to remove templates, but complex devices are required.

Furthermore, in 2012, a new method for the removal of the surfactant from the pores of mesoporous materials employing ultrasonic irradiation in ethanolic solution was presented.[35]

However, a method for template removal should have the following properties: efficient removal of the template, short operation time, reduced organic solvent consumption, regular (well-organized or systematic) structure retention and the possibility for surfactant recovery

In this work, methanol as solvent in the presence of ultrasonic waves was used to remove the template and the effect of ultrasonic wave and methanol solvent on the structure of MCM-41 were investigated. Additionally, the obtained results were compared with those of a calcined sample. The results indicated that the samples kept their porous structures and structural shrinkage was minimized. Moreover, the surface area and pore volume of the samples were higher than those for the calcined samples were. Thus, methanol as solvent in the presence of ultrasonic waves functioned effectively.

EXPERIMENTAL

Preparation of hexagonal mesoporous silica

The surfactant-templated MCM-41 was synthesized by a familiar room temperature method.[35,36]

Template removal using ultrasound waves

The ultrasound-assisted template removal was performed in a 7500S ultrasonic device (Sairan Instrument Company, Iran) with an ultrasound power of 600 W, heating power of 800 W and a frequency of 28 kHz, equipped with a timer and a temperature controller. In general, 0.5 g of MCM-41 was dispersed in 75 mL of methanol in a beaker. Then, the suspension was immersed in water in the ultrasonic device and irradiated for 15 min at 40 °C. A mechanical stirrer at a speed of 300 rpm was used during the treatment. After ultrasonic irradiation, the sample was recovered by centrifugation, washed with cold methanol and dried at 60 °C for 6 h [MCM-41(US1)]. For certain samples, this procedure was repeated for two more successive steps [MCM-41(US2)].

Template removal using thermal calcination

For comparison, the template was also removed by thermal calcination. The fresh sample was heated under air at 550 °C and held for 5 h (MCM-41(C-550)). Then the sample was cooled to room temperature. The total time for the complete removal was 12.4 h.

Characterization of the as-synthesized, calcined and sonicated powders and the supernatant solutions

A Philips PW1840 diffractometer with CuK_α radiation was used to record the powder XRD patterns of the MCM-41 samples within a 2θ range of 1–10°. The XRD patterns were recorded using an automatic divergence slit system. Thermogravimetric analysis (TGA) was performed on a TGA 1500 instrument (Polymer Laboratories) to estimate the residual amount of the template in the MCM-41 samples after sonochemical treatment. The measurements

were performed under static air from room temperature to 600 °C at a heating rate of 10 °C min^{-1}. In addition, the concentration of CTAB in the supernatant solution was determined by using a double-beam UV spectrophotometer at 375 nm and in the presence of 0.02 mL of 0.1 % picric acid in 0.002 M NaOH and 10 mL of chloroform per 1.0 mL of the supernatant.[37] The specific surface areas of the sonicated and calcined MCM-41 samples were estimated based on the data provided by a Sibata surface area apparatus 1100. The sample was degassed at 250 °C for 2 h prior to nitrogen physisorption measurements. The FTIR spectra of the bare MCM--41 and the treated MCM-41 samples were obtained using a Shimadzu FTIR-8900 spectrophotometer.

Adsorption test

Methylene blue (MB) solutions were prepared from a commercially available product (Merck, 1.59270) dissolved in distilled water. For the adsorption experiments, 100 mg of the as-synthesized MCM-41 or any of the sonicated MCM-41 samples were added into 100 mL of MB solutions at a concentration of 25 ppm and pH of 5.5. The solution was stirred for about 30 min for the sorption process to reach equilibrium.

The solution and the solid phase were separated by centrifugation. A Shimadzu UV-2100 spectrophotometer was employed for measuring the MB concentration.

RESULTS AND DISCUSSION

Structural characterization

The XRD diffraction patterns of the as-prepared, sonicated and calcined MCM-41 materials are shown in Fig. 2. Three peaks were observed in all cases.

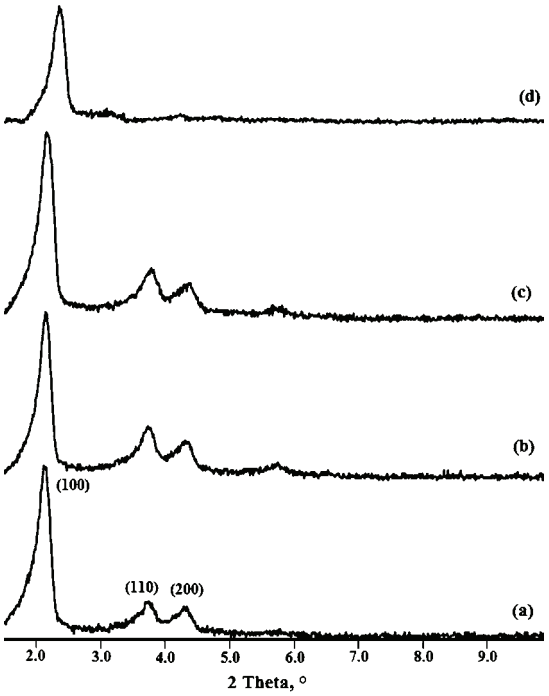

Fig. 2. Low-angle XRD patterns for the MCM-41 samples: a) MCM-41, b) MCM-41 (US1), c) MCM-41 (US2) and d) MCM-41 (C-550).

The first peak was detected at around 2θ = 2.150° and the two small intensity peaks were detected at 2θ 3.73 and 4.73°. These diffraction peaks were indexed as the 2D hexagonal arrangement with the reflection of (100), (110) and (200).[38] The structural parameter (d-spacing) calculated from the diffraction angles is given in Table I. The XRD patterns showed that ordered mesoporous structures were preserved in all the sonicated samples. However, the weaker reflections corresponding to the planes (110) and (200) could hardly be seen in the pattern of the calcined MCM-41(C-550) sample. The frequent disappearance of these weak reflections was assigned to disordering of the array of meso channels of MCM-41 samples subjected to a calcination step.[39] The small shift of the main diffraction peak toward a higher 2θ value for MCM-41 (C-550) was due to shrinkage of the sample that occurred because of the template removal by calcinations.[40]

TABLE I. Comparison of the physicochemical properties of porous materials treated by ultrasound waves and thermal calcinations; S_{BET}: apparent surface area calculated by the BET method; V_m: pore volume; d_{100}: LA-XRD spacing of the 100 reflection of a hexagonal plane array of pores; L: crystallite size calculated by the Sherrer equation (L = = $k\lambda/\beta\cos\theta$); a_0: cell constant, $a_0 = 2d_{100}/\sqrt{3}$; W_d: pore size

Sample	S_{BET} / $m^2.g^{-1}$	V_m /$cm^3.g^{-1}$	2θ / °	d_{100} / Å	L / nm	a_0 / Å	W_d / Å
MCM-41 (1)	811	0.288	2.140	41.29	38.1	47.7	29.70
MCM-41 (US1)	1215	0.432	2.145	41.54	37.7	47.9	37.60
MCM-41 (US2)	1320	0.470	2.145	41.54	37.6	47.9	38.40
MCM-41 (C-550)	1276	0.454	2.205	40.07	37.3	46.3	33.41

The degree of template removal was verified by BET analysis based on physisorption of nitrogen and calculation of the specific surface area of the sonicated samples. Table I shows the results of the sonication in methanol solvent at 40 °C and for 15 min and thermal calcination for the removal of CTAB template from the pores of MCM-41. The table also contains the results of the treatment of MCM-41 by stirring in methanol at 40 °C in the absence of ultrasound irradiation (MCM-41 (1)). It is evident from Table I that stirring of MCM-41 in methanol solutions without sonication led to the partial removal of template from the pores of MCM-41, as indicated by the resulting pore volume and surface area. However, using ultrasound irradiation for the treatment of MCM-41 in methanol at the same temperature (40 °C) for the same time (15 min), a greater increase in the surface area and pore volume resulted. In fact, the calculated specific surface area for MCM-41 (1) of 811 m^2 g^{-1} increased to 1215 m^2 g^{-1} for MCM-41 (US1) due to the ultrasound irradiation.

Repeating the sonication under the same conditions affected the value of the surface area. Table I shows that the calculated surface area for MCM-41 (US1) was 1215 m^2 g^{-1}, which increased to 1320 m^2 g^{-1} for MCM-41 (US2) that had undergone a second 15 min sonication step. These samples were studied further

by thermogravimetric analysis (discussed later) and it was found that the amount of template remaining in the structure following 15 min sonication were very small. Therefore, at this stage it is obvious that although template removal from MCM-41 is feasible by the treatment with alcohols, such as methanol, application of ultrasound irradiation greatly increased the speed and the efficiency of the removal.[36] The specific surface area for MCM-41 (C-550), prepared by thermal treatment at 550 °C of the as-synthesized MCM- 41 was 1276 m^2 g^{-1}. The values of the surface areas for the sonicated MCM-41 samples (around 1200 m^2 g^{-1} or higher) were comparable with that of the thermally treated sample (1276 m^2 g^{-1}). This proximity is an indication that the employed sonication procedure was successful in the removal of the template from MCM-41.

The FTIR absorbance spectra of the as-prepared and sonicated MCM-41 materials are shown in Fig. 3. A broad band around 3200–3500 cm^{-1} appears for all samples, which is partially caused by the O–H stretching vibration mode of

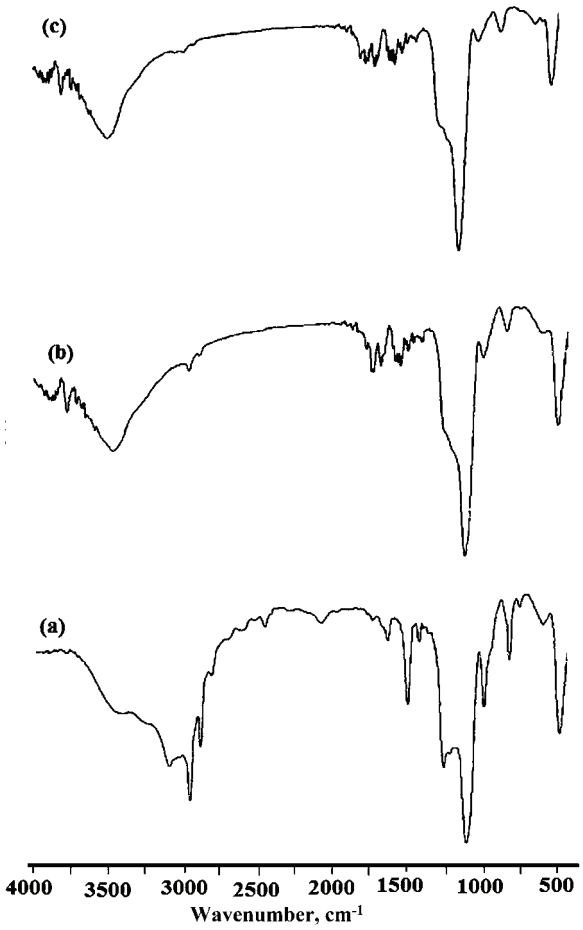

Fig. 3. FTIR spectra of the MCM--41 samples: a) MCM-41, b) MCM--41 (US1) and c) MCM-41 (US2).

adsorbed water molecules, the bending vibration mode of which is responsible for the band recorded at 1630 cm^{-1}. The absorption bands at around 2858–2925 cm^{-1} and 1375–1475 cm^{-1} observed in the spectrum of the as-prepared MCM-41 could be assigned to C–H stretching and bending vibrations of the template CTAB.[41] After treatment (sonication), the C–H vibration peaks are nearly indiscernible. This suggests the efficient removal of the surfactant template by the sonication methods. These bands were absent in the FTIR spectrum of MCM-41 (C-500) because of the complete removal of the template from MCM-41 by calcination.

Thermogravimetric analysis was employed to determine quantitatively the degree of surfactant removal from the sonicated MCM-41 materials. The thermograms for the as-synthesized MCM-41 and for those sonicated at 40 °C in methanol for 15 min and for two consecutive 15-min periods are shown in Fig. 4. The thermograms were recorded from 20 to 600 °C. In the temperature range up to 150 °C, physisorbed water was released from the pores. From 150 °C to about 340 °C, the remaining template was successfully decomposed. At temperatures above 340 °C, the weight loss could be attributed to water released from silanol condensation and to the oxidation of a small amount of carbonaceous residues from incomplete template combustion. The amount of template could therefore be estimated from the weight loss between 150 and 340 °C.[15] These amounts were approximately 57, 7 and 1 % for MCM-41, MCM-41 (US1) and MCM-41 (US2), respectively. These data show that most of the template molecules had been released from MCM-41.

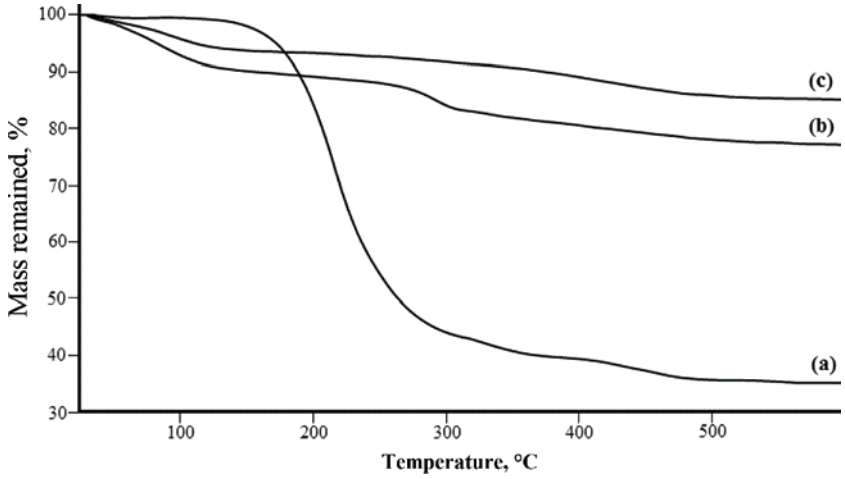

Fig. 4. TGA curves of the samples before and after template removal: a) MCM-41, b) MCM-41 (US1) and c) MCM-41 (US2).

Mechanism of cationic surfactant extraction from the pores of MCM-41

The data in Table I revealed that ultrasound irradiation played essential roles in the removal of the template from the pores of MCM-41. It was already established that organic solvents such as methanol or ethanol cause disruption of the surfactant aggregates.[42,43] Due to this disintegration, the surfactant monomers are released into the organic solvent and can be eluted. It is known that the critical micelle concentration (cmc) for CTAB in methanol is much higher than that in water. Therefore, the micelles of CTAB that were formed during the synthesis process of MCM-41 in aqueous media can be disrupted by treating MCM-41 in methanol. The ultrasound irradiation makes the disruption faster and more efficient *via* a synergistic effect.[36]

The role of ultrasound in the disintegration of the micelles could be attributed to the shear forces generated by bubble implosion during ultrasound irradiation. There are several reports to describe this role of ultrasound and consequent forces in the disruption or segregation of the micelles.[44–46] During sonication, bubble implosion occurs, which results in liquid jets of high velocity forming shear forces. The shear forces break the integrity of the micelles and convert them to free surfactant molecules.

In addition, it should be taken into account that upon ultrasound irradiation, degradation of the surfactant molecules may also occur. From the previous studies, it could be learnt that only surfactant monomers are susceptible to degradation by a sonochemical process and their presence as micelles would shield them from the irradiation.[47,48] In fact, the hydrophobic tail of the surfactant cannot be directly exposed to a bubble ‘‘hot spot’’ when it is pointed into the core of the micelle. Therefore, provided that the ultrasound irradiation causes only micelle disruption, the intact template could be recovered at the end of the template removal procedure.

Investigation of the effects of sonication on the surfactant structure by UV and FTIR spectroscopy

Due to decomposition of surfactant monomers during sonochemistry processes, the possibility of destruction of surfactant molecules by ultrasound irradiation should be considered. Ultrasonic irradiation was applied to disturb order in the micelles so surfactant molecules in the micelles de-aggregate. In order to obtain useful information about the structural integrity of the surfactant molecules that were removed from MCM-41 and transferred into the methanol solvent, further studies are required. The FTIR spectrum of the supernatant solution after treatment in the presence of ultrasound could be useful.

The FTIR spectrum of the supernatant after 15 min sonication of MCM-41 (US1) is shown in Fig. 5b. For the sake of comparison, the spectrum of a methanolic solution of pure CTAB containing approximately the same amount of

CTAB is presented in Fig. 5a. The two bands at 2891 and 2974 cm^{-1} correspond to C–H vibrations of the surfactant molecules in methanol. On comparing the FTIR spectra, it is readily observable that the C–H stretching vibration bands do not significantly change. This shows that the CTAB molecules had preserved their structure after sonication in methanol. However, these results are based on FTIR spectroscopy (qualitative analysis); hence, a more comprehensive study and quantitative analysis are required.

To obtain the necessary information about the structure and composition of the surfactant and determine the amount of surfactant present in the supernatant solutions after exposure of samples to ultrasonic waves, a special spectrophotometric method was used. In this method, the solutions remaining from MCM-41 samples that had been irradiated by ultrasound waves for 2, 4, 6, 8, 10 and 12 min at 40 °C in methanol were studied spectrophotometrically.

After ultrasound irradiation, the micelles in the methanol environment disrupted slowly and consequently by adding picric acid, ion pairs were formed with the monomers of surfactant and the ion pairs transferred from the aqueous phase to the organic phase. The absorbance of the organic phase was read at λ_{max} = = 375 nm.

According to UV–Vis spectra (Fig. 6), it was found that the micelles in the MCM-41 structure break from each other and monomers are released into the methanol. Although the spectrum of samples MCM-41 (US2), MCM-41 (US4), MCM-41 (US6) and MCM-41 (US8) showed increases in the concentration of surfactant CTA^+ with increasing sonication time, the spectra of samples MCM-

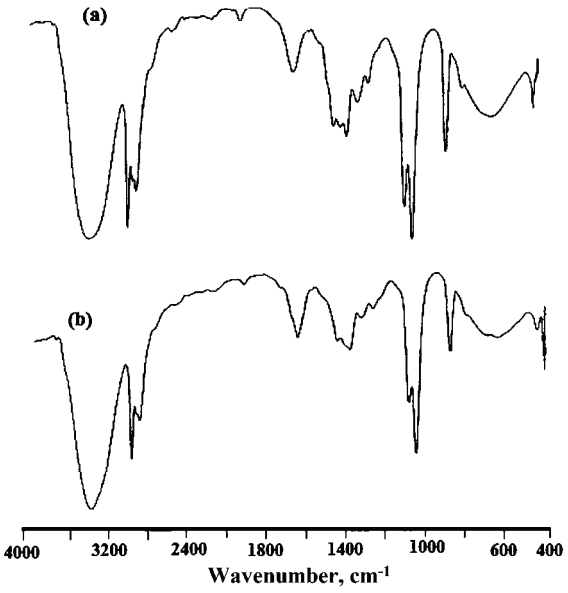

Fig. 5. FTIR spectra for a) the prepared solution of CTAB in methanol and b) the methanol supernatant after 15 min sonication of MCM-41.

-41 (US10) and MCM-41 (US12) showed gradually decreasing concentration of the surfactant. Reduction in the surfactant concentration means that degradation of surfactant molecules occurred at longer sonication times.

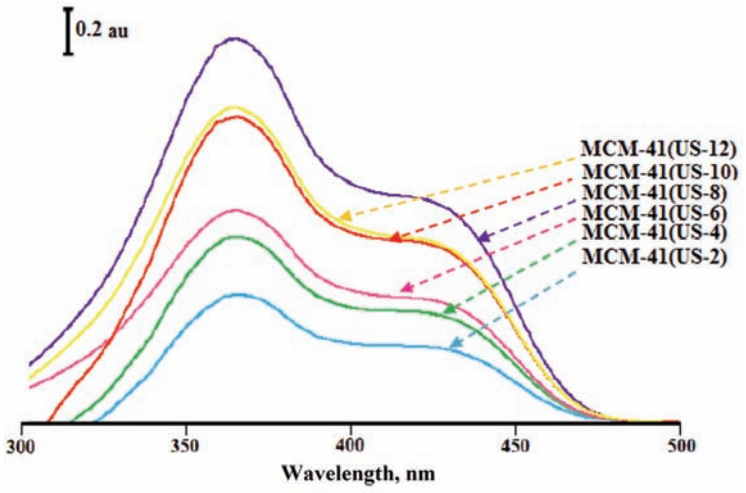

Fig. 6. UV–Vis spectra for the methanol supernatants after various times.

Thus, it can be stated that ultrasonic vibrations increase the molecular movement of the surfactant molecules away from each other following micelle disruption in a methanolic solution. Consequently, surfactant micelles are released from MCM-41 mesoporous pores into organic solvents. Since the hydrophobic tail of the organic template is pointed into the core of the micelle, they will not be damaged by the ultrasonic vibrations, which can only cause accelerated disruption of micelles in methanol solvent. When the micelles are converted to monomers, they may be attacked by hydroxyl radicals through their hydrophilic heads in bulk solution; as a result, they lose their own nature as a CTAB surfactant monomer. The alkyl chain of the surfactant may be separated from the head of the alkyl ammonium; hence, the C–H stretching vibration bands in the FTIR spectra do not change but the CTAB molecules are not identified by spectrophotometric methods.

Performance of the sonicated MCM-41 materials in MB adsorption

The as-synthesized and modified MCM-41 samples were checked for removal of MB from water. In a typical experiment, 100 mg of the adsorbent was suspended in 100 mL of water containing 25 ppm of MB and the contact time between the MB solutions and the adsorbents was 30 min. Within this period, the suspension was stirred, then filtered and the dye concentration in the solution was determined. MCM-41 (US1) showed the highest adsorption capacity, well above

that of MCM-41 (C-550) and MCM-41 (US2). While, the adsorption of MB onto the as-synthesized MCM-41 was much lower than onto sonicated MCM-41 samples (Fig. 7). These results suggest that the absence of CTA^+ inside of sonicated MCM-41 affects the sorption of MB by these adsorbents. The pH_{pzc} value of 4.1 for MCM-41 (C-550) clearly shows that at the employed experimental conditions (pH ≈5.5), the surface charge was negative and the electrostatic interaction between MB and MCM-41 (C-550) or the sonicated MCM-41 sample was very likely.

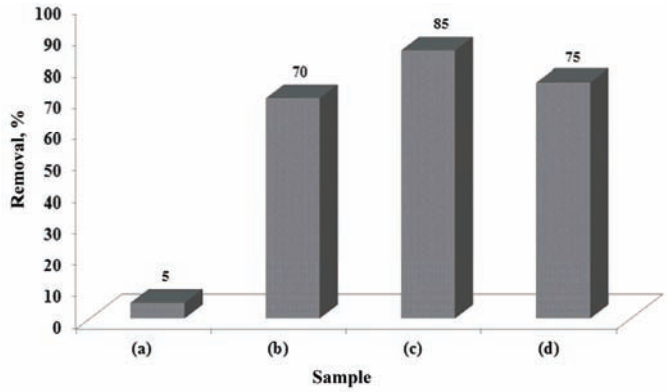

Fig. 7. MB removal by the adsorbents: a) MCM-41, b) MCM-41 (US1), c) MCM-41 (US2) and d) MCM-41 (C-550).

CONCLUSIONS

Ultrasound waves were successfully applied for CTAB removal from mesoporous MCM-41. The perfect hexagonal pore structure of MCM-41 was preserved. Sonication of a methanol solution containing the as-synthesized MCM-41 leads to disruption of the micelles that fill the pores of MCM-41. Compared to the rate of template removal using thermal calcination, the rate with the sonication method was very short (15 min). The surfactant molecules were released into methanol and could be recovered for reuse. The effectiveness of the sonicated prepared MCM-41 as an adsorbent was confirmed using the adsorption MB. In addition, no hazardous chemicals were used during sonication template removal. The sonication template removal is a fast, facile, low cost, and environmentally friendly alternative to the conventional thermal calcination method for the template removal from MCM-41.

ИЗВОД

ПРИМЕНА УЛТРАЗВУКА И МЕТАНОЛА ЗА БРЗО УКЛАЊАЊЕ СУРФАКТАНТА СА ПОВРШИНЕ MCM-41

MOHAMMAD. A. ZANJANCHI и SHAGHAYEGH. JABARIYAN

Department of Chemistry, Faculty of Science, University of Guilan, P. O. Box 1914, Rasht 41335, Iran

Ултразвучни таласи су успешно примењени за уклањање темплата са мезопорозног молекулског сита MCM-41. Примењено је ултразвучно озрачивање од 28 kHz у метанолу као растварачу да би се спречила мицеларна агрегација молекула сурфактанта, цетилтриметиламонијум-бромида, који је испуњавао поре MCM-41 приликом синтезе. Соникацијом у трајању од 15 min на умереној темеператури од 40 °C, већина молекула сурфактанта је уклоњена са праха MCM-41. Брзина уклањања темплата при ултразвучном озрачивању (15 min) је већа од брзине уклањања која се постиже калцинацијом и при том је добијена перфектно уређена хексагонална структура пора што је потврђено применом дифракције X-зрачења (XRD) и адсорпцијом азота, док загревање до високих температура резултује у скупљању пора што има утицај на површинска својства материјала. У току ове процедуре, молекули сурфактанта се ослобађају у метанол и могу се поново користити. Ефикасност на овај начин припремљеног MCM-41 као адосорбента је потврђена адсорпцијом метиленског плавог (MB).

(Примљено 12. јануара, ревидирано 12. априла 2013)

REFERENCES

1. G. J. A. Chiffoleau, T. A. Steinberg, M. Veidt, G. F. Stickley, *Ultrasonics* **39** (2001) 173
2. B. G. Pollet, *Int. J. Hydrogen Energy* **35** (2010) 11986
3. C. Yu, Q. Shu, C. Zhang, Z. Xie, Q. Fan, *J. Porous Mater*. **19** (2012) 3
4. T. J. Mason, J. P. Lorimer, *Sonochemistry*, Ellis Harwood, New York, 1988, p. 1
5. P. Chowdhury, T. Viraraghavan, *Sci. Total Environ.* **407** (2010) 2474
6. T. J Mason, *Foreword*, to *Theoretical and Experimental Sonochemistry Involving Inorganic Systems*, P. Pankaj, M. Ashokkumar, Eds., Springer, New York, 2010
7. Y. Adewuyi, *Ind. Eng. Chem. Res.* **40** (2001) 4681
8. K. S. Suslick, *Sci. Am*. **260** (1989) 80
9. Q. Huo, D. I. Margolese, U. Ciesla, P. Feng, T. E. Gier, P. Sieger, R. Leon, P. M. Petroff, F. Schüth, D. I. Stucky, *Nature* **368** (1994) 317
10. G. Øye, W. R. Glomm, T. Vralstad, S. Volden, H. Magnusson, M. Stöcker, J. Sjöblom, *Adv. Colloid Interface Sci*. **123**–**126** (2006) 17
11. J. Y. Ying, C. P. Mehnert, M. S. Wong, *Angew. Chem. Int. Ed*. **38** (1999) 56
12. M. Kruk, M. Jaroniec, A. Sayari, *J. Phys. Chem., B* **101** (1997) 583
13. M. L. Occelli, S. Biz, *J. Mol. Catal., A* **151** (2000) 225
14. M. T. J. Keene, R. D. M. Gougeon, R. Denoyel, R. K. Harris, J. Rouquerol, P. L. Llewellyn, *J. Mater. Chem*. **9** (1999) 2843
15. F. Kleitz, W. Schmidt, F. Schüth, *Microporous Mesoporous Mater*. **65** (2003) 1
16. J. Goworek, A. Kierys, R. Kusak, *Microporous Mesoporous Mater*. **98** (2007) 242
17. S. Hitz, R. Prins, *J. Catal*. **168** (1997) 194
18. W. A. Gomes, L. A. M. Cardoso, A. R. E. Gonzaga, L. G. Aguiar, H. M. C. Andrade, *Mater. Chem. Phys*. **93** (2005) 133
19. P. T. Tanev, T. Pinnavaia, *J. Chem. Mater*. **8** (1996) 2068
20. C. Y. Chen, H. X. Li, M. E. Davis, *Microporous Mater*. **2** (1993) 17

21. N. Lang, A. Tuel, *Chem. Mater*. **16** (2004) 1961
22. A. H. Lu, W. C. Li, W. Schmidt, F. Schüth, *J. Mater. Chem*, **16** (2006) 3396.
23. M. T. J. Keene, R. Denoyel, P. L. Llewellyn, *Chem. Commun*. (1998) 2303
24. E. Meretei, J. Halász, D. Méhn, Z. Kónya, T. I. Korányi, J. B. Nagy, I. Kiricsi, *J. Mol. Struct*. **651–653** (2003) 323
25. K. C. Hsu, K. J. Chao, S. F. Chen, H. K. Li, P. Y. Wu, *Thin Solid Films* **517** (2008) 686
26. H. Cai, D. Zhao, *Microporous Mesoporous Mater*. **118** (2009) 513
27. J. Kecht, T. Bein, *Microporous Mesoporous Mater*. **116** (2008) 123
28. L. Xiao, J. Li, H. Jin, R. Xu, *Microporous Mesoporous Mater*. **96** (2006) 413
29. B. Tian, X. Liu, C. Yu, F. Gao, Q. Luo, S. Xie, B. Tu, D. Zhao, *Chem. Commun*. (2002) 1186
30. T. L. Lai, Y. Y. Shu, Y. C. Lin, W. N. Chen, C. B. Wang, *Mater. Lett*. **63** (2009) 1693
31. P. Pootawang, N. Saito, O. Takai, *Thin Solid films* **519** (2011) 7030
32. Y. Liu, Y. Pan, Z. J. Wang, P. Kuai, C. Liu, *J. Catal. Commun*. **11** (2010) 551
33. Z. Huang, L. Huang, S. C. Shen, C. C. Poh, K. Hidajat, S. Kawi, S. C. Ng, *Microporous Mesoporous Mater*. **80** (2005) 157
34. Z. Huang, L. Xu, J. H. Li, S. Kawi, A. H. Goh, *Sep. Purif. Technol*. **77** (2011) 112
35. S. Jabariyan, M. A. Zanjanchi, *Ultrason. Sonochem*. **19** (2012) 1087
36. M. A. Zanjanchi, S. Asgari, *Solid State Ionics* **171** (2004) 277
37. A. Gurses, M. Yalcin, M. Sozbilir, C. Dogar, *Fuel Process. Technol*. **81** (2003) 57
38. J. S. Beck, J. C. Vartuli, W. J. Ruth, M. E. Leonowiez, C. T. Kresge, K. D. Schmitt, C. T. Chu, D. H. Olson, E. W. Sheppard, S. B. Higgins, J. B. Higgins, J. L. Schlenker, *J. Am. Chem. Soc*. **114** (1992) 10834
39. L. Huang, H. Xiao, Y. Ni, *Colloids Surf., A* **247** (2004) 247
40. M. Jaroniec, M. Kruk, H. J. Shin, R. Ryoo, Y. Sakamoto, O. Terasaki, *Microporous Mesoporous Mater*. **48** (2001) 127
41. B. Zohra, K. Aicha, S. Fatima, B. Nourredine, D. Zoubir, *Chem. Eng. J*. **136** (2008) 295
42. M. Cantero, S. Rubio, D. Pérez-Bendito, *J. Chromatogr., A* **1120** (2006) 260
43. L. Sun, C. Zhang, L. Chen, J. Liu, H. Jin, H. Xu, L. Ding, *Anal. Chim. Acta* **638** (2009) 162
44. N. Miyoshi, T. Takeshita, V. Misik, P. Riesz, *Ultrason. Sonochem*. **8** (2001) 367
45. A. Vercet, R. Oria, P. Marquina, S. Crelier, P. Lopez-Buesa, *J. Agric. Food Chem*. **50** (2002) 6165
46. A. Madadlou, M. E. Mousavi, Z. Emam-Djomeh, M. Ehsani, D. Sheehan, *Ultrason. Sonochem*. **16** (2009) 644
47. H. Destaillats, H. M. Hung, M. R. Hoffmann, *Environ. Sci. Technol*. **34** (2000) 311
48. R. Singla, F. Grieser, M. Ashokkumar, *J. Phys. Chem., A* **113** (2009) 2865.

Journal of the Serbian Chemical Society
JSCS-info@shd.org.rs • www.shd.org.rs/JSCS
J. Serb. Chem. Soc. *79* (1) 39–52 (2014)
JSCS–4563
UDC 547.532+547.532+547.78+544.6.076.32–033.5–039.26:543.55
Original scientific paper

Electrochemical behavior of lansoprazole at a multiwalled carbon nanotubes–ionic liquid modified glassy carbon electrode and its electrochemical determination

LI-HONG LIU[1,2], WEI YOU[1], XUE-MEI ZHAN[1] and ZUO-NING GAO[1]*

[1]*College of Chemistry and Chemical Engineering, Ningxia University, Yinchuan, 750021, China and* [2]*Department of Chemistry, Heihe College, Heilongjiang 164300, China*

(Received 12 December 2012, revised 3 May 2013)

Abstract: The electrochemical behavior of lansoprazole (LNS) was investigated at a glassy carbon electrode (GCE) and the GCE modified by a gel containing multiwalled carbon nanotubes (MWCNTs) and a room-temperature ionic liquid (RTIL) of 1-butyl-3-methylimidazolium hexafluorophosphate ($BMIMPF_6$) in 0.10 M phosphate buffer solution of pH 6.8. It was found that an irreversible anodic oxidation peak with an E_{pa} of 1.060 V_{SCE} appeared at the MWCNTs––RTIL/GCE. Under the optimized experimental conditions a linear calibration curve was obtained over the concentration range from 5.0 μM to 0.20 mM by differential pulse voltammetry with a limit of detection (*LOD*, *S*/*N* = 3) of 0.28 μM. In addition, the novel MWCNTs–RTIL/GCE was also characterized by electrochemical impedance spectroscopy and the proposed method was successfully applied in the quantitative electrochemical determination of LNS content in commercial tablet samples. The determination results met the determination requirements.

Keywords: lansoprazole; MWCNTs; RTIL; 1-butyl-3-methylimidazolium hexafluorophosphate; electrochemical determination.

INTRODUCTION

Lansoprazole (LNS, chemically known as (*R/S*)-2-{[3-methyl-4-(2,2,2-trifluoroethoxy)pyridin-2-yl]methylsulfinyl}-1*H*-benzo[*d*]imidazole, is a benzimidazole derivative (tradename Takepron®), the structure of which is shown in Fig. 1, which is related to omeprazole. LNS is a permanent, potent and non-reversible proton pump inhibitor that suppresses gastric acid secretion through an interaction with (H^+/K^+)-adenosine triphosphatase (ATPase) in the secretary membranes of the gastric parietal cells.[1] LNS is effective in the treatment of various peptic diseases, including duodenal ulcers, peptic ulcer, reflux esophagitis and

* Corresponding author. E-mail: gaozn@nxu.edu.cn
doi: 10.2298/JSC121216059L

Zollinger–Ellison syndrome,[2,3] and its therapeutic effect excels omeprazole.[4] Like the most compounds of this class, LNS is acid labile and reversibly transformed to sulfenamides in acidic media.[5,6] Thus it must be administrated in the form of enteric coated granules in capsules to prevent gastric decomposition and improve its systematic bioavailability.[7] Various techniques have been developed for the studies of LNS in pharmaceutical dosage forms, human serum and plasma, including spectrophotometry,[8–13] high-performance liquid chromatography with ultraviolet detection,[14–17] liquid chromatography coupled with tandem mass spectrometry (LC/MS),[18] thin-layer chromatography with fluorescence[19] or ultraviolet detection,[20] capillary electrophoresis,[21,22] flow analysis[23] and flow injection analysis.[24] In addition, a few of electrochemical techniques have been reported, including cathodic polarography,[25] adsorptive stripping square-wave voltammetry at a hanging mercury drop electrode,[26,27] anodic voltammetry[28,29] and alternating current polarography at a dropping mercury electrode.[30] However, the methods related to spectrophotometry, chromatography, capillary electrophoresis and flow analysis require time-consuming manipulation steps, expensive instruments and special training. The electrochemical methods mentioned above involving a mercury electrode have environmental pollution issues and mostly discuss only the electrochemical reduction of LNS. For these reasons, herein, a rapid, simple and accurate electrochemical method was developed using a glassy carbon electrode (GCE) modified with multi-walled carbon nanotubes (MWCNTs) and a room-temperature ionic liquid (RTIL), *i.e.*, 1-butyl-3-methylimidazolium hexafluorophosphate ($BMIMPF_6$) (MWCNTs–RTIL/GCE).

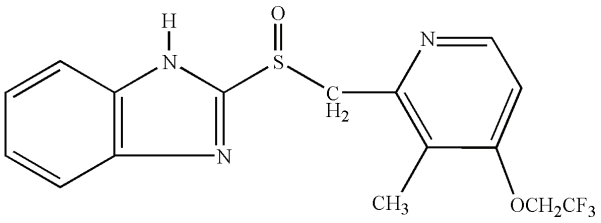

Fig. 1. Structure of lansoprazole.

Carbon nanotubes (CNTs), discovered by Lijima[31] in 1991 using transmission electron microscopy, have a special structure, and mechanical, electronic and chemical properties,[32,33] for which reasons they are widely applied in chemical, physical and materials science. When used as electrode-modifying materials, CNTs have the ability to promote charge-transfer reactions.[34–38] RTILs are compounds consisting entirely of ions that exist in the liquid state at around room temperature.[39,40] They have good chemical and physical properties, such as good chemical and thermal stability, negligible vapor pressure, high conductivity, good biocompatibility, low toxicity and a wide electrochemical window.[41–46] Accord-

ing to the literature,[47] MWCNTs are untangled after treatment with RTILs, mainly because of cross-linking of the nanotube bundles mediated by local molecular ordering of the RTIL resulting from "cation–π" interactions between imidazolium and nanotubes. At the present, the research and application of MWCNTs––RTIL modifiers have been reported. According to the above facts, a combination of MWCNTs and an RTIL could be favorable for the fabrication of modified electrode. Such electrodes could be successfully applied in the electrocatalysis of bioelectrochemical reactions, the fabrication of biosensors and the detection of the various kinds of biomolecules.[48–61]

As a continuation of previous work,[62–68] the use of MWCNTs and the ionic liquid $BMIMPF_6$, based on their synergy to form a novel composite thin-film material at a GCE, is described herein for the electrochemical determination of LNS in commercial tablet form.

EXPERIMENTAL

Apparatus

All electrochemical experiments were carried out using an Electrochemistry Workstation CHI660A (CHI Instrument, USA). A personal computer was used for data storage and processing. The working electrodes used in voltammetry experiments were a CHI104 glassy carbon electrode with 3 mm diameter and glassy carbon electrode modified by MWCNTs and room temperature ionic liquid (RTIL–MWCNTs/GCE). A platinum wire and a saturated calomel electrode (SCE) served as the auxiliary and the reference electrodes, respectively. All potentials measured and reported in this work were *versus* SCE.

Reagents

Lansoprazole (Batch No. 4090401, Purity > 99 %), was from Kangya Pharmaceutical Ltd. (Ningxia Hui Autonomous Region, China) and used without further purification. Lansoprazole tablets (batch No. 080801; labeled value of 15 mg per tablet) were from ShengFan Pharmaceutics Ltd. (Henan province, China). 1-Butyl-3-methylimidazolium hexafluorophosphate ($BMIMPF_6$, purity > 99 %) was obtained from Shanghai Chengjie Chemical Co. Ltd., China). The MWCNTs (provided by prof. Fei Wei, Chemical Engineering College of Tsinghua University, China) were functionalized to give carboxylic carbon nanotubes following a literature procedure.[69] Unless otherwise stated, a 0.10 M Na_2HPO_4–NaH_2PO_4 buffer solution (PBS) of pH 6.8 was used as the supporting electrolyte. All other chemicals were of analytical grade and used as received. All solutions were prepared in doubly distilled water and thoroughly flushed with high purity nitrogen to remove oxygen from the solutions in the electrochemical cell. All experiments were performed at room temperature.

Fabrication of modified electrodes

Before the modification, a glassy carbon electrode was polished with 0.3 μm α-Al_2O_3 slurry on the polishing micro-cloth, rinsed thoroughly with distilled water and ultrasonically successively in acetone and doubly distilled water for 10 min to remove any remaining polishing alumina. 0.50 mg mL^{-1} of homogeneous black suspension was prepared by dispersing 1 mg of functionalized MWCNTs into 2 mL of *N*,*N*-dimethyl formamide (DMF) /H_2O (1:1) aqueous solution with the aid of ultrasonic stirring for 15 min, then 12 μL of the black MWCNTs suspension was dropped directly on GCE surface with a microsyringe and the solvent was evaporated under the infrared lamp to obtain MWCNTs/GC. 12 mg of MWCNTs

mixed with 200 μL of $BMIMPF_6$ was ground for about 20 min in a mortar to give a viscous MWCNTs–RTIL gel, and then a proper amount of the gel was transferred on the cleaned electrode surface by mechanically rubbing, thus a MWCNTs–RTIL/GCE was fabricated.

The influence of the amount of the MWCNTs dispersion, from 1–15 μL, on the oxidation peak currents of LNS was examined by CV. On increasing the amount of the MWCNTs dispersion, the number of the catalytic sites for LNS oxidation increased, whereby the oxidation peak current increased gradually. When the amount of MWCNTs dispersion exceeded 15 μL, the cast film was thicker and blocked electron transfer. Due to uncompensated resistive effects or to a lowering of the charge transfer rate, the peak currents decreased. In addition, solvent evaporation required a longer waiting time. Therefore, 12 μL of MWCNTs dispersion was cast on the GCE to fabricate the MWCNTs/GCE.

The ratio of $BMIMPF_6$ to MWCNTs was optimized through observing the peak current of 50 μM of LNS in 0.10 M PBS by CV. The experimental results indicated that the peak currents of LNS remained essentially constant in the range of $BMIMPF_6$–MWCNTs ratio of 200/13 to 200/9 μL mg^{-1}. When more (or less) of the RTIL was employed, the gel for fabricating the modified electrode was not well formed. Hence a $BMIMPF_6$–MWCNTs ratio of 200/12 μL mg^{-1} was chosen as appropriate. Furthermore, the thickness of MWCNTs–RTIL modified layer was controlled by the minimum redox potential difference (ΔE_p) and the maximum peak current (I_p) of $K_3[Fe(CN)_6]$ at the modified electrode.

RESULTS AND DISCUSSION

Electrochemical impedance spectroscopy (EIS) of the bare GCE and the modified electrode

Electrochemical impedance spectroscopy can generally provide useful information on the impedance changes of the electrode surface during the fabrication process.[70,71] By using the $Fe(CN)_6^{3-/4-}$ redox couple as an electrochemical probe, the Nyquist plots of the different electrodes as shown in Fig. 2 with frequencies ranging from 1 Hz to 100 kHz were obtained. It was found from the curves in Fig. 2 that the interfacial electron transfer resistance was nearly to zero at MWCNTs/GCE, which indicated that the MWCNTs formed high electron conduction pathways between the electrode and the electrolyte.[72] At high frequencies near the origin, MWCNTs–RTIL/GCE represented an obvious smaller semicircle than that of the bare GCE and RTIL/GCE, which is related to good ionic conductivity and the least charge-transfer resistance of MWCNTs–RTIL/ /GCE. At low frequencies, MWCNTs–RTIL/GCE represented a linear tail with a maximal slope among the different electrodes, which indicated that the MWCNTs–RTIL/GCE obviously improved the diffusion of ferricyanide toward the electrode surface, as reported in the literature.[73]

Cyclic voltammetric behavior of lansoprazole

The cyclic voltammetric behavior of MWCNTs–RTIL/GCE, MWCNTs/ /GCE and the bared GCE in 0.10 mM LNS were investigated at a scanning rate of 50 mV s^{-1} in 0.10 M of PBS over the potential range of 0–1.20 V, as shown by the curves in Fig. 3. From these curves, it could be seen that a large and well-

-defined anodic peak appeared at 1.06 V at the MWCNTs–RTIL/GCE (Fig. 3a). No corresponding reduction peak was observed in the reverse scan, indicating the irreversibility of the electrochemical oxidation reaction.

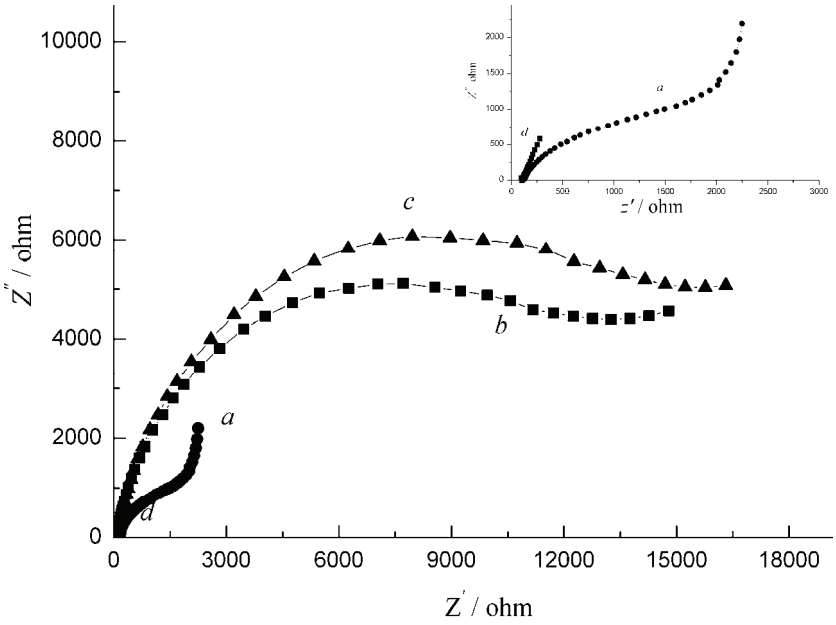

Fig. 2. Complex plane plots of a) MWCNTs–RTIL/GCE, b) bare GCE, c) RTIL/GCE and d) MWCNTs/GCE in 1.0 mM $Fe(CN)_6^{3-/4-}$ + 0.10 M KCl. Frequency range: 1–10^5 Hz.

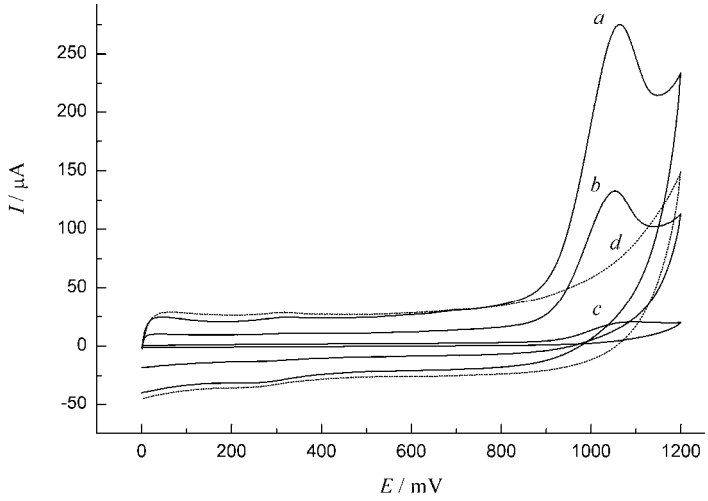

Fig. 3. Cyclic voltammograms of a) MWCNTs–RTIL/GCE, b) MWCNT/GCE and c) GCE in the presence and d) MWCNTs–RTIL/GCE in the absence of 0.10 mM of lansoprazole in 0.10 M PBS (pH 6.8). Scan rate: 50 mV s^{-1}.

By comparison MWCNTs/GCE and the bare GCE, it is seen that the LNS oxidation peak potential is hardly shifted, but the peak current increased by almost two times in contrast to that at the MWCNTs/GCE and fifteen times to that at the bare GCE, which indicated that the electrochemical oxidation reaction of LNS could be improved significantly by the MWCNTs–RTIL/GCE, which is based on the synergy of MWCNTs and RTIL. This may be explained as follows: first, the electrochemical oxidation of LNS occurred easily at thermodynamically favorable potentials and the reaction rate increased kinetically at the MWCNTs–––RTIL/GCE; secondly, the MWCNTs themselves, with nano-scaled dimensions, have a particular electronic structure, high electrical conductivity and topological defects present on their surfaces, which can be readily and completely used as an electrochemical sensing unit, yielding higher sensitivity, and can bear both basal plane sites and edge plane like sites/defects in their structures, which may have caused the electrocatalytic efficiency during the electro-oxidation process.[74–76] Finally, MWCNTs are untangled after treatment with RTIL, mainly because of cross-linking of the nanotube bundles mediated by local molecular ordering of the RTIL resulting from "cation–π" interactions between imidazolium and the nanotubes.[47] Thus, the MWCNTs–RTIL gel can act as a promoter to increase the heterogeneous electron transfer rate, and catalyze very well the lansoprazole electrochemical oxidation reaction.

The effects of the experimental conditions on the peak current and potential of the catalytic oxidation

The effect of various media on the peak current and potential of the catalytic oxidation of LNS could be easily observed from CV. The voltammetric behaviors of LNS at scanning rate 50 mV s^{-1} in different electrolytes, such as aqueous NaCl, CH_3COONa, $NaNO_3$, Na_2SO_4 and CH_3COONa–CH_3COOH, Britton–––Robinson buffer solution and Na_2HPO_4–NaH_2PO_4 (PBS), were investigated. The experimental results showed that in 0.10 M aqueous PBS, LNS had a relative well-defined oxidation peak; thus, 0.10 M PBS was chosen as the supporting electrolyte.

The effect of pH on the anodic peak current and the peak potential for 0.10 mM LNS were studied in 0.10 M PBS over the pH range 5.5–10.0 to avoid degradation and the results are shown in Fig. 4. From Fig. 4, curve a, it could be seen that the anodic peak potentials shifted linearly in the negative direction up to pH 8.0 (inset plot in Fig. 4) with the linear equation being:

$$E_p / \text{mV} = -60\text{pH} + 1502 \ (R = 0.9989) \quad (1)$$

The correlation coefficient was 0.9989. The slope of –60 mV pH^{-1} is very similar to the theoretical value of 59 mV pH^{-1}, which indicated that the number of electrons transferred and the number of proton participating in the electrochemical oxidation reaction were the same. The intercept of the two segments, which

occurred at pH 8.0 may be related to the pK_a of LNS[77] and are in accordance with literature data.[28] Fig. 4, curve b shows that the anodic peak current varies with change in pH values. The peak current reaches its maximum at pH 6.5; thus, pH 6.8 was chosen for the further experiment.

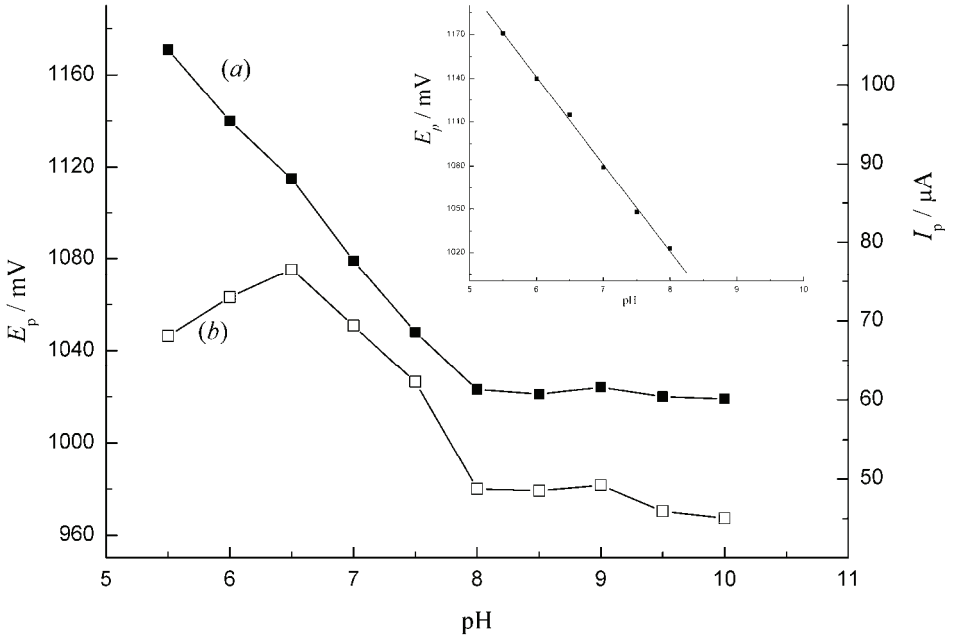

Fig. 4. Effect of pH on a) E_p and b) I_p of 0.10 mM lansoprazole at a MWCNTs–RTIL/GCE by CV. The inset plot is the dependence of pH on E_p from pH 5.5 to pH 8.0. Scan rate: 50 mV s^{-1}.

The effect of the scan rate in CV experiments with 0.10 mM LNS at the MWCNTs–RTIL/GCE is as follows. With increasing potential scanning rate, the peak current increased and the peak potential shifted positively, which implied irreversibility of the electrode reaction processes. The oxidation peak current *versus* the square root of the scan rate was a straight line as shown in Fig. 5, curve b, as expected for a diffusion-controlled electrode reaction process. The linear regression equation is expressed as:

$$I_{pa} / \mu A = 29.88 + 10.19v^{1/2} / (mV^{1/2}\ s^{-1/2})\ (R = 0.9987) \quad (2)$$

The oxidation peak potential (E_{pa}) shifted in the positive direction with increasing scan rate (v), and the relationship between E_{pa} / V and v / V s^{-1} was in accordance with the following equation:

$$E_{pa} / mV = 894.5 + 88.88\log v\ (R = 0.9929) \quad (3)$$

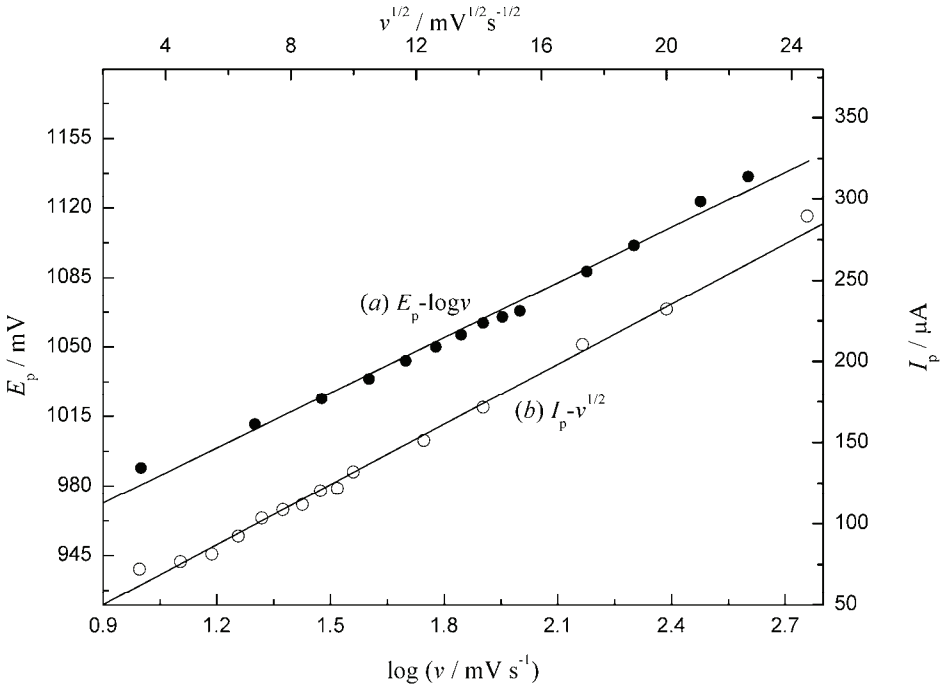

Fig. 5. a) Dependence of the peak potential on the logarithm of the scan rate (log *v*) and b) dependence of the peak current on the square root of the scan rate ($v^{1/2}$).

In brief, the electrode reaction process the most probably one-electron and one-proton irreversible electrochemical oxidation reaction, which indicated that the oxidetion occurs mainly on the benzimidazolem, and its metabolites may be 5′-hydroxy-lansoprazole and lansoprazole sulfone. It is likely that the generation of a radical cation from the oxidation of lansoprazole (*e.g.*, by rearrangement, fragmentation or addition of water) occurs before it can be reduced back to neutral, which is in accord with the literature.[28]

Electrochemical kinetics

Diffusion coefficient. The real area of the electrode and the apparent diffusion coefficient of LNS were determined by chronocoulometry (CC):[78]

$$Q = \frac{2nFAcD^{1/2}t^{1/2}}{\pi^{1/2}} + Q_{dl} + Q_{ads} \quad (6)$$

where, Q is the total charge, n is the number of electrons transferred in the electrochemical oxidation reaction, A is the electrode surface area (cm^2), c is the concentration of the electro-active species in the solution (M), D is the diffusion coefficient (cm^2 s^{-1}) and t is the time (ms). The real area of the MWCNTs––RTIL/GCE was determined to be 0.498 cm^2 from the slopes of Q *vs.* $t^{1/2}$ curves

using 5.0 mM $Fe(CN)_6^{3-}$ as a model compound. As the number of electron transferring of LNS was calculated to be one and the concentration (c) was 0.10 mM, the diffusion coefficient (D) could be calculated to be 1.9×10^{-2} cm^2 s^{-1}.

Electrode reaction rate constant, k_f. The rate constant (k_f) of the electrode could be determined by chronoamperometry (CA) using the following:[79]

$$\mathrm{I}(t) = nF\,\mathrm{A}k_\mathrm{f}c\left[1-\frac{2\mathrm{H}\sqrt{t}}{\sqrt{\pi}}\right] \tag{7}$$

where:

$$H = \frac{k_\mathrm{f}}{D_\mathrm{Ox}^{1/2}} + \frac{k_\mathrm{b}}{D_\mathrm{Rd}^{1/2}} \tag{8}$$

For an irreversible electrochemical oxidation reaction, the reduction rate constant, k_b, is 0, therefore:

$$H = k_\mathrm{f} \Big/ D_\mathrm{Ox}^{1/2} \tag{9}$$

When t approaches zero, a plot of $I(t)$ *vs.* $t^{1/2}$ gives a good straight line. Therefore, k_f could be calculated to be 7.20×10^{-2} s^{-1} from the slope and the intercept of the CA curve.

In order to check the electrochemical responses of the MWCNTs–RTIL/ /GCE for LNS, time–steady-state current response curves were determined and the experimental results are shown in Fig. 6. The current response signals of the

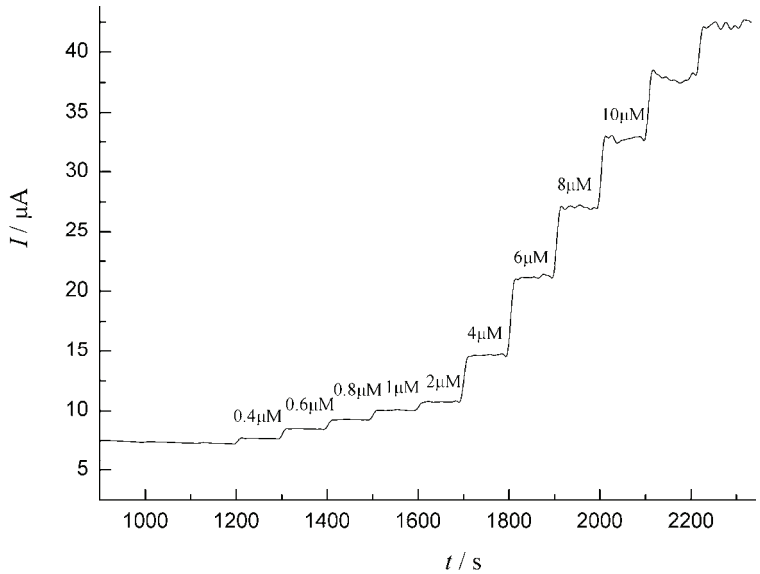

Fig. 6. Time-dependent steady state currents obtained at the RTIL–MWCNTs/GCE while increasing the LNS concentration at 0.998 V at a stirring rate of 100 rpm.

MWCNTs–RTIL/GCE are proportional to the LNS concentrations. The response time was less than four seconds and the least response concentration was 0.4 μM. Thus, the electrode could be used for the quantitative electrochemical determination of LNS having both a low detection limit and a high sensitivity.

Application of the electrochemical determination

Differential pulse voltammetric (DPV) behavior of LNS. The DPV behaviors of 0.10 mM LNS at the MWCNTs–RTIL/GCE, MWCNT/GCE and GCE in 0.10 M PBS under the optimized experimental conditions (amplitude, 65 mV, pulse width, 0.05 s, and scanning potential increment, 4 mV) were examined. An irreversible oxidation peak of LNS at the MWCNTs–RTIL/GCE appeared around 0.960 V, and the LNS itself showed a more sensitive DPV response at the MWCNTs–RTIL/GCE in contrast to that at the bare GCE and at the MWCNTs/ /GCE. The degree of increase was in quite good agreement with that of CV.

The peak currents of electrocatalytic oxidation of LNS with variation of its concentration were investigated at the MWCNTs–RTIL/GCE. A linear calibration curve was obtained over the concentration range 5.0 μM–0.20 mM with the linear regression equation:

$$I_{pa} / \mu A = 4.641 + 192.3(c / mM) \; (R = 0.9972) \qquad (10)$$

The limit of detection (*LOD*) was 0.28 μM according to $S/N = 3$ ($n = 10$).

Under the optimized experimental conditions, the direct determination of 50 μM LNS in 0.10 M PBS was checked in the presence of some common compounds and ions found in pharmaceutical formulations. The determination results showed that within a relative error of ±5 %, 200-fold of K^+, Na^+, Cl^-, NO_3^-, SO_4^{2-} and 100-fold of glucose, saccharose did not affect the LNS current response, which suggested that the proposed voltammetric method had excellent selectivity toward LNS.

In order to examine the reproducibility and the stability of the MWCNTs–––RTIL/GCE, the determinations were performed ten times using one MWCNTs–––RTIL/GCE; a relative standard deviation (*RSD*) of 1.7 % was obtained. The oxidation peak currents for LNS at six independent MWCNTs–RTIL/GCEs were measured, the current response deviated by only 4.3 %. The proposed modified electrode was stored at ambient temperature over a period of 2 h, then dipped in distilled water or activated in PBS blank solution; the current response of LNS deviated by less than 3.0 %. These experimental results showed the good reproducibility and stability of the modified electrode.

Compared with other reported methods[8–24] and the reported electrochemical methods[25–30] (Table I), it is clear that the fabrication of MWCNTs–RTIL/GCE is simple, easy and reproducible. The procedure for the determination of LNS is rapid, inexpensive and pollution-free and requires neither sample pretreatment nor any time-consuming derivatization reaction or deposition steps. Although the

minimum detectability, sensitivity and accuracy of the proposed method may be not as good as those reported[8–30] in the determination of LNS for complicated samples, it is believed that the reported method. as a simpler, quicker, less time consuming method, could still be an alternative in LNS determination in commercial pharmaceutics preparations.

TABLE I. Comparison the characteristics of the proposed method with those of other reported electrochemical methods for the determination of LNS

Linear detection range, mol dm^{-3}	*LOD* / mol dm^{-3}	Reference
1.145×10^{-7}–3.25×10^{-5}	8.59×10^{-8}	25
1.0×10^{-9}–5.0×10^{-8}	2.5×10^{-10}	26
1.0×10^{-9}–5.0×10^{-8}	2.5×10^{-10}	27
2.0×10^{-7}–5.0×10^{-5}	1.0×10^{-8}	28
5.73×10^{-6}–5.15×10^{-5}	5.41×10^{-7}	29
1.145×10^{-6}–5.73×10^{-5}	5.4×10^{-8}	30
5.0×10^{-6}–2.0×10^{-4}	2.8×10^{-7}	This work

Determination of LNS in commercial LNS tablets

In order to ascertain its potential application in the analysis of commercial tablet samples, the proposed method was employed to determine the LNS content in LNS tablets. Ten LNS tablets with a labeled amount of 15 mg per tablet were homogeneously ground into a powder in a mortar. Subsequently, the required amount of the powder was accurately weighed, dissolved in doubly distilled water, transferred quantitatively into a 100 mL volumetric flask and made up to the mark with doubly distilled water. Finally, a known amount of the sample solution was added into 0.10 M pH 6.8 PBS solution and determined by DPV.

The proposed method was successfully applied to the quantitative electrochemical determination of LNS in commercial tablets, evidencing 15 mg LNS per tablet with a relative standard deviations of 1.20–2.91 % based on the average of six replicate measurements. The accuracy was also judged by applying the standard addition method and the mean recoveries were 97.6–100.3 %. The results of these determination implied that there were no significant differences between the proposed method and the reported conventional methods with respect to reproducibility, accuracy, and precision. In other words, the proposed method is convenient and efficient for the determination of LNS with the advantages of simplicity, sensitivity and rapidity.

CONCLUSIONS

The electrochemical behavior, electrochemical kinetics and the quantitative electrochemical determination of LNS were investigated for the first time by several electrochemical methods based on the application of a MWCNTs–RTIL/ /GCE. A well-defined irreversible electrocatalytic oxidation peak was obtained. The electrocatalytic oxidation reaction of LNS at a MWCNTs–RTIL/GCE is a

diffusion-controlled electrode reaction process involving the transfer of one electron accompanied by the participation of one proton. Additionally, the electrochemical kinetic parameters were determined. From the obtained results, an accurate and precise method was proposed, which could be an alternative method for the quantitative electrochemical determination of LNS in commercial pharmaceutical formulations.

Acknowledgements. This work was financially supported by the Natural Science Foundation of Ningxia, China (NZ1147), and the Scientific Research Fund of Heilongjiang Provincial Education Department, China (12511347).

И З В О Д

ЕЛЕКТРОХЕМИЈСКО ПОНАШАЊЕ И ДЕТЕКЦИЈА ЛАНСОПРАЗОЛА НА ЕЛЕКТРОДИ ОД СТАКЛАСТОГ УГЉЕНИКА МОДИФИКОВАНОЈ ВИШЕСЛОЈНИМ УГЉЕНИЧНИМ НАНО-ЦЕВИМА У ЈОНСКОЈ ТЕЧНОСТИ

LI-HONG LIU[1,2], WEI YOU[1], XUE-MEI ZHAN[1] и ZUO-NING GAO[1]

[1]*College of Chemistry and Chemical Engineering, Ningxia University, Yinchuan, 750021, China* и [2]*Department of Chemistry, Heihe College, Heilongjiang 164300, China*

Електрохемијско понашање лансопразола је испитивано на електроди од стакластог угљеника (GCE) и на истој електроди модификованој гелом који је садржао вишеслојне угљеничне нано-цеви (MWCNTs) у ниско-температурној јонској течности (RTIL) 1-бутил-3-метилимидазолијум-хексафлуорофосфат (BMIMPF$_6$). Испитивања су вршена у 0,10 M фосфатном пуферу pH 6,8. Утврђено је да се на електроди MWCNTs–RTIL/GCE појављује иреверзибилни анодни струјни максимум на потенцијалу 1,060 V_{3KE}. Применом методе диференцијалне пулсне волтаметрије, под оптимизованим експерименталним условима добијена је линеарна калибрациона крива у опсегу концентрација од 5,0 μM до 0,20 mM са границом детекције (*LOD*, $S/N = 3$) од 0,28 μM. Осим тога, електрода MWCNTs–RTIL/GCE је карактерисана спектроскопијом електрохемијске импеданције. Предложена метода је успешно примењена за квантитативно електрохемијско одређивање садржаја лансопразола у комерцијалним таблетама.

(Примљено 12. децембра 2012, ревидирано 3. маја 2013)

REFERENCES

1. W. F. James, *Am. J. Med*. **117** (2004) 14
2. A. E. Zimmermann, B. G. Katona, *Pharmacotherapy* **17** (1997) 308
3. D. Jaspersen, K. L. Diehl, H. Schoeppner, P. Geyer, *Aliment. Pharmacol. Ther*. **12**(1998)49
4. G. Coruzzi, M. Adami, G. Bertaccini, *Gen. Pharmacol.* **26** (1995**)** 1027
5. P. Richardson, C. J. Hawkey, W. A. Stack, *Drugs* **56** (1998) 307
6. G. Sachs, J. M. Shin, C Briving, B. Wallmark, S. Hersey, *Annu. Rev. Phamacol. Toxicol*. **35** (1995) 277
7. C. M. Spencer, D. Faulds, *Indian Drugs*. **48** (1994**)** 404
8. A. V. Kasturf, P. G. Yeole, A. P. Sherje, *Asian J. Chem*. **19** (2007) 3612
9. A. A. Syed, A. Syeda, *Bull. Chem. Soc. Ethiop*. **21** (2007) 315
10. N. Rahman, Z. Bano, S. N. H. Azmi, M. Kashif, *J. Serb. Chem. Soc*. **71** (2006) 1107

11. A. A. M. Wahbi, O. A. Razak, A. A. Gazy, H. Mahgoub, M. S. Moneeb, *J. Pharm. Biomed. Anal.* **30** (2002)1133
12. A. A. M. Moustafa, *J. Pharm. Biomed. Anal*. **22** (2000) 45
13. N. Ozaltin, *J. Pharm. Biomed. Anal.* **20** (1999) 599
14. H. Katsuki, A. Hamada, C. Nakamura, K. Arimori, M. Nakano, *J. Chromatogr., B* **757** (2001) 127
15. T. Uno, N. Y. Furukori, T. Takahata, K. Sugawara, T. Tateishi, *J. Chromatogr., B* **816** (2005) 309
16. K. V. S. P. Rao, G. V. Kumar, K. V. Kumari, L. D. Srinivas, G. Prabhakar, *Asian J Chem.* **18** (2006) 798
17. M. Miura, H. Tada, T. Suzuki, *J. Chromatogr., B* **804** (2004) 389
18. M. Song, X. Gao, T. J. Hang, A. D. Wen, *J. Pharm. Biomed. Anal*. **48** (2008) 1181
19. K. K. Pandya, V. D. Mody, M. C. Satia, I. A. Modi, R. I. Modi, B. K. Chakravarthy, T. P. Gandhi, *J. Chromatogr., B* **693** (1997) 199
20. A. P. Argekar, S. S. Kunjir, *J. Planar Chromatogr.-Mod. TLC* **9** (1996) 296
21. A. Tivesten, S. Folestad, V. Schonbacher, K. Swenson, *Chromatographia* **49** (1999) S7
22. D. Dogrukol-Ak, M. Tuncel, H. Y. Aboul-Enein, *Chromatographia* **54** (2001) 527
23. C. I. C. Silvestre, J. L. M. Santos, J. L. F. C. Lima, M. A. Feres, E. A. G. Zagatto, *Microchem. J*. **94** (2010) 60
24. D. Yeniceli, D. Dogrukol-Ak, M. Tuncel, *J. Pharm. Biomed. Anal*. **36** (2004) 145
25. C. Yardimci, N. Ozaltin, *Analyst* **126** (2001) 361
26. A. Radi, *Microchem. J*. **73** (2002) 349
27. A. Radi, *Anal. Lett*. **35** (2002) 2449
28. A. Radi, *J. Pharm. Biomed. Anal*. **31** (2003) 1007
29. F. Belal, N. El-Enany, M. Rizk, *J. Food Drug Anal.***12** (2004) 102
30. N. El-Enany, F. Belal, M. Rizk, *J. Biochem. Biophys. Methods* **70** (2008) 889
31. S. Lijima, *Nature* **354** (1991) 56
32. P. M. Ajayan, *Chem. Rev*. **99** (1999) 1787
33. T. W. Odom, J. L. Huang, P. Kim, C. M. Lieber, *Nature* **391** (1998) 62
34. J. M. Nugent, K. S. V. Santhanam, A. Rubio, P. M. Ajayan, *Nano Lett*. **1** (2001) 87
35. X. Dai, G. G. Wildgoose, R. G. Compton, *Analyst* **131** (2006) 901
36. C. Hu, X. Chen, S. Hu, *J. Electroanal. Chem.* **586** (2006) 77
37. R. Antiochia, I. Lavagnini, *Anal. Lett*. **39** (2006) 1643
38. F. Ricci, A. Amine, D. Moscone, G. Palleschi, *Anal. Lett.* **36** (2003)1921
39. J. S. Moulthrop, R. P. Swatloski, G. Moyna, R. D. Rogers, *Chem. Commun*. **12** (2005) 1557
40. H. M. Lou, S. Dai, P. V. Bonnesen, A. C. Buchanan, J. D. Holbery, N. J. Bridges, R. D. Rogers, *Anal. Chem.* **76** (2004) 3078
41. T. Welton, *Chem. Rev*. **99** (1999) 2071
42. M. Kosmulski, R. A. Osteryoung, M. Ciszkowska, *J. Electrochem. Soc.* **147** (2000) 1454
43. P. Yu, Y. Q. Lin, L. Xiang, L. Su, J. Zhang, L. Q. Mao, *Langmuir* **21** (2005) 9000
44. P. Wassercheid, W. Keim, *Angew. Chem. Int. Ed*. **39** (2000) 3772
45. A. A. Ensafi, H. Karimi-Maleh, *Drug Test. Anal*. **3** (2011) 325
46. J. G. Huddlestion, H. D. Willauer, R. P. Swatloski, A. E. Visser, R. D. Rogers, *Chem. Commun*. **16** (1998) 1765
47. T. Fukushima, A. Kosaka, Y. Ishimura, T. Yamamoto, T. Takigawa, N. Ishii, T. Aida, *Science* **300** (2003) 2072

48. A. M. Kazemi S. M. A. Khalilzadeh, H. Karimi-Maleh, M. B. P. Zanousi, *Int. J. Electrochem. Sci.* **8** (2013) 1938
49. M. Fouladgar, H. Karimi-Maleh, *Ionics* **19** (2013) 1163
50. A. A. Ensafi, H. Bahrami, H. Karimi-Maleh, *Mater. Sci. Eng., C* **33** (2013) 831
51. H. Beitollah, M. Goodarzian, M. A. Khalilzadeh, H. Karimi-Maleh, M. Hassanzadeh, M. Tajbakhsh, *J. Mol. Liq.* **173** (2012) 137
52. T. Tavana. M. A. Khalilzadeh, H. Karimi-Maleh, A. A. Ensafi, H. Beitollah, D. Zareyee, *J. Mol. Liq.* **168** (2012) 69
53. S. Salmanpour, T. Tavana, A. Pahlavan, M. A. Khalilzadeh, A. A. Ensafi, H. Karimi-Maleh, H. Beitollah, E. Kowsari, *Mater. Sci. Eng., C* **32** (2012) 1912
54. A. A. Ensafi, M. Lzadi, B. Rezaei, H. Karimi-Maleh, *J. Mol. Liq.* **174** (2012) 42
55. A. A. Ensafi, M. Izadi, H. Karimi-Maleh, *Ionics* **19** (2013) 137
56. M. Asnaashariisfahani, H. Karimi-Maleh, H. Ahmar, A. A. Ensafi, A. R. Fakhari, M. A. Khalilzadeh, F. Karimi, *Anal Methods* **4** (2012) 3275
57. M. Keyvanfard, R. Shakeri, H. Karimi-Maleh, K. Alizad, *Mater. Sci. Eng., C* **33** (2013) 811
58. A. Mokhtari, H. Karimi-Maleh, A. A. Ensafi, H. Beitollahi, *Sens. Actuators, B* **169** (2012) 96
59. H. Yaghoubian, H. Karimi-Maleh, M. A. Khalilzadeh, F. Karimi, *J. Serb. Chem. Soc.* **74** (2009) 1443
60. A. A. Ensafi. H. Karimi-Maleh, *J. Electroanal. Chem.* **640** (2010) 75
61. H. Beitollahi, H. Karimi-Maleh, H. Khabazzadeh, *Anal. Chem.* **80** (2008) 9848
62. Z. N. Gao, Y. Q. Sun, W. You, *Chin. J. Anal. Chem.* **37** (2009) 553 (in Chinese)
63. X. M. Zhan, L. H. Liu, Z. N. Gao, *J. Solid State Electrochem.* **15** (2011) 1185
64. Y. Q. Sun, W. You, Z. N. Gao, *Acta Pharm. Sin.* **43** (2008) 396 (in Chinese)
65. X. M. Zhan, W. You, Z. N. Gao, *Chin. J. Pharm. Anal.* **29** (2009)1543 (in Chinese)
66. J. W. Chen, C. Q. Duan, Z. N. Gao, *Chin. J. Anal. Chem.* **40** (2012) 447 (in Chinese)
67. L. H. Liu, C. Q. Duan, Z. N. Gao, *J. Serb. Chem. Soc.* **77** (2012) 483
68. Y. M. Zhang, C. Q. Duan, Z. N. Gao, *J. Serb. Chem. Soc.* **78** (2013) 281
69. S. C. Tsang, Y. K. Chen, P. J. F. Harris, M. L. H. Green, *Nature* **372** (1994) 159
70. J. J. Feng, G. Zhao, J. J. Xu, H. Y. Chen, *Anal. Biochem.* **342** (2005) 280
71. M. R. Shahmiri, A. Bahari, H. Karimi-Maleh, R. Hosseinzadeh, N. Mirnia, *Sens. Actuators, B* **177** (2013) 70
72. C. L. Xiang, Y. J. Zou, L. X. Sun, F. Xu, *Electrochem. Commun.* **10** (2008) 38
73. *Impedance Spectroscopy: Theory, Experiment, and Applications*, 2nd ed., E. Barsoukov, J. R. Macdonald, Eds., Wiley, Hoboken, NJ, 2005, p. 258
74. P. J. Britto, K. S. V. Santhanam, A. Rubio, J. A. Alonso, P. M. Ajayan, *Adv. Mater.* **11** (1999) 154
75. M. Musameh, N. Lawrence, J. Wang, *Electrochem. Commun.* **7** (2005) 14
76. C. E. Banks, R. G. Compton, *Analyst* **131** (2006) 15
77. B. Delhotal Landes, J. P. Petite, B. Flouvat, *Clin. Pharmacokinet.* **28** (1995) 458
78. A. J. Bard, L. R. Faulkner, *Electrochemical Methods Fundamentals and Applications*, Wiley, New York, 1980, p. 200
79. H. Q. Wu, Y. F. Li, *Electrochemical Kinetics*, China Higher Education Press, Beijing, and Springer, Berlin, 1998, p. 96.

Journal of the Serbian Chemical Society
JSCS-info@shd.org.rs • www.shd.org.rs/JSCS
J. Serb. Chem. Soc. 79 (1) 53–62 (2014)
JSCS–4564
UDC *Famotidin+612.461:543.552+544.6.076.32–36:615.015.3
Original scientific paper

Sensitive voltammetric determination of famotidine in human urine and tablet dosage forms using an ultra trace graphite electrode

SULTAN YAGMUR[1], SELEHATTIN YILMAZ[1]*, GULSEN SAGLIKOGLU[1], BENGI USLU[2], MURAT SADIKOGLU[3] and SIBEL A. OZKAN[2]

[1]Canakkale Onsekiz Mart University, Faculty of Science and Arts, Department of Analytical, Chemistry, 17020, Canakkale, Turkey, [2]Ankara University, Faculty of Pharmacy, Department of Analytical Chemistry, 06100, Ankara, Turkey and [3]Gaziosmanpasa University, Faculty of Education, Department of Science Education, 60100, Tokat, Turkey

(Received 10 February, revised 19 May 2013)

Abstract: In this study, the direct and sensitive determination of famotidine based on its electrochemical oxidation was investigated in spiked human urine and tablet dosage forms. The electrochemical measurements were performed in various buffer solutions in the pH range 0.88–12.08 at an ultra trace graphite electrode (UTGE) by cyclic voltammetry (CV) and differential pulse voltammetry (DPV) techniques. The best results were obtained for the quantitative determination of famotidine by the DPV technique in 0.5 mol L^{-1} H_2SO_4 solution (pH 0.30). In this strong acid medium, one irreversible anodic peak was observed. The effects of pH and scan rate on the peak current and peak potential were investigated. The diffusion-controlled nature of the peak was established. For optimum conditions described in the experimental section, a linear calibration curve for DPV analysis was constructed in the famotidine concentration range 2×10^{-6}–9×10^{-5} mol L^{-1}. The limit of detection (*LOD*) and limit of quantification (*LOQ*) were 3.73×10^{-7} and 1.24×10^{-6} mol L^{-1} at a UTGE, respectively. The repeatability, precision and accuracy of the developed technique were checked by recovery studies in spiked urine and tablet dosage forms.

Keywords: famotidine; voltammetry; ultra trace graphite electrode; determination; human urine; dosage forms.

INTRODUCTION

Famotidine 3-{[2-(diaminomethyleneamino)thiazol-4-yl]methylthio}-*N'*-sulfamoylpropanimidamide, Scheme 1, is a histamine H_2-receptor antagonist that is used to treat duodenal ulcers and prevent their recurrence. It is also used to treat gastric ulcers and Zollinger–Ellison disease.[1–3] The drug is applied both orally

* Corresponding author. E-mail: seletyilmaz@hotmail.com
doi: 10.2298/JSC130210055Y

and intravenously as an infusion. Therapeutic trials have shown that 20 mg famotidine twice daily or 40 mg at bedtime may be an effective alternative to standard doses of cimetidine in healing duodenal ulcers. The therapeutic level in plasma is 50 μg mL^{-1}. About 15–22 % of famotidine binds to plasma proteins and between 17–30 % of the drug appears unchanged in the urine.[1–3]

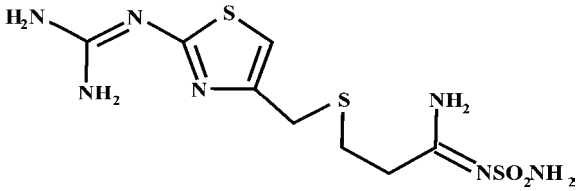

Scheme 1. The structural formula of famotidine.

Methods for the assay of famotidine in pharmaceutical dosage forms and biological materials are usually based on high performance liquid chromatographic (HPLC) techniques with ultraviolet detectors[3–9] or a tandem mass spectrometer.[9–10]

Such applications are, however, time consuming. Other analytical methods have been limited to spectrophotometric and spectrofluorimetric,[11] potentiometric[12] and high performance thin layer chromatographic techniques.[13–14]

Hitherto, only a few papers have been published about the electro-analytical determination of famotidine based on its reduction behavior.[15,16] In this study, famotidine was determined in human urine and tablet dosage forms using an ultra trace graphite electrode by a voltammetric technique.

This technique is particularly well suited for the quantitative determination of redox couples immobilized on an electrode surface.[17–19] This proposed voltammetric technique could be applied directly to the analysis of pharmaceutical dosage forms and biological samples.

EXPERIMENTAL

Apparatus

A Model Metrohm 757 VA Trace Analyzer (Herisau, Switzerland) was used for the voltammetric measurements, with a three-electrode system consisting of an ultra trace graphite working electrode (UTGE, surface size φ = 3 mm, Metrohm), a platinum wire auxiliary electrode and an Ag/AgCl (NaCl 3 mol L^{-1}, Metrohm) reference electrode. The UTGE was polished with aluminum oxide on an alumina polish pad. Then its surface was rinsed with deionized water (DI) and ethanol consequently. Oxygen was removed from the supporting electrolyte solution by passing argon gas (analytically pure of 99.99 %) for 5 min before all measurements. The argon gas was passed for 30 s before each measurement. In each new experiment, a new bare electrode surface was used.

All pH measurements were performed with Model Metrohm 744 pH meter (Herisau, Switzerland). All measurements were realized at ambient laboratory temperature (15–20 °C).

For the analytical applications, the following parameters were employed: differential pulse voltammetry (DPV) – pulse amplitude 50 mV; pulse time 0.04 s, voltage step 0.009 V. Potential step 10 mV and scan rate in the range 10–1000 mV s^{-1} (cyclic voltammetry, CV).

Reagents

Famotidine and its Famoser® tablet dosage forms were kindly supplied by Ilsan Inc. (Istanbul, Turkey). A stock solution of 1.0×10^{-2} mol L^{-1} was prepared by dissolving an accurate mass of famotidine in an appropriate volume of ultrapure deionized water (DI) and 20 μL HNO_3. This solution was kept in a refrigerator until the experiments were performed. The working solutions for the voltammetric investigations were prepared by dilution of the stock solution with DI. All solutions were protected from light and were used within 24 h to avoid decomposition. 0.5 mol L^{-1} sulfuric acid (pH 0.30), 0.067 mol L^{-1}; phosphate buffer, pH 4.45–7.39 (Na_2HPO_4 and NaH_2PO_4 as buffer components were purchased from Riedel); 0.2 mol L^{-1} acetate buffer, pH 3.50–5.60 (Riedel); 0.04 mol L^{-1} Britton–Robinson buffer, pH: 2.12–12.00 (acetic acid, Riedel, 100 %); boric acid (Merck) and phosphoric acid (Carlo Erba, 85 m/m %) were used for the supporting electrolytes. The DI water used throughout the experiments with 18.2 MΩ cm^{-1} was obtained from a Sartorius Arium model of ultrapure water system.

Calibration graph for quantitative determination

Famotidine was dissolved in DI to obtain a 1×10^{-2} mol L^{-1} stock solution. This solution was diluted with DI to obtain diluted famotidine concentrations. For the optimum conditions described in the experimental section, a linear calibration curve for DPV analysis was constructed in the famotidine concentration range of 2×10^{-6}–9×10^{-5} mol L^{-1}. The repeatability, accuracy and precision were checked.

Working voltammetric procedure for spiked human urine

Urine obtained daily from a volunteer was diluted 1:9 with DI. Firstly, 9.4 mL of 0.5 mol L^{-1} H_2SO_4 was put into the voltammetric cell and its voltammogram was taken as the blank. Then 600 μL of the diluted urine solution was added to this solution and its voltammogram was taken as the urine blank. Subsequently, to obtain a 4×10^{-6} mol L^{-1} cell concentration, 40 μL of urine sample (1 mL urine + 8 mL deionized water + 1 mL of 1×10^{-2} mol L^{-1} famotidine stock solution) was added into the voltammetric cell and its voltammogram was recorded. Then, 20 μL of 1×10^{-3} M famotidine standard solution was added four times and the voltammograms of the resulting solutions were individually recorded after each addition. The calibration curve was plotted using obtained results.[17–19]

Working voltammetric procedure for spiked tablet dosage forms

Ten tablets were weighed and ground to a fine powder. From this powder, a 1×10^{-2} mol L^{-1} solution was prepared with deionized water in a 10 mL volumetric flask. The contents of the flask were centrifuged for 20 min at 4000 rpm to affect complete dissolution and then diluted to volume with the same solvent. Appropriate solutions were prepared by taking suitable aliquots of the clear supernatant liquor and diluting with the selected supporting electrolyte solution. Each solution was transferred into the voltammetric cell. Argon was passed through the solution for 5 min before each measurement. The amount of famotidine was found from the calibration curve.

RESULTS AND DISCUSSION

Electrochemical oxidation of famotidine

In this study, the electrochemical oxidation process and the determination of famotidine were realized by the CV and DPV techniques. The results of the CV measurements performed at a UTGE using 1×10^{-4} mol L^{-1} famotidine solution at a scan rate of 100 mV s^{-1} in various supporting electrolytes and buffers are given in Fig. 1. Cyclic voltammetric measurements showed that an irreversible oxidation process of famotidine occurred.

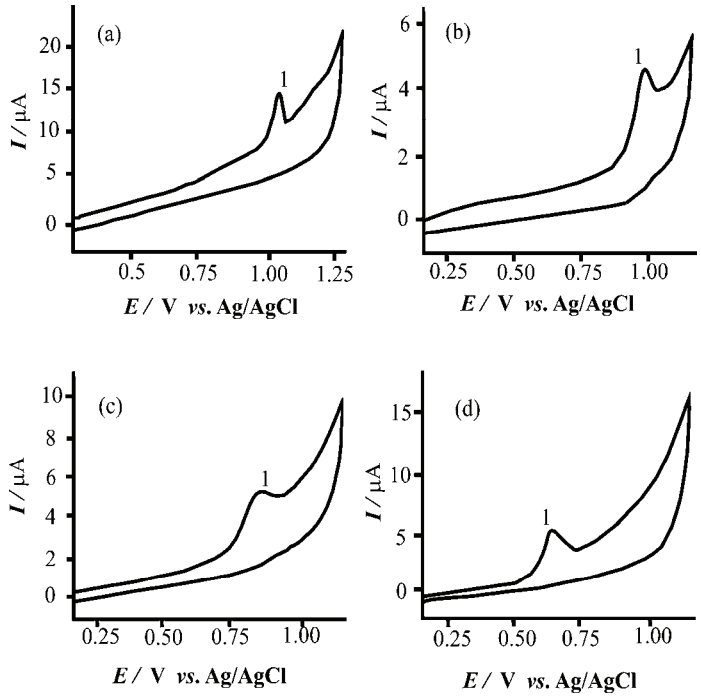

Fig. 1. Cyclic voltammograms of a UTGE electrode in different electrolytes containing 1×10^{-4} mol L^{-1} famotidine; a) 0.5 mol L^{-1} sulfuric acid at pH 0.30, b) 0.2 mol L^{-1} acetate buffer at pH 3.50, c) 0.067 mol L^{-1} phosphate buffer at pH 5.45 and d) 0.04 mol L^{-1} Britton–Robinson buffer at pH 8.02. Scan rate, 100 mV s^{-1}.

The peak potential and the peak current of famotidine were evaluated as in relation to the effects of various scan rates between 10–1000 mV s^{-1}. Scan rate studies were then performed to assess whether the processes at the UTGE were under diffusion or adsorption control.[16–20] Two tests were employed for this procedure. The linear relationship obtained between the peak current and square root of the scan rate between 10–1000 mV s^{-1} was I_p / μA = $0.2489v^{1/2} - 0.6652$ (correlation coefficient, R = 0.998). The correlation coefficient was very close to 1.0, showing that the current was diffusion-controlled. A plot of the logarithm of

the peak current *versus* the logarithm of the scan rate gave a straight line with a slope of 0.6571 (very close to 0.5), which is the expected value for a diffusion controlled current.[17–19]

In order to obtain the optimum experimental conditions, some variables affecting the peak current and peak potential, *i.e.*, pH and supporting electrolyte, for a 5×10^{-5} mol L^{-1} famotidine solution were studied at the UTGE using the proposed voltammetric techniques. The voltammetric response was strongly pH dependent. The peak potential shifted to more negative values with increasing pH (Fig. 2a).

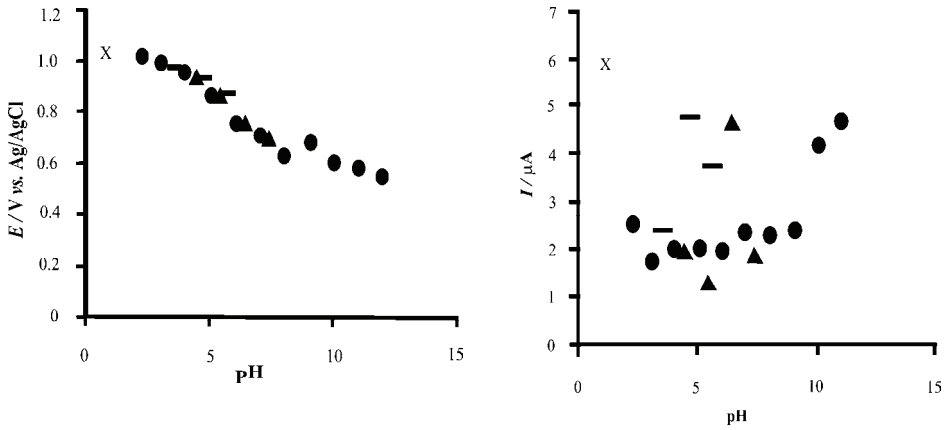

(a) (b)

Fig. 2. Effect of pH and on the DPV peak potential (a) and current (b) in 5×10^{-5} mol L^{-1} famotidine; (–) acetate (0.2 mol L^{-1}), (▲) phosphate (0.067 mol L^{-1}) and (•) Britton–Robinson buffers (0.04 mol L^{-1}) and (X) sulfuric acid.

The peak current was maximal at pH 0.30 in 0.5 mol L^{-1} H_2SO_4 solution. Thus, this pH value and supporting electrolyte were chosen for the electro-analytical studies (Fig. 2b).

The DPV technique and 0.5 mol L^{-1} H_2SO_4 solution (pH 0.30) were also selected for further work because they gave not only the highest peak current, but also the best peak shape.

Validation parameters for the quantitative analysis

Based on the electrochemical oxidation of famotidine, DPV techniques were used for the quantitative determination of the pure drug in spiked urine. The optimum experimental conditions were chosen from the studies of the variation of the peak current on pulse amplitude and potential step. Using the optimum conditions described in the experimental section, the voltammograms for various concentrations of famotidine were recorded in 0.5 mol L^{-1} H_2SO_4 solutions pH 0.30 at the UTGE by the applied technique (Fig. 3).

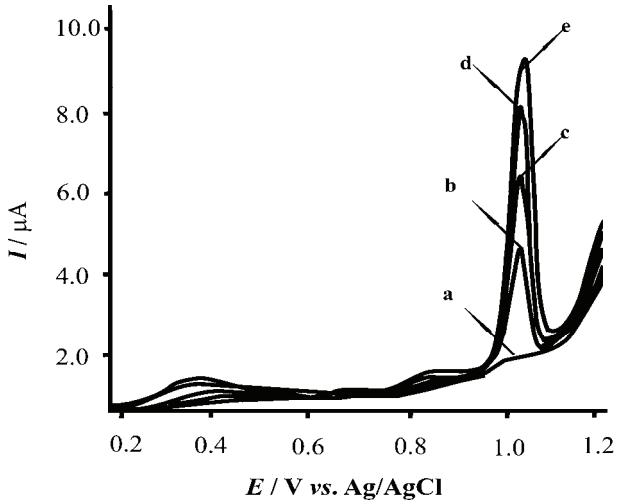

Fig. 3. DPV voltammograms of a UTGE in famotidine solutions. a) Blank, 0.5 mol L^{-1} H_2SO_4 solution (pH 0.30), b) 3.0×10^{-5}, c) 5.0×10^{-5}, d) 7.0×10^{-5} and e) 9.0×10^{-5} mol L^{-1} famotidine.

Quantitative evaluation based on the linear correlation between the oxidation peak current and concentration was performed. Due to this, good correlations were obtained for famotidine in the concentration range 2×10^{-6}–9×10^{-5} mol L^{-1}. The equation of the calibration plot was I_p / μA = 8.0324×10^4(c / mol L^{-1}) – – 0.0398 with a correlation coefficient of r = 0.999 at the UTGE by the DPV technique. Regression data for the calibration plots of famotidine are given in Table I.

TABLE I. Analytical parameters of famotidine obtained in 0.5 mol L^{-1} H_2SO_4 by the DPV technique

Parameter	UTGE
Measured potential, V	1.02
Linear concentration range, mol L^{-1}	2×10^{-6}–9×10^{-5}
Slope, μA M	8.03×10^4
Intercept, μA	–0.0398
Correlation coefficient, *r*	0.999
SE of slope	3.30×10^3
SE of intercept	0.0130
Number of measurements, *N*	10
LOD / mol L^{-1}	3.73×10^{-7}
LOQ / mol L^{-1}	1.24×10^{-6}
Repeatability of peak current, *RSD* / %	1.77
Reproducibility of peak current, *RSD* / %	0.48
Repeatability of peak potential, *RSD* / %	0.69
Reproducibility of peak potential, *RSD* / %	1.26

Validation of the procedure for the quantitative determination of famotidine was examined *via* the evaluation of the limit of detection (*LOD*), limit of quantification (*LOQ*), repeatability, reproducibility, accuracy and precision for the DPV technique (Table I).

The *LOD* and *LOQ* were calculated on the oxidation peak current using the following equations: $LOD = 3s/m$ and $LOQ = 10s/m$ (s is the standard deviation of the peak current for six runs and m is the slope of the calibration curve).[16–19] The achieved limits of detection and quantification were 3.73×10^{-7} and 1.24×10^{-6} mol L^{-1} at the UTGE. The repeatability of the current measurement was calculated for the DPV technique from ten independent runs as 3.27 % *RSD* for 7×10^{-5} mol L^{-1} and 1.77 % *RSD* for 1.0×10^{-5} mol L^{-1} at the UTGE.

The reproducibility of the current measurement was also calculated by the DPV technique from ten independent runs as 0.97 % *RSD* for 7×10^{-5} mol L^{-1} and 0.48 % *RSD* for 1.0×10^{-5} mol L^{-1} famotidine solution at the UTGE, respectively.

Application to human urine samples

The possibility of applying the voltammetric procedure to the quantitative determination of famotidine in spiked human urine was also successfully tested by standard additions of pure drug as described in the experimental section. The voltammograms for famotidine in spiked human urine are given in Fig. 4.

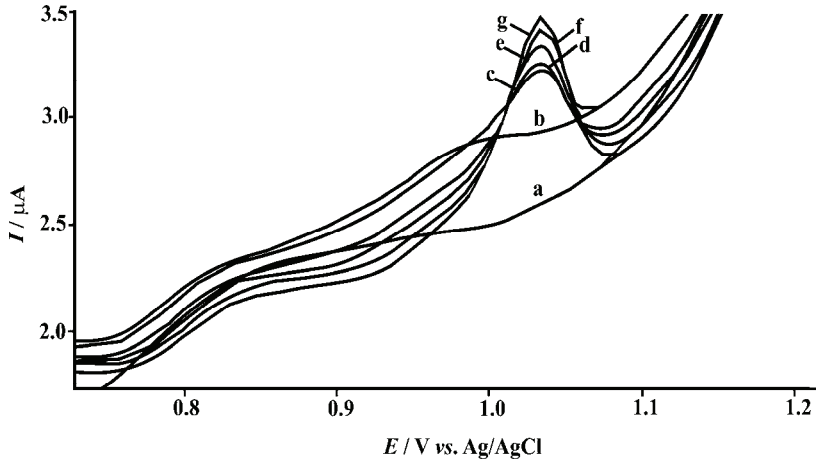

Fig. 4. DPV voltammograms of a UTGE for famotidine in spiked human urine; a) blank (0.5 mol L^{-1} H_2SO_4 solution, pH 0.30); b) a + 600 μL urine (1:9); c) 4.0×10^{-6} mol L^{-1} famotidine with urine; d) 2.0×10^{-6}; e) 4.0×10^{-6}; f) 6.0×10^{-6} and g) 8.0×10^{-6} mol L^{-1} famotidine.

The found amount of famotidine in human urine was calculated from the related linear regression equations. The results of these analyses are summarized in Table II.

TABLE II. Application of the DPV technique at a UTGE to the quantitative determination of famotidine in spiked human urine samples with recovery results

Medium	Human urine
Famotidine spiked, mol L^{-1}	4.00×10^{-6}
Famotidine found, mol L^{-1}	4.08×10^{-6}
Number of measurements, *N*	5
Average recovery, %	102.00
RSD / %	0.42
Bias, %	2.00

As can be seen in Table II, good recovery of famotidine was achieved from this type of matrix at the UTGE. The quantitative assay of spiked urine samples by the proposed technique involved only dilution of spiked urine samples, so it is timesaving and no other procedure steps are required.

Pharmaceutical applications

The amount of famotidine in Famoser® tablets was calculated by reference to the appropriate calibration plots. The results obtained are given in Table III. The proposed technique could be applied with great success to famotidine in tablets without any interference at the UTGE.

TABLE III. The quantitative determination of famotidine in Famoser® tablets by the DPV technique at UTGE

Parameter	Result
Labeled, mg	40.00
Amount found, mg	41.97
RSD / %	2.72
Bias, %	4.92
Famotidine spiked, mg	5.00
Found, mg	5.17
Recovery, %	103.5
Bias, %	3.50
RSD of recovery, %	2.04

The proposed technique was checked by performing recovery tests. To determine whether excipients in the tablets interfered with the analysis, the accuracy of the proposed methods were evaluated by recovery tests after addition of known amounts of pure drug to pre-analyzed formulations of famotidine (Table III).

The results showed the validity of the proposed techniques for the quantitative determination of famotidine in tablets. The proposed DPV technique proved to be sufficiently precise and accurate for reliable electro-analytical analysis of famotidine.

CONCLUSION

In this study, the determination of famotidine based on its electrochemical oxidation at a UTGE was studied by voltammetric techniques. From the CV measurements, it was understood that the electrode reaction process is irreversible and pH dependent. The DPV technique was successfully applied to the quantitative determination of famotidine in 0.5 mol L^{-1} H_2SO_4 solution (pH 0.30) in spiked human urine and commercial drug samples. The analysis was performed with good recoveries without any interference from the excipients in spiked human urine and tablet dosage forms.

The principal advantage of this proposed technique over other techniques is that it may be applied directly to the analysis of pharmaceutical dosage forms and to biological samples without the need for extensive sample preparation, since there was no interference from the excipients and endogenous substances. Another advantage is that the developed techniques are rapid, requiring about 5 min to run any sample. This paper is not intended to be a study of the pharmacodynamic properties of famotidine, because only healthy volunteers were used for sample collection and results might be of no significance. It only indicated that the possibility of monitoring this compound makes the technique useful for pharmacokinetic and pharmacodynamic purposes.[17–19]

The proposed voltammetric techniques might be a rapid and simple alternative to more complicated chromatographic (HPLC) or spectrometric (UV) techniques for routine analysis of famotidine.

Acknowledgments. The authors gratefully acknowledge the Scientific and Technical Research Council of Turkey (TUBITAK, Grant No.: TBAG-2173; 102T062). The authors would like to thank Ilsan Inc. (Istanbul, Turkey) for supplying pure famotidine and its tablet dosage forms for the development of the proposed voltammetric technique.

ИЗВОД

ВОЛТАМЕТРИЈСКО ОДРЕЂИВАЊЕ ФАМОТИДИНА У ХУМАНОМ УРИНУ И ТАБЛЕТНИМ ДОЗИРАНИМ ОБЛИЦИМА ПРИМЕНОМ ЕКСТРЕМНО ОСЕТЉИВЕ ГРАФИТНЕ ЕЛЕКТРОДЕ

SULTAN YAGMUR[1], SELEHATTIN YILMAZ[1], GULSEN SAGLIKOGLU[1], BENGI USLU[2], MURAT SADIKOGLU[3] и SIBEL A. OZKAN[2]

[1]Canakkale Onsekiz Mart University, Faculty of Science and Arts, Department of Analytical, Chemistry, 17020, Canakkale, Turkey, [2]Ankara University, Faculty of Pharmacy, Department of Analytical Chemistry, 06100, Ankara, Turkey и [3]Gaziosmanpasa University, Faculty of Education, Department of Science Education, 60100, Tokat, Turkey

У овом раду је директно и осетљиво одређивање фамотидина, базирано на електрохемијској оксидацији, испитивано на оптерећеним узорцима урина и таблетним дозираним облицима. Електрохемијска мерења су извођена у различитим пуферима pH опсега 0,88–12,08, на екстремно осетљивој електроди (UTGE) цикличном волтаметријом (CV) и диференцијалном пусном волтаметријом (DPV). Најбољи резултати за одређивање фамотидина су добијени DPV техником у раствору H_2SO_4 концентрације 0,5 mol L^{-1}

(pH 0,30). Запажа се један иреверзибилан анодни пик у јако киселој средини. Испитивани су ефекат pH и брзине промене потенцијала на струју и потенцијал пика. Процес регистрован волтаметријским пиком је дифузионо контролисан. Конструисана је линеарна калибрациона крива за оптималне услове, у опсегу концентрација фамотидина 2×10^{-6}–9×10^{-5} mol L^{-1}. Граница детекције (*LOD*) и граница квантификације (*LOQ*) на UTGE износе $3{,}73\times10^{-7}$ и $1{,}24\times10^{-6}$ mol L^{-1}, односно репродуктивност, прецизност и тачност развијене методе су проверени помоћу „*recovery*“ студија на оптерећеним узорцима урина и таблетним дозираним облицима.

(Примљено 10. фебруара, ревидирано 19. маја 2013)

REFERENCES

1. G. B. Onoa, V. Moreno, *J. Inorg. Biochem.* **72** (1998) 141
2. J. A. Squella, C. Rivera, L. Lemus, I. J. Nunez-Vergara, *Microchim. Acta* **1** (1990) 343
3. S. Skrzypek, W. Ciesielski, A. Sokołowski, S. Yilmaz, D. Kazmierczak, *Talanta* **66** (2005) 1146
4. T. C. Dowling, R. F. Frye, *J. Chromatogr., B* **732** (1999) 239
5. C. Ho, H. M. Haung, S. Y. Hsu, C. Y. Shaw, B. L. Chang, *Drug. Dev. Ind. Pharm.* **25** (1999) 379
6. Y. R. Tahboub, M. F. Zaater, N. M. Najib, *Quim. Anal.* **17** (1998) 117
7. A. Zarghi, H. Komeilizadeh, M. Amini, L. Kimiagar, *Pharmacol. Commun.* **4** (1998) 77
8. B. Cakir, A. U. Tosun, M. F. Sahin, *Pharm. Sci.* **3** (1997) 493
9. M. A. Campanero, I. Bueno, M. A. Arangoa, M. Escolar, E. G. A. Quetglas, J. R. Lopez-Ocariz, *J. Chromatogr., B* **76** (2001) 321
10. L. Zhong, R. Eisenhandler, K. C. J. Yeh, *Mass Spectrom.* **36** (2001) 736
11. A. K. S. Ahmad, M. A. Kawy, M. Nebsen, *Anal. Lett.* **32** (1999) 1403
12. J. Petkovic, D. Minic, Z. Koricanac, T. Jovanovic, *Pharmazie* **53** (1998) 163
13. R. E. Simon, L. K. Walton, Y. L. Liang, M. B. Denton, *Analyst* **126** (2001) 446
14. J. Novakovic, *J. Chromatogr., A* **846** (1999) 193
15. J. A. Squella, G. Valencia, I. Lemus, L. J. Nunez-Vergara, *J. Assoc. Anal. Chem.* **72** (1989) 549
16. V. Mirceski, B. Jordanoski, S. Komorsky-Lovric, *Portugaliae Electrochim. Acta* **16** (1998) 43
17. S. Yilmaz, B. Uslu, S. A. Ozkan, *Talanta* **54** (2001) 351
18. S. A. Ozkan, B. Uslu, *Anal. Bioanal. Chem.* **372** (2002) 582
19. S. Yilmaz, M. Sadikoglu, G. Saglikoglu, S. Yagmur, G. Askin, *Int. J. Electrochem. Sci.* **3** (2008) 1534.

Journal of the Serbian Chemical Society
JSCS-info@shd.org.rs • www.shd.org.rs/JSCS
J. Serb. Chem. Soc. 79 (1) 63–76 (2014)
JSCS–4565
UDC 543.3:546.74'73'56'47:544.77:
66.061.35:543.544.5.068.7
Original scientific paper

Ionic liquid-based dispersive liquid–liquid microextraction combined with high performance liquid chromatography–UV detection for the simultaneous pre-concentration and determination of Ni, Co, Cu and Zn in water samples

ALIREZA ASGHARI[1]*, MEHRI GHAZAGHI[1], MARYAM RAJABI[1], MAHDI BEHZAD[1] and MEHRORANG GHAEDI[2]

[1]*Department of Chemistry, Semnan University, Semnan 35195-363, Iran and* [2]*Department of Chemistry, Yasouj University, Yasouj 75918-74831, Iran*

(Received 22 June 2012, revised 11 January 2013)

Abstract: Ionic liquid-based dispersive liquid–liquid microextraction (IL––DLLME) coupled with high performance liquid chromatography (HPLC) with UV detection was developed for the simultaneous extraction and determination of nickel, cobalt, copper and zinc ions. In the proposed approach, salophen (*N*,*N*′-bis(salicylidene)-1,2-phenylenediamine) was used as a chelating agent, the ionic liquid, 1-hexyl-3-methylimidazolium hexafluorophosphate, and acetone were selected as extracting and dispersive solvents, respectively. After extraction, phase separation was performed by centrifugation and the sedimented phase (ionic liquid) was solubilized in acetonitrile and directly injected into the HPLC for subsequent analysis. Baseline separation of the metal ion complexes was achieved on a RP-C18 column using a gradient elution of mixtures of methanol–acetonitrile–water as the mobile phase at a flow rate of 1.0 mL min^{-1}. The influence of variables such as sample pH, concentration of the chelating agent, amount of ionic liquid (extraction solvent), disperser solvent volume, extraction time, salt effect and centrifugation speed were studied and optimized. Under the optimum conditions, an enrichment factor of 222 was obtained. The detection limits for Ni, Co, Cu and Zn were 0.8, 1.6, 1.9 and 2.8 μg L^{-1}, respectively. The relative standard deviation (*RSD*) was in the range 3.6–5.0 % for all of the investigated metal ions. The proposed procedure was successfully applied to the determination of the studied metal ions in water samples.

Keywords: nickel; cobalt; copper; zinc; dispersive liquid–liquid microextraction; salophen; HPLC–UV.

* Corresponding author. E-mail: aasghari@semnan.ac.ir
doi: 10.2298/JSC062212081A

INTRODUCTION

Nickel, cobalt, copper and zinc are essential trace elements in the human body. Although these elements are required for the fulfillment of multiple functions in the organism, they are harmful at high concentrations.[1] The accurate and precise quantification of low concentrations of metal ions is possible by either using very sensitive instrumental techniques or performing enrichment/separation methods. Several separation and pre-concentration procedures, including: liquid–liquid extraction (LLE),[2–5] solid phase extraction (SPE),[6–11] cloud point extraction (CPE),12–14 and co-precipitation,15–17 have been developed in this regard. These methods, despite of their advantages, suffer from limitations, such as significant chemical additives, solvent losses, complex equipment, large secondary wastes, unsatisfactory enrichment factors and high time consumption, that limit their application. A new trend in analytical chemistry is miniaturization of pre-concentration techniques to reduce the consumption of reagents and decrease waste generation.[18] As a result, several novel micro-extraction techniques, such as solid-phase microextraction (SPME)[19,20] and liquid-phase micro-extraction (LPME),[21–24] have been developed. SPME is expensive, its fiber is fragile and has limited lifetime and sample carry-over can be a problem.[25] LPME was developed as a solvent-minimized sample pretreatment procedure that is inexpensive and, since very little solvent is used, there is minimal exposure to toxic organic solvents.[26,27] However, this method suffers from some disadvantages, such as: fast stirring would tend to form air bubbles,[28] the extraction is time-consuming and equilibrium could not be attained even after a long time in most cases.[23]

Efforts to overcome these limitations have led to the development of dispersive liquid–liquid micro-extraction (DLLME) with the advantages of short extraction time, ease of operation, and small amounts of applied solvents.[29] These quite new methods of sample preparation, which are used in the separation and pre-concentration of metals, could solve some of the problems encountered with conventional pretreatment techniques. In DLLME, a mixture of a water-immiscible extraction solvent and a water-miscible dispersive solvent is rapidly injected into an aqueous sample solution by syringe. A cloudy solution containing fine droplets of the extraction solvent dispersed entirely in the aqueous phase is formed, which is attributed to the dispersive role of the dispersive solvent. The analytes in the sample are extracted into fine droplets of the extraction solvent, the mixture is then exposed to centrifugation and the sedimented phase containing the analytes of interest is then analyzed by gas chromatography (GC) or high performance liquid chromatography (HPLC) or by conventional analytical techniques. The DLLME method is simple, rapid and low cost, and has high recovery and enrichment factors. This method was successfully applied for the pre-concentration of organic and inorganic species in environmental samples.[30–36]

Atomic spectrometric techniques are commonly used in multi-element analysis, but most of them, especially flame atomic absorption spectrometry, need milliliter volumes of samples. Inductively coupled plasma–atomic emission spectrometry (ICP-AES) and inductively coupled plasma–mass spectrometry (ICP-MS) require complicated operation, high cost of maintenance, expensive apparatus and need well-controlled experimental conditions. HPLC is a good alternative technique, which is a simple and relatively cheap method. In DLLME, the sedimented phase has micro-liter volumes that can be fully injected into the HPLC column. To the best of our knowledge, there are only two reports in the literature on the pre-concentration and determination of cobalt and iron,[37] and copper and zinc[38] by the DLLME–HPLC method.

The main objective of this study was to explore the applicability of DLLME coupled with HPLC-UV for the development of a new method for the simultaneous pre-concentration and determination of nickel, cobalt, copper and zinc in water samples. In this research, an ionic liquid (IL) was used as the extraction solvent. The IL decreases the toxicity of the procedure *via* decreasing the consumption of chlorinated solvents and allows the facile injection into the reversed--phase system after dilution. Ionic liquid can effectively shield residual silanols and improve the peak shapes.[39] The effects of various experimental parameters, such as the sample pH, concentration of ligand, amount of ionic liquid, kind and volume of the disperser solvent, extraction time, speed of centrifugation and salt effect, were studied and optimized.

EXPERIMENTAL

Apparatus

Chromatographic separations were realized using a Knauer HPLC system consisting of a K-1001 quaternary solvent delivery pump with an online degasser, a UVD K-2600 detector capable of detecting at four wavelengths, and a sampling valve with 20 µL sample loop (Knauer, Germany). A reversed-phase Perfectsil target C_{18} column (250 mm×4.6 mm I.D., 5-µm particle size) was used for separation at ambient temperature and ChromGate software package was employed to acquire and process the chromatographic data. The mobile phase used for the analysis consisted of methanol (A), water (B); and acetonitrile (C) at a flow rate of 1 mL min^{-1}. The following gradient was used: 0 min, 10 % A, 30 % B, 60 % C; 3–3.5 min, 50 % A, 30 % B, 20 % C; 3.5–10 min, 0 % A, 20 % B, 80 % C. The UV-detector was set at 436 nm. A Hettich centrifuge model EBA 20 (Hettich, Germany) was used for phase separation. A BEL PHS-3BW pH-meter (BEL, Italy) with a combined glass–calomel electrode was used for pH adjustment.

Reagents and solutions

Methanol (HPLC-grade), water, acetone and acetonitrile were provided by Merck (Darmstadt, Germany). Analytical grade nitrate salts of nickel, cobalt, and acetate salts of copper and zinc (all from Merck, Darmstadt, Germany) were of the highest available purity and used without any further purification. All other chemicals used were of analytical reagent grade. All solutions were purchased in double distilled water. The stock solutions of Ni(II),

Co(II), Cu(II) and Zn(II), 1000 mg L^{-1}, were prepared by carefully weighing the solid salts and dissolving in double distilled water in 100 mL volumetric flasks. A standard solution of metal ions was prepared daily by suitable dilution of the stock solution with doubly distilled water. 1-Hexyl-3-methylimidazolium hexafluorophosphate ([hmim][PF_6]) was purchased from IoLiTec (Germany). Acids, bases and the other materials and salts were obtained from Merck (Darmstadt, Germany). The ligand of *N*,*N*′-bis(salicylidene)-1,2-phenylenediamine (salophen, Fig. 1) was synthesized and purified according to a previously reported procedure.[40] A 0.01 mol L^{-1} solution of salophen in ethanol was prepared by dissolving the proper amount of the reagent. The pH of solutions was adjusted to 6.5 by dissolving the required amount of acetic acid (0.4 mol L^{-1}) in distilled water and drop wise addition of sodium hydroxide solution.

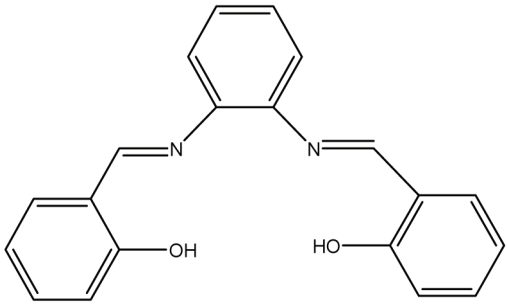

Fig. 1. Structural formula of salophen.

Four water samples, *i.e.*, Kan River, tap, well and mineral water, were used to validate the proposed method. The tap, well and Kan River waters were collected from Tehran (Iran). Bottled mineral water was purchased from a local supermarket. All samples were filtered through a filter paper (Whatman, No. 42) prior to use for the DLLME procedure. The water samples were subjected to ultra violet light for 2 h to kill all microorganisms.

Ionic liquid-based DLLME procedure

The pH of the sample solution (10.0 mL) containing 10 μg L^{-1} of Ni(II), Co(II), Cu(II) and Zn(II), and 1.0×10^{-2} mol L^{-1} salophen was adjusted to 6.5 by adding hydrochloric acid and/or sodium hydroxide in the presence of sodium acetate in a 15 mL screw-cap conical-bottom glass centrifuge tube. Then, a binary solution containing 400 μL of acetone as the disperser solvent and 130 mg of ionic liquid (1-hexyl-3-methylimidazolium hexafluorophosphate ([hmim][PF_6])) as the extracting solvent was rapidly injected into the sample solution using a 1.0 mL gastight syringe (Hamilton). A cloudy solution (water/acetone/IL) consisting of very fine droplets of IL dispersed in the solution was formed and the metal ions–salophen complexes were extracted into the fine droplets of IL. The mixture was gently shaken and then centrifuged for 5 min at 4000 rpm. As a result, the fine droplets of IL with a volume of 5 μL settled at the bottom of the centrifuge tube. All the aqueous phase was removed with a syringe. Then, the sedimented phase (IL-phase) was dissolved in acetonitrile to a total volume of 40 μL and injected into the HPLC-UV for separation and determination. The chromatogram showing the separation of nickel, cobalt, copper and zinc complexes with salophen is shown in Fig. 2.

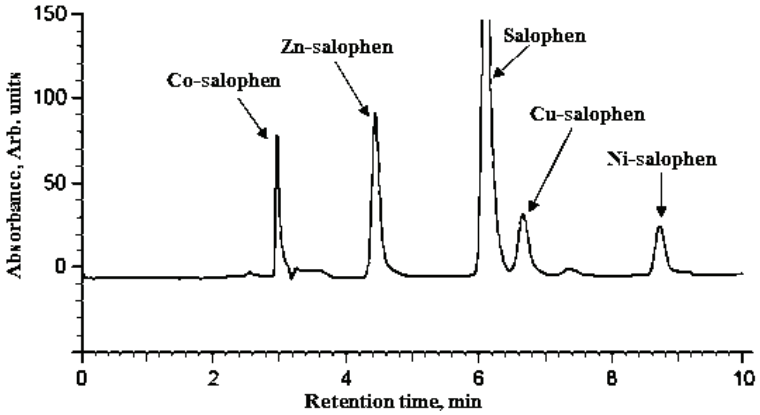

Fig. 2. IL–DLLME–HPLC chromatogram for a mixture of the metal complexes. Conditions: Ni(II), 40.0; Co(II), 60.0; Cu(II), 20.0 and Zn(II), 50.0 μg L^{-1}; 1.0×10^{-2} mol L^{-1}; salophen, 130 mg [hmim][PF_6]; 400 μL acetone; 4000 rpm centrifuge speed; gradient eluent program at a flow rate of 1 mL min^{-1} and detection at 436 nm.

RESULTS AND DISCUSSION

In the present work, IL-DLLME combined with HPLC-UV was developed for the simultaneous determination of Ni(II), Co(II), Cu(II) and Zn(II) ions in water samples. To obtain a high extraction recovery, the influence of effective parameters such as pH, amounts of IL and disperser solvents, concentration of chelating agent and salt and co-existing ions should be optimized.

Influence of pH

The pH has a significant influence on the metal–ligand complex formation and subsequent extraction. The effect of pH on the DLLME pre-concentration of Ni(II), Co(II), Cu(II) and Zn(II) ions was studied in the pH range 2.0–10.0. The results are illustrated in Fig. 3. The progressive decrease in the extraction of metal ions of interested at low pH values was due to competition of hydrogen ion with analytes for reaction with salophen. At high pH values, hydrolysis of the cations occurs. The extraction recoveries were the highest for all metal ions at pH 6.5. Therefore, pH 6.5 was selected for further studies.

Influence of the ligand concentration

The concentration of salophen has a direct effect on the formation of the complexes of the metal ions and their subsequent extraction and pre-concentration. The effect of salophen concentration on the extraction recoveries of Ni(II), Co(II), Cu(II) and Zn(II) ions was studied in the range of 1.0×10^{-3}–-4.0×10^{-2} mol L^{-1}, and the results are shown in Fig. 4. With increasing salophen concentration up to 0.01 mol L^{-1}, the maximum metal ions extraction was achieved and with higher amounts of salophen concentrations, the recoveries

became nearly constant. Therefore, a salophen concentration of 0.01 mol L^{-1} was selected for the further experiments.

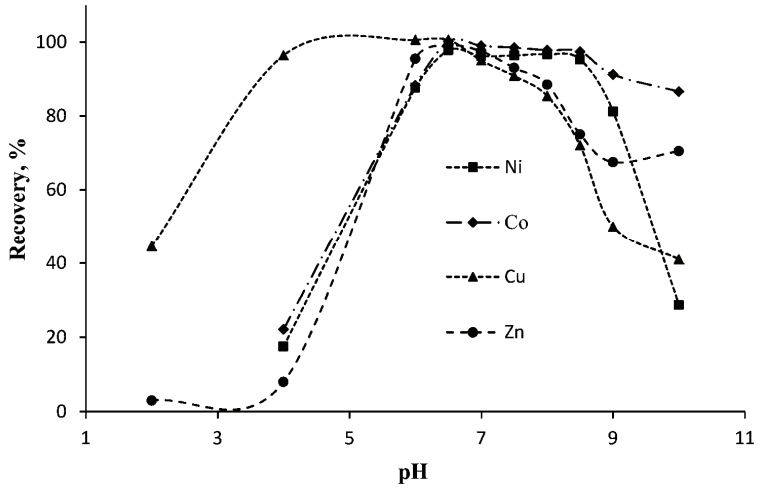

Fig. 3. Influence of pH on the extraction recovery of metal ions obtained by DLLME. Extraction conditions: sample volume 10.0 mL; disperser solvent (acetone) volume 0.40 mL; salophen 1.0×10^{-2} mol L^{-1}; amount of [hmim][PF_6] 130 mg; concentration of: Ni(II) 40.0, Co(II) 60.0; Cu(II) 20.0 and Zn(II) 50.0 μg L^{-1}.

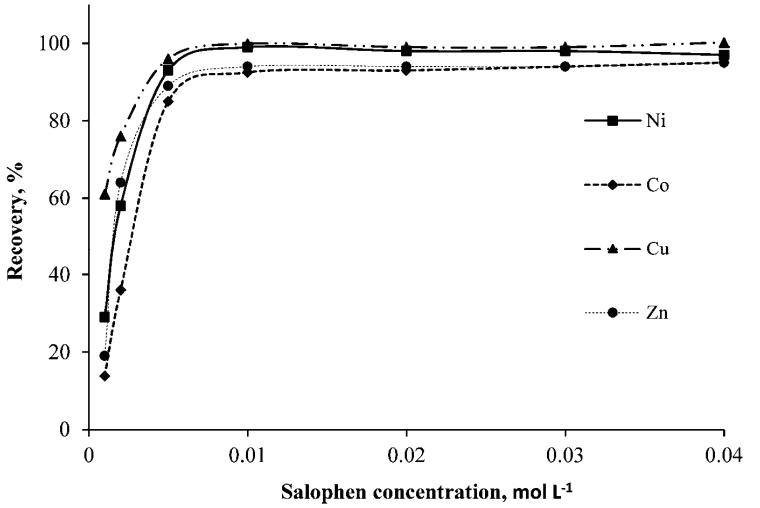

Fig. 4. Influence of the concentration of the ligand on the extraction recovery of metal ions obtained by DLLME. Extraction conditions: sample volume 10.0 mL; disperser solvent (acetone) volume 0.40 mL; amount of [hmim][PF_6] 130 mg; concentration of: Ni(II) 40.0, Co(II) 60.0; Cu(II) 20.0 and Zn(II) 50.0 μg L^{-1}.

Influence of the amount of ionic liquid

The extraction solvent should have special characteristics including low solubility in water, capability of extraction of the target compounds, higher density than water and good chromatographic behavior. Most of the halogenated solvents applied in DLLME have all of the above properties, but these compounds are highly toxic and their direct injection to reverse phase HPLC is impossible. ILs represents a good and efficient alternative to the conventional chlorinated organic solvents in the DLLME procedure. In the present study, the IL ([hmim][PF_6]) was used as the extraction solvent. To examine the effect of the IL, solutions containing different amounts of the ionic liquid were subjected to the same IL–DLLME procedure and the results are shown in Fig. 5. The results indicate that with increasing amount of ionic liquid, the extraction recovery of metal ions increased *via* improving their ability for trapping and extraction of target compounds. At values greater than 130 mg, some of IL could not be dispersed into the aqueous solution as infinitesimal drops, and existed as larger drops, which decreased the contact area between metal complexes and the IL drops. Reduction of the extraction recovery at higher values of IL (>130 mg) was probably due to a decrease in the ratio between the dispersive solvent and the extractant. This decreases the number of formed droplets available for extraction, which lowers the extraction efficiency.[41,42] Based on these observations, 130 mg of the IL were used in the further experiments.

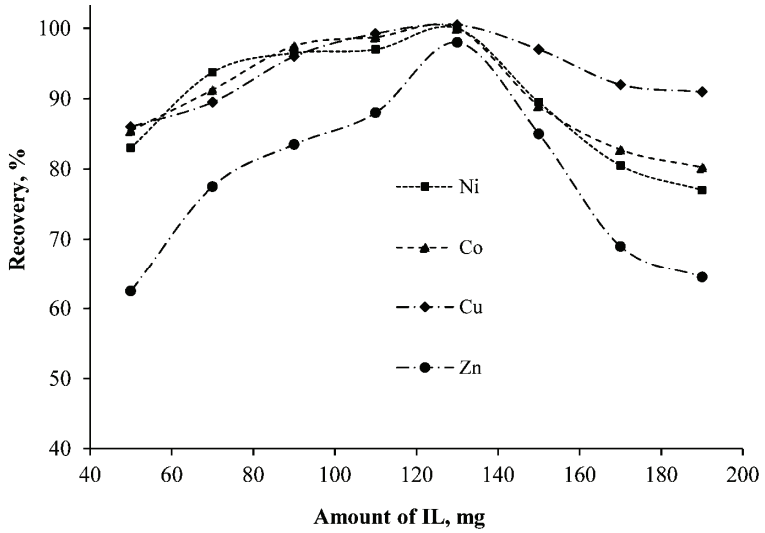

Fig. 5. Influence of the amount of ionic liquid on the extraction recovery of metal ions obtained by DLLME. Extraction conditions: sample volume 10.0 mL; disperser solvent (acetone) volume 0.40 mL; salophen amount 1.0×10^{-2} mol L^{-1}; concentration of: Ni(II) 40.0, Co(II) 60.0; Cu(II) 20.0 and Zn(II) 50.0 μg L^{-1}.

Influence of the type and volume of the dispersive solvent

The choice of the dispersive solvent to be used in a DLLME procedure is very important in order to achieve an effective pre-concentration of analytes. The candidate solvents must have the appropriate miscibility in both the extraction solvent and the sample solution in order to form a distinct cloudy solution. Hence, four possible disperser solvents, *i.e.*, methanol, ethanol, acetonitrile and acetone, were tested. A series of sample solutions were studied by using 400 µL of each solvent containing 130 mg of [hmim][PF_6] (extraction solvent). The extraction recoveries are given in Fig. 6. The results show that acetone is the best disperser solvent. Acetone was therefore selected for the subsequent studies. The volume of disperser solvent affects the solubility of the extraction solvent in the water solution and the volume of the settled phase, which have influences on the extraction recovery and enrichment factor. To acquire the optimal volume, experiments were performed with different volumes of acetone (0, 100, 200, 300, 400, 600 and 800 µL) containing 130 mg [hmim][PF_6]. As shown in Fig. 7, the extraction recoveries of the analytes show an initial increase and then decrease with increasing volume of acetone. At low volumes of acetone, a cloudy solution was not completely formed, and hence the extraction recovery of the analyte was low, while at larger volumes of acetone, the solubility of [hmim][PF_6] in the aqueous solution increased and the extraction recovery decreased. According to the obtained results, 400 µL acetone was chosen in order to obtain a high extraction recovery and the maximum pre-concentration factor.

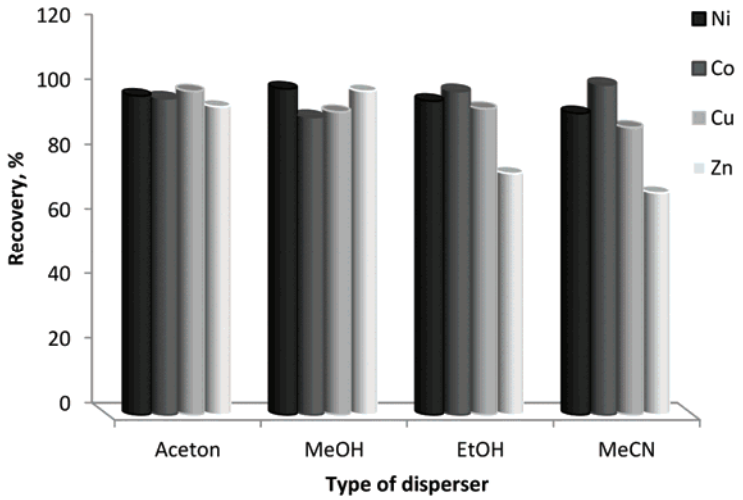

Fig. 6. Influence of the type of dispersive solvent on the extraction recovery of metal ions obtained by DLLME. Extraction conditions: sample volume 10.0 mL; disperser solvent volume 0.40 mL; salophen amount 1.0×10^{-2} mol L^{-1}; ionic liquid amount 130 mg; concentration of: Ni(II) 40.0; Co(II) 60.0; Cu(II) 20.0 and Zn(II) 50.0 µg L^{-1}.

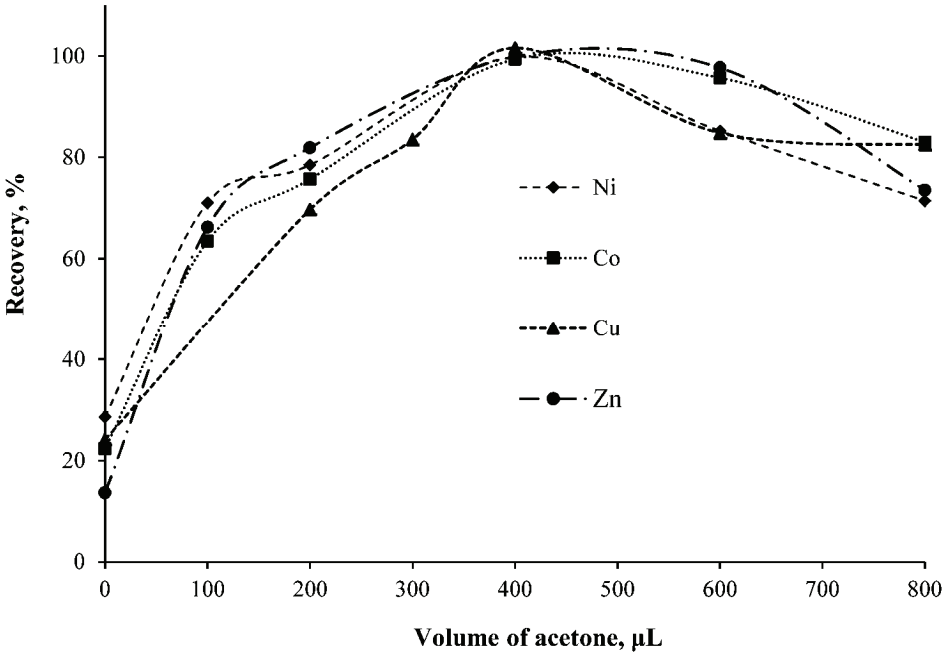

Fig. 7. Influence of the volume of the disperser solvent on the extraction recovery of metal ions obtained from DLLME. Extraction conditions: sample volume 10.0 mL; salophen amount 1.0×10^{-2} mol L^{-1}; amount of [hmim][PF_6] 130 mg; concentration of: Ni(II) 40.0; Co(II) 60.0; Cu(II) 20.0 and Zn(II) 50.0 µg L^{-1}.

Influence of the extraction time

An extraction process is time dependent. The extraction time in this experiment was defined as the interval between injection of the mixture of methanol and IL and the start of centrifugation. To evaluate the optimum extraction time, similar experiments were undertaken at time intervals in the range 0–20 min. The results showed that the extraction time had no significant effect on the extraction efficiency. It could be concluded that the extraction process is fast and immediately after the formation of the cloudy solution, equilibrium is achieved due to the large surface area between the IL droplets and the aqueous phase. Consequently, a short time was required for the extraction. Therefore, the phase separation by centrifugation was performed immediately after mixing the reagents.

Centrifugation parameters

In DLLME process, centrifugation affects the size of the settled phase and the concentration of analyte in the extraction phase. In this regard, a set of similar experiments were conducted and it was observed that centrifuging the cloud mixture for 5 min at 4000 rpm results in an efficient and suitable phase sepa-

ration leading to an oil phase that can be efficiently introduced into the HPLC system. Hence, 5 min at 4000 rpm was chosen for the further experiments.

Influence of ionic strength

The effect of ionic strength on the extraction efficiency was evaluated by adding various amounts of $NaNO_3$ (0.0–1.0 mol L^{-1}) into the sample solutions, the other parameters being kept constant. The results confirmed that the addition of salt up to 0.6 mol L^{-1} has no significant effect on the extraction efficiency and the extractions of all species were quantitative. On increasing the ionic strength (from 0.6 to 1.0 mol L^{-1}), the solubility of the extraction solvent (IL) in the aqueous phase increases. As a result, the volume of the sedimented phase decreases, which reduce the extraction recoveries. These observations revealed the possibility of using this method for the pre-concentration of the target analytes from saline solutions of up to 0.6 mol L^{-1}.

Influence of co-existing ions

The influence of various co-existing ions in the water samples on the recovery of the investigated metal ions in the DLLME process was studied. In these experiments, 10.0 mL of solutions containing 200.0 μg L^{-1} of metal ions and various amounts of interfering ions was treated according to the recommended procedure. Tolerance limit was defined as the analyte ion/interferent ratio that caused an error smaller than ±5 %. The interferences were investigated and from the observations (Table I), it can be concluded that the method is suitable for trace metal enrichment in the presence of high amounts of co-existing ions.

TABLE I. Interference study for nickel, cobalt, copper and zinc determination

Species	Tolerance limit[a]			
	w_{ion}/w_{Ni}	w_{ion}/w_{Co}	w_{ion}/w_{Cu}	w_{ion}/w_{Zn}
Mg^{2+}, Ca^{2+}, K^+, Na^+, Li^+, NO_3^-, Cl^-, F^-, I^-, SO_4^-	1000	1000	1000	1000
Cd^{2+}	1000	1000	1000	500
Ba^{2+}	1000	1000	1000	500
Al^{3+}	1000	1000	1000	25
Mn^{2+}	25	1000	1000	1000
Sn^{2+}	500	1000	1000	500
Cu^{2+}	25	50	–	100
Zn^{2+}	100	100	50	–
Ni^{2+}	–	100	25	50
Co^{2+}	50	–	50	50
Ag^+	25	25	1000	50
Cr^{3+}	1000	50	50	10
Pb^{2+}	25	10	25	10
Fe^{2+}	10	10	10	10

[a]Concentration of each metal ion was 200 μg L^{-1}

Analytical figures of merit

The characteristics of the performance of the optimized method, including linear range, reproducibility, limit of detection (*LOD*) and enhancement factor, are summarized in Table II. Linearity was observed in the ranges 2.5–300.0 μg L^{-1} for Ni(II), 6.0–350.0 μg L^{-1} for Co(II), 7.0–700.0 μg L^{-1} for Cu(II) and 22.0–500.0 μg L^{-1} for Zn(II). Each analyte exhibited good linearity with correlation coefficients (R^2) ranging from 0.990 to 0.998. The reproducibility of the method was checked for seven replicate extractions of spiked water samples at concentration levels of 80.0 μg L^{-1} and the relative standard deviation (*RSD*) varied between 3.6 and 5.1 %. The *LOD* values, based on signal-to-noise ratio of 3, were in the range of 0.8–2.8 μg L^{-1}. The enrichment factor, which was about 222 for all species, was obtained from the ratio of sample volume before and after extraction.

TABLE II. Values of merit for the proposed method

Parameter	Ni	Co	Cu	Zn
Dynamic linear range, μg L^{-1}	2.5–300.0	6.0–350.0	7.0–700.0	9.5–500.0
Calibration equation, μg L^{-1}	$y = 25482x$ – – 10659	$y = 4160x$ + + 47084	$y = 22303x$ – – 83814	$y = 22531x$ + + 11570
R^2	0.997	0.998	0.990	0.990
LOD / μg L^{-1} (n = 5)	0.8	1.6	1.9	2.8
RSD / % (n = 10)	4.2	5.0	5.1	3.6
Enrichment factor	222	222	222	222
Enhancement factor[a]	113.8	22.0	70.9	73.5

[a]The enhancement factor is the slope ratio of the calibration graph after and before extraction

Analysis of real samples

The practical applicability of the recommended method was evaluated by extracting four metal ions from different water samples, *i.e.*, tap, well, mineral and river water. The water samples were collected in acid-leached polyethylene bottles and filtered through a filter paper (Whatman, No. 42) before analyses to remove suspended particulate materials. The samples were subjected to UV irradiation for 2 h with a 160 W UV-lamp. Each sample was spiked with target species at two different concentration levels and analyzed in triplicate using the developed DLLME procedure. The obtained results (Table III) indicate that the matrices of the real water samples did not have an obvious effect on the proposed IL–DLLME method for pre-concentration and determination of the analytes in the water samples.

TABLE III. Determination of the metal ions in different water samples; ND – not detected

Sample	Added µg L^{-1}	Ni		Co		Cu		Zn	
		Found[a] µg L^{-1}	Recovery %	Found µg L^{-1}	Recovery %	Found µg L^{-1}	Recovery %	Found µg L^{-1}	Recovery %
Tap water[b]	0.0	11.7±0.5	–	ND	–	17.4±0.5	–	321.4±9.4	–
	10.0	21.1±0.8	94.0	10.3±0.4	103.0	26.8±0.7	94.0	331.2±10.1	98.0
	20.0	31.0±1.2	96.6	19.2±0.5	96.0	36.9±0.7	97.5	340.7±9.8	96.5
River	0.0	7.3±0.3	–	6.8±0.4	–	19.2±0.6	–	64.9±2.0	–
water[c]	20.0	26.3±1.1	95.0	25.8±0.9	95.0	38.4±1.2	96.0	83.8±2.8	94.5
	30.0	37.3±1.2	100.0	35.8±0.8	96.7	47.6±1.3	94.7	94.8±1.8	99.7
Well	0.0	11.8±0.7	–	10.0±0.5	–	24.1±0.6	–	79.0±2.1	–
water[d]	10.0	21.7±1.0	99.0	19.6±0.9	96.0	34.3±0.8	102.0	88.6±1.9	96.0
	20.0	30.8±0.9	95.0	28.9±0.8	94.5	43.3±0.9	96.0	98.1±2.5	95.5
Mineral	0.0	10.2±0.6	–	ND	–	13.8±0.7	–	37.0±0.9	–
water[e]	10.0	20.5±0.8	103.0	9.5±0.5	95.0	23.4±0.9	96.0	47.2±1.1	102.0
	20.0	29.5±0.9	96.5	19.6±0.9	98.0	32.8±1.1	95.0	56.9±1.6	99.5

[a]mean±standard deviation (n = 3); [b]Tehran, Iran water; [c]Kan River (Tehran, Iran) water; [d]Shahriar (Tehran, Iran) well water; [e]Damavand company

CONCLUSIONS

A new method consisting of ionic liquid-based dispersive liquid–liquid microextraction combined with HPLC-UV was described for the determination of zinc, copper, cobalt and nickel in environmental water samples. In the proposed procedure, salophen was successfully used as the complexing agent for preconcentration of the metal ions. This led to the development of a simple, rapid, sensitive with high pre-concentration factor method. Additionally, the employment of the ionic liquid exhibited some advantages, such as a reduction of exposure to toxic solvent, the possibility of obtaining more reproducible results since evaporation of the extractant is not required, and a directly analyzable extract is obtained in a short-single step. The results obtained in this work demonstrated that the proposed method is applicable for the analysis of trace amounts of Zn, Cu, Co and Ni in water samples.

Acknowledgements. The authors gratefully acknowledge the financial support for this project from the Semnan University Research Council.

И З В О Д

ДИСПЕРЗИВНА МИКРОЕКСТРАКЦИЈА ТЕЧНО–ТЕЧНО БАЗИРАНА НА ЈОНСКИМ ТЕЧНОСТИМА СПРЕГНУТА СА ВИСОКОЕФИКАСНОМ ТЕЧНОМ ХРОМАТОГРАФИЈОМ СА UV ДЕТЕКЦИЈОМ ЗА ИСТОВРЕМЕНО ПРЕКОНЦЕНТРИСАЊЕ И ОДРЕЂИВАЊЕ Ni, Co, Cu И Zn У УЗОРЦИМА ВОДА

ALIREZA ASGHARI[1], MEHRI GHAZAGHI[1], MARYAM RAJABI[1], MAHDI BEHZAD[1] и MEHRORANG GHAEDI[2]

[1]*Department of Chemistry, Semnan University, Semnan 35195-363, Iran* и [2]*Department of Chemistry, Yasouj University, Yasouj 75918-74831, Iran*

Развијена је метода дисперзивне микроекстракције течно–течно базиране на јонским течностима (IL–DLLME) спрегнуте са високоефикасном течном хроматографијом (HPLC) уз UV детекцију, за истовремену екстракцију и одређивање никла, кобалта, бакра и цинка. У предложеном приступу коришћен је салофен (*N,N*′-бис(салисилиден)-1,2-фенилендиамин) као хелирајући реагенс; јонска течност, 1-хексил-3-метилимидазолиум-хексафлуорофосфат, и ацетон су изабрани као раствори за екстракцију, односно диспергување. Раздвајање фаза после екстракције изведено је центрифугирањем, а сталожена фаза (јонска течност) је растворена у ацетонитрилу и директно инјектирана у HPLC систем за анализу. Раздвајање комплекса метала је изведено помоћу RP-C18 колоне применом градијентног елуирања смеша са метанол–ацетонитрил–вода мобилном фазом са брзином протока од 1,0 mL min^{-1}. Испитиван је и оптимизован утицај промењљивих као што су: pH узорка, концентрација хелирајућег реагенса, количина јонске течности (екстракционог раствора), запремине раствора за диспергување, времена екстракције, соног ефекта и брзине центрифугирања. Под оптималним условима добијен је фактор концентрисања од 222. Границе детекције Ni, Co, Cu и Zn износиле су: 0,8, 1,6, 1,9 и 2,8 μg L^{-1}, редом. Релативна стандардна девијација (*RSD*) је била у опсегу 3,6–5,0 % за све испитиване јоне метала. Предложена процедура је била успешно примењена за одређивање јона метала у узорцима вода.

(Примљено 22. јуна 2012, ревидирано 11. јануара 2013)

REFERENCES

1. C. K. Wong, A. P. Pak, *Bull. Environ. Contam. Toxicol.* **73** (2004) 190
2. A. R. K. Dapaah, N. Takano, A. Ayame, *Anal. Chim. Acta* **386** (1999) 281
3. D. Zendelovska, G. Pavlovsk, K. Cundeva, T. Stafilov, *Talanta* **54** (2001) 139
4. I. Komjarova, R. Blust, *Anal. Chim. Acta* **576** (2006) 221
5. M. Ghaedi, F. Ahmadi, A. Shokrollahi, *J. Hazard. Mater.* **142** (2007) 272
6. M. Ghaedi, F. Ahmadi, A. Shokrollahi, *J. Hazard. Mater.* **142** (2007) 272
7. M. Ghaedi, F. Ahmadi, M. Soylak, *J. Hazard. Mater.* **147** (2007) 226
8. M. Ghaedi, F. Ahmadi, M. Soylak, *Ann. Chim.* **97** (2007) 277
9. M. Ghaedi, M. R. Fathi, F. Marahel, F. Ahmadi, *Feresen. Environ. Bull.* **14** (2005) 1158
10. M. Ghaedi, A. Shokrollahi, A. H. Kianfar, A. S. Mirsadeghi, A. Pourfarokhi, M. Soylak, *J. Hazard. Mater.* **154** (2008) 128
11. V. Gurnani, A. K. Singh, B. Venkataramani, *Talanta* **61** (2003) 889
12. A. Shokrollahi, M. Ghaedi, O. Hossaini, N. Khanjari, M. Soylak, *J. Hazard. Mater.* **160** (2008) 435
13. S. Candir, I. Narin, M. Soylak, *Talanta* **77** (2008) 289
14. F. Shemirani, R. R. Kozani, Y. Assadi, *Microchim. Acta* **157** (2007) 81
15. G. Doner, A. Ege, *Anal. Chim. Acta* **547** (2005) 14
16. V. Umashankar, R. Radhamani, K. Ramadoss, D. S. R. Murty, *Talanta* **57** (2002) 1029
17. U. Divrikli, L. Elci, *Anal. Chim. Acta* **452** (2002) 231
18. F. R. P. Rocha, L. S. G. Teixeira, J. A. Nóbrega, *Spectrosc. Lett.* **42** (2009) 1532
19. D. Djozan, Y. Assadi, *Chromatographia* **60** (2004) 313
20. D. Djozan, Y. Assadi, S. Hosseinzadeh, *Anal. Chem.* **73** (2001) 4054
21. M. R. Khalili, Y. Yamini, S. Shariati, J. A. Jonsson, *Anal. Chim. Acta* **585** (2007) 286
22. T. S. Ho, T. Vasskog, T. Anderssen, E. Jensen, K. E. Rasmussen, S. P. Bjergaard, *Anal. Chim. Acta* **592** (2007) 1
23. F. Ahmadi, Y. Assadi, M. R. M. Hosseini, M. Rezaee, *J. Chromatogr., A* **1101** (2006) 307
24. E. Psillakis, N. Kalogerakis, *Trends Anal. Chem.* **22** (2003) 565
25. P. Helena, I. K. Locita, *Trends Anal. Chem.* **18** (1999) 272
26. L. Zhao, H. K. Lee, *J. Chromatogr., A* **919** (2001) 381
27. S. Pedersen-Bjergaard, K. E. Rasmussen, *Anal. Chem.* **71** (1999) 2650
28. P. Li, Y. M. Qiu, H. X. Cai, Y. Kong, Y. Z. Tang, D. N. Wang, M. X. Xie, *Chin. J. Chromatogr.* **24** (2006) 14
29. M. Rezaee, Y. Assadi, M. R. M. Hosseini, E. Aghaee, F. Ahmadi, S. Berijani, *J. Chromatogr., A* **1116** (2006) 1
30. J. S. Chiang, S. D. Huang, *Talanta* **75** (2008) 70
31. M. A. Farajzadeh, M. Bahram, J. A. Jonsson, *Anal. Chim. Acta* **591** (2007) 69
32. E. Z. Jahromi, A. Bidari, Y. Assadi, M. R. M. Hosseini, M. R. Jamali, *Anal. Chim. Acta* **585** (2007) 305
33. H. M. Jiang, Y. C. Qin, B. Hu, *Talanta* **74** (2008) 1160
34. P. Liang, J. Xu, Q. Li, *Anal. Chim. Acta* **609** (2008) 53
35. M. Shamsipur, M. Ramezani, *Talanta* **75** (2008) 294
36. N. Shokoufi, F. Shemirani, Y. Assadi, *Anal. Chim. Acta* **597** (2007) 349
37. M. A. Farajzadeh, M. Bahram, M. R. Vardast, *J. Sep. Sci.* **32** (2009) 4200
38. M. A. Farajzadeh, M. Bahram, M. R. Vardast, *CLEAN – Soil Air Water* **38** (2010) 466
39. J. F. Liu, J. A. Jonsson, G. B. Jiang, *Trends Anal. Chem.* **24** (2005) 20
40. D. Chen, A. E. Martell, *Inorg. Chem.* **26** (1987) 1026
41. P. X. Baliza, L. S. G. Teixeira, V. A. Lemos, *Microchem. J.* **93** (2009) 220
42. M. B. Melwanki, M. R. Fuh, *J. Chromatogr., A* **1207** (2008) 24.

Journal of the Serbian Chemical Society
JSCS-info@shd.org.rs • www.shd.org.rs/JSCS
J. Serb. Chem. Soc. *79* (1) 77–87 (2014)
JSCS–4566
UDC 547–326+547.37:541.25:
532.13/.14.08+536.7
Original scientific paper

Densities, refractive indices and viscosities of the binary mixtures of dimethyl phthalate or dimethyl adipate with tetrahydrofuran

ANDJELA B. KNEŽEVIĆ-STEVANOVIĆ, JELENA D. SMILJANIĆ, SLOBODAN P. ŠERBANOVIĆ[#], IVONA R. RADOVIĆ[#] and MIRJANA LJ. KIJEVČANIN*[#]

Faculty of Technology and Metallurgy, University of Belgrade, Karnegijeva 4, P. O. Box 35-03, 11120 Belgrade, Serbia

(Received 7 April, revised 23 April 2013)

Abstract: Densities, refractive indices and viscosities of the binary mixtures of dimethyl phthalate (or dimethyl adipate) + tetrahydrofuran have been measured at eight temperatures (288.15 to 323.15 K) and atmospheric pressure. All measurements were performed using an Anton Paar DMA 5000 digital vibrating-tube densimeter, Anton Paar RXA 156 refractometer and Anton Paar SVM 3000/G2 digital Stabinger viscometer, respectively. From the experimental densities, refractive indices and viscosities, the excess molar volumes, V^E, deviations of refractive indices, Δn_D, and viscosity deviations, $\Delta\eta$, were calculated.

Keywords: experimental measurements; excess molar volumes; deviations of refractive indices; viscosity deviations; esters; ethers.

INTRODUCTION

This article is a continuation of previous research dealing with the experimental determination of volumetric and transport properties of binary and ternary mixtures containing different organic solvents, such as alcohols and aromatics, chlorinated aromatics, esters, ketones, chlorinated alkanes or amines.[1–10] An intention of this study is to provide a set of volumetric and transport data in order to asses the influence of temperature and molecular structure on the behaviour of mixtures of esters (dimethyl phthalate or dimethyl adipate) and ethers (tetrahydrofuran). From the theoretical viewpoint, this is an important source of information for the characterization of interactions between components and is helpful in understanding the liquid state theory, as well. Besides, esters and ethers are widely used in a variety of industrial and consumer applications, and hence, knowledge of their physical properties is of great importance from a practical

* Corresponding author. E-mail: mirjana@tmf.bg.ac.rs
[#] Serbian Chemical Society member.
doi: 10.2298/JSC130407045K

point of view, too. Phthalates are widely used in the automobile, cable, medical equipment and the toy industries, as plasticizers and as performance enhancers in the manufacture of glues and paints. Dimethyl phthalate is used as an additive for plastics, which increases their flexibility, transparency and stability. Dimethyl adipate is an organic solvent for inks, coatings and adhesives, an emollient that can be used in the manufacture of agrochemicals, synthetic leather, paint strippers, plasticizers, or as a food additive and pigment dispersant. Tetrahydrofuran is primarily used as an industrial solvent for poly(vinyl chloride) and varnishes.

In the present work, measured densities, ρ, refractive indices, n_D, and viscosities, η, are reported for the two binary systems containing dimethyl phthalate (or dimethyl adipate) and tetrahydrofuran at eight temperatures (from 288.15 to 323.15 K) and atmospheric pressure. The excess molar volumes, V^E, deviations of the refractive indices, Δn_D, and viscosity deviations, $\Delta\eta$, of the investigated mixtures were calculated from the measured data.

To the best of our knowledge, ρ, n_D and η experimental data are not available for the investigated binary systems and no V^E, Δn_D and $\Delta\eta$ values were found in the currently published articles.

EXPERIMENTAL

Materials

All products were of high purity (mass fraction purity > 0.99) and used without further purification: dimethyl phthalate (>0.99) was supplied by Fluka, while dimethyl adipate (≥0.99) and tetrahydrofuran (min 0.995) were Merck products. Two different bottles of Merck-supplied high purity tetrahydrofuran (min 0.995) were used in the experimental work: one was used in the experiments with dimethyl phthalate and another in the experiments with dimethyl adipate. All the organic liquids were stored in brown glass bottles under an inert nitrogen atmosphere. Pure components were degassed in an ultrasonic bath shortly before sample preparation. Densities, refractive indices and viscosities of the pure components at the temperatures 293.15 and 298.15 K, together with the corresponding literature values,[11–19] are listed in Table I.

TABLE I. Density, ρ, refractive index, n_D, and viscosity, η, values of the studied pure components

T / K	ρ / 10^3 kg m^{-3}		n_D		η / mPa s	
	Exp.	Lit.	Exp.	Lit.	Exp.	Lit.
			Tetrahydrofuran			
298.15	0.882330[a]	0.882358[11]	1.404984[a]	1.40496[13]	0.48821[a]	0.456[12]
	0.882402[b]	0.882502[12]	1.404322[b]		0.47984[b]	0.460[13]
			Dimethyl phthalate			
298.15	1.186933	1.18657[14]	1.513544	1.5137[15], 1.513[16]	13.847	13.76169[14]
			Dimethyl adipate			
293.15	1.061928	1.06190[17]	–	–	3.2894	3.36[19]
298.15	–	–	1.426356	1.4215[17], 1.4283[18]	2.9101	2.98[19]

[a]First bottle, system with dimethyl phthalate; [b]second bottle, system with dimethyl adipate

Apparatus and procedure

The densities of the binary mixtures, and corresponding pure substances were measured with an Anton Paar DMA 5000 digital vibrating U-tube densimeter having a stated accuracy $\pm 5\times10^{-3}$ kg m^{-3}. The temperature in the cell was measured by means of two integrated Pt 100 platinum thermometers with a stability of better than ± 0.002 K; the temperature was regulated to ±0.001 K with a built-in solid-state thermostat. The refractive indices were measured by an Anton Paar RXA 156 refractometer with a stated accuracy of $\pm 5\times10^{-5}$, and the temperature was controlled with an internal Peltier thermostat to ±0.03 K. The viscosities were measured with an Anton Paar SVM 3000/G2 digital Stabinger viscometer, with a stated accuracy of ±0.1 % of the measurement value and the temperature was regulated with an uncertainty of ±0.01 K by a built in solid-state thermostat.

In order to minimize evaporation of the volatile solvents and to avoid errors in the compositions, all mixtures presented in this paper were prepared by mass using the cell and a previously described procedure.[20,21] The masses were measured using a Mettler AG 204 balance, with a precision of 1×10^{-7} kg. The uncertainty in the calculation of the mole fraction was less than $\pm 1\times10^{-4}$. All molar quantities were based on the IUPAC relative atomic mass table. The experimental uncertainty (from repeated measurements) in the density, refractive index and viscosity measurements were about $\pm 1\times10^{-2}$ kg m^{-3}, $\pm 1\times10^{-4}$ and < 1.5 %, respectively, while the average uncertainty in the excess molar volume, refractive index deviation and viscosity deviation were estimated at $\pm 3\times10^{-9}$ m^3 mol^{-1}, $\pm 2\times10^{-4}$ and better than $\pm 3\times10^{-3}$ mPa s, respectively.

RESULTS AND DISCUSSION

Excess molar volumes V^E were calculated from the density data by the equation:

$$V^E = \sum_{i=1}^{N} x_i M_i \left[\left(1/\rho\right) - \left(1/\rho_i\right) \right] \quad (1)$$

where N is the number of components; x_i is the mole fraction of component i in the mixture; M_i is its molecular weight; ρ and ρ_i are the measured densities of the mixture and the pure component i, respectively.

The refractive index deviations, Δn_D, were calculated as follows:

$$\Delta n_D = n_D - \sum_{i=1}^{N} x_i n_{Di} \quad (2)$$

where n_D and n_{Di} are the measured refractive indices of the mixture and the pure component i, respectively.

The viscosity deviations, $\Delta\eta$, were calculated from the equation:

$$\Delta\eta = \eta - \sum_{i=1}^{N} x_i \eta_i \quad (3)$$

where η and η_i are the measured viscosities of the mixture and the pure component i, respectively.

The results of V^E, Δn_D and $\Delta\eta$ were correlated with the Redlich–Kister (RK) Equation:[22]

$$Y = x_i x_j \sum_{p=0}^{k} A_p (2x_i - 1)^p \quad (4)$$

where Y denotes V_{ij}^E / m^3·mol^{-1}, Δn_D, or $\Delta\eta$ / mPa·s, A_p, are the adjustable parameters of the related property, and the number of adjustable parameters (k + 1) was determined using the F-test.[23]

The results of ρ, V^E, n_D, Δn_D, η and $\Delta\eta$ for the investigated binaries, in the temperature range and over the entire concentration range, are summarized in Table S-1 of the Supplementary material to this paper. Table II lists the coefficients A_p for the V^E, Δn_D and $\Delta\eta$ at each temperature separately, and the corresponding root-mean-square deviations (σ) given by the equation:

$$\sigma = \left(\sum_{i=1}^{m} \left(Y_{\text{exp},i} - Y_{\text{cal},i} \right)^2 \Big/ m \right)^{1/2} \quad (5)$$

where m is the number of experimental data points.

The results were also fitted and explained using the reduced excess molar volume, V^E/x_1x_2, refractive index deviation, $\Delta n_D/x_1x_2$, and viscosity deviation, $\Delta\eta/x_1x_2$.

TABLE II. Parameters A_p of Eq. (4) and the corresponding root mean square deviations, σ

T / K	A_0	A_1	A_2	A_3	A_4	$\sigma\times10^2$
Dimethyl phthalate (1) + tetrahydrofuran (2)						
V^E / 10^{-6} m^3 mol^{-1}						
288.15	–2.6986	0.3765	0.3855	1.0737	–	0.85
293.15	–2.7797	0.3896	0.4101	1.1170	–	0.87
298.15	–2.8622	0.4216	0.3845	1.1240	–	0.85
303.15	–2.9520	0.4544	0.3826	1.1361	–	0.85
308.15	–3.0495	0.4699	0.3800	1.1922	–	0.87
313.15	–3.1571	0.4934	0.3777	1.2369	–	0.89
318.15	–3.2404	0.6075	0.2676	1.0932	–	0.76
323.15	–3.3078	0.6088	0.3930	0.9423	–	0.79
Δn_D						
288.15	0.0849	–0.0325	0.0124	–0.0063	–	0.01
293.15	0.0853	–0.0327	0.0117	–0.0068	–	0.01
298.15	0.0855	–0.0327	0.0126	–0.0076	–	0.01
303.15	0.0861	–0.0329	0.0120	–0.0082	–	0.01
308.15	0.0862	–0.0313	0.0123	–0.0128	–	0.01
313.15	0.0858	–0.0313	0.0132	–0.0124	–	0.01
318.15	0.0863	–0.0308	0.0128	–0.0132	–	0.01
323.15	0.0861	–0.0309	0.0155	–0.0152	–	0.02

TABLE II. Continued

T / K	A_0	A_1	A_2	A_3	A_4	$\sigma\times10^2$
Dimethyl phthalate (1) + tetrahydrofuran (2)						
			$\Delta\eta$ / mPa s			
288.15	–33.4291	–20.0319	–11.3009	–4.4937	–	2.43
293.15	–23.9657	–13.2136	–6.6039	–2.2368	–	2.10
298.15	–17.6840	–8.8378	–3.8201	–1.2562	–	1.89
303.15	–13.3160	–6.1789	–2.4057	–0.4603	–	1.51
308.15	–10.2461	–4.3833	–1.4981	–0.0010	–	1.27
313.15	–8.0454	–2.9403	–0.6578	–0.7116	–	1.87
318.15	–6.3678	–2.2431	–0.6323	0.1581	–	0.89
323.15	–5.1077	–1.7111	–0.5757	0.5363	–	0.80
Dimethyl adipate (1) + tetrahydrofuran (2)						
			V^E / 10^{-6} m^3 mol^{-1}			
288.15	–0.1986	0.1311	–0.1620	–0.0862	0.2422	0.02
293.15	–0.2335	0.1434	–0.1640	–0.0810	0.2390	0.01
298.15	–0.2725	0.1567	–0.1634	–0.0822	0.2297	0.01
303.15	–0.3152	0.1705	–0.1616	–0.0768	0.2215	0.01
308.15	–0.3593	0.1872	–0.1697	–0.0761	0.2196	0.02
313.15	–0.4086	0.2037	–0.1764	–0.0697	0.2204	0.02
318.15	–0.4612	0.2247	–0.1821	–0.0683	0.2178	0.02
323.15	–0.5190	0.2463	–0.1947	–0.0594	0.2206	0.03
			Δn_D			
288.15	0.0153	–0.0057	0.0028	–0.0019	–	0.001
293.15	0.0158	–0.0060	0.0030	–0.0019	–	0.001
298.15	0.0163	–0.0060	0.0030	–0.0023	–	0.001
303.15	0.0169	–0.0068	0.0027	–0.0010	–	0.001
308.15	0.0174	–0.0066	0.0026	–0.0017	–	0.001
313.15	0.0178	–0.0067	0.0026	–0.0020	–	0.001
318.15	0.0180	–0.0069	0.0028	–0.0020	–	0.001
323.15	0.0184	–0.0067	0.0026	–0.0022	–	0.001
			$\Delta\eta$ / mPa s			
288.15	–1.7896	–0.0179	0.0909	–0.0164	–0.0088	0.08
293.15	–1.4060	0.0285	0.0519	–0.0027	0.0264	0.04
298.15	–1.1035	0.0621	0.0004	–0.0073	0.0962	0.04
303.15	–0.8827	0.0868	–0.0111	–0.0347	0.0494	0.14
308.15	–0.6952	0.1021	–0.0925	–0.0198	0.1344	0.15
313.15	–0.5431	0.1447	–0.0766	–0.0850	0.0353	0.14
318.15	–0.4063	0.0614	–0.3521	0.0455	0.3789	0.12
323.15	–0.2925	0.1094	0.0610	–0.2807	0.0478	0.10

The dependence V^E–x_1, Δn_D–x_1 and $\Delta\eta$–x_1, respectively, for the systems measured in this work are shown in Fig. 1.

The calculated V^E/x_1x_2, $\Delta n_D/x_1x_2$ and $\Delta\eta/x_1x_2$ values, respectively, are plotted as a function of the mole fraction of an ester in Fig. 2. The nonlinear curves obtained for all the investigated systems represent their evident non-ideal behaviour.

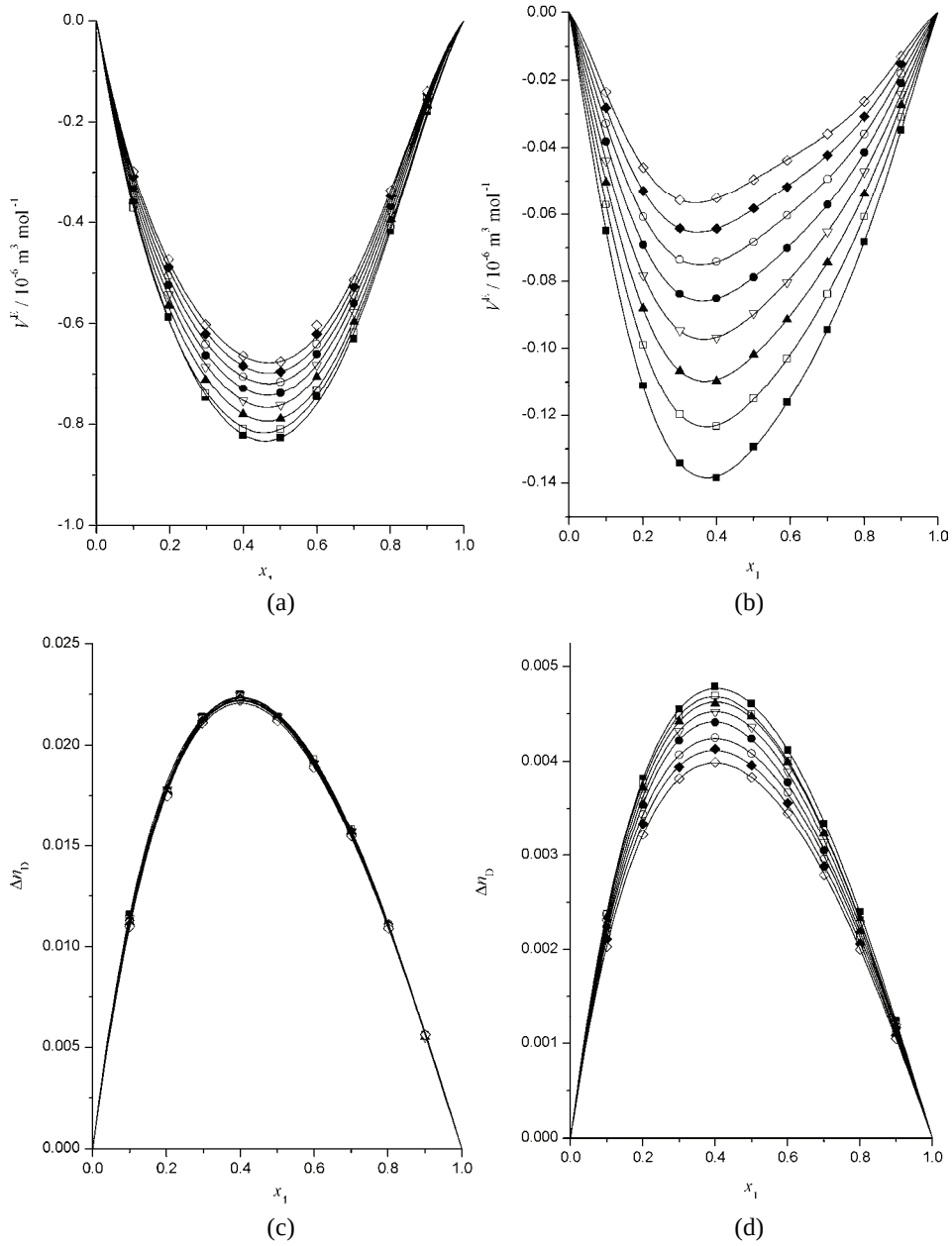

Fig. 1. Data for the binary systems: a) V^E values for dimethyl phthalate (1) + tetrahydrofuran (2), b) V^E values for dimethyl adipate (1) + tetrahydrofuran (2), c) Δn_D values for dimethyl phthalate (1) + tetrahydrofuran (2) and d) Δn_D values for dimethyl adipate (1) + tetrahydrofuran (2). The symbols refer to experimental data points at: ◊, 288.15; ◆, 293.15; ○, 298.15; ●, 303.15; ▽, 308.15; ▲, 313.15; □, 318.15; ■, 323.15 K. The lines present the results calculated by Eq. (4) with the parameters presented in Table II.

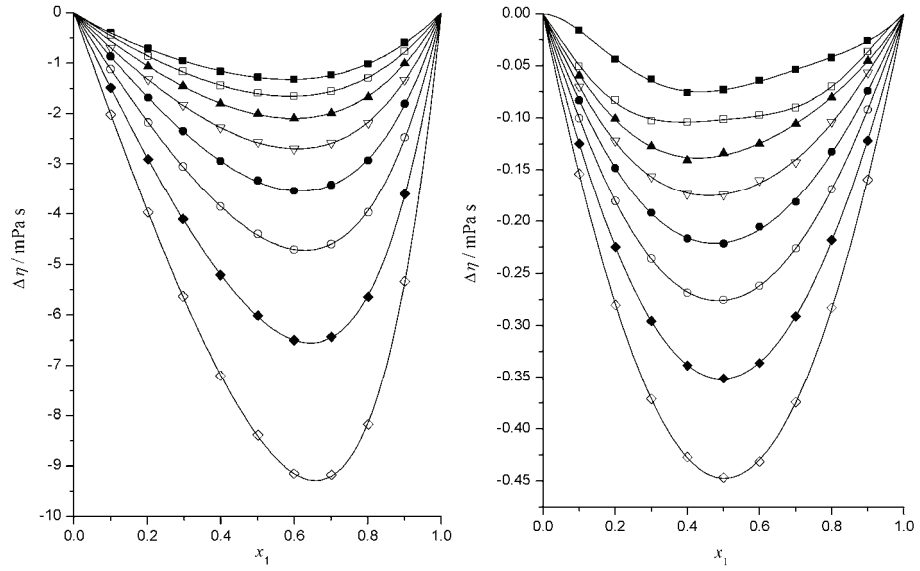

(e) (f)

Fig. 1. (Continued). e) $\Delta\eta$ values for dimethyl phthalate (1) + tetrahydrofuran (2) and f) dimethyl adipate (1) + tetrahydrofuran (2).

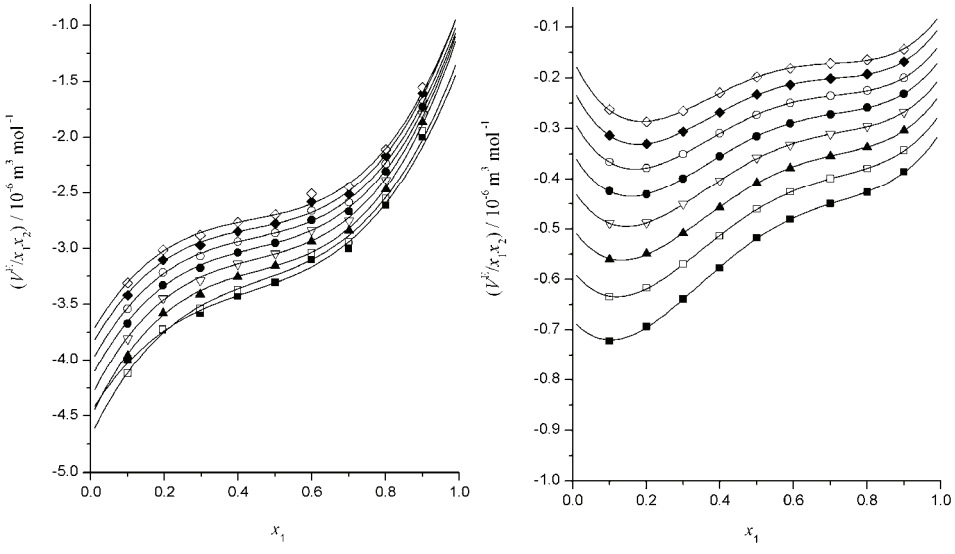

(a) (b)

Fig. 2. Data for the binary systems: a) values of (V^E/x_1x_2) for dimethyl phthalate (1) + tetrahydrofuran (2) and b) dimethyl adipate (1) + tetrahydrofuran (2). The symbols refer to experimental data points at: ◊, 288.15; ◆, 293.15; ○, 298.15; ●, 303.15; ▽, 308.15; ▲, 313.15; □, 318.15; ■, 323.15 K. The lines present the results calculated by Eq. (4) with the parameters presented in Table II.

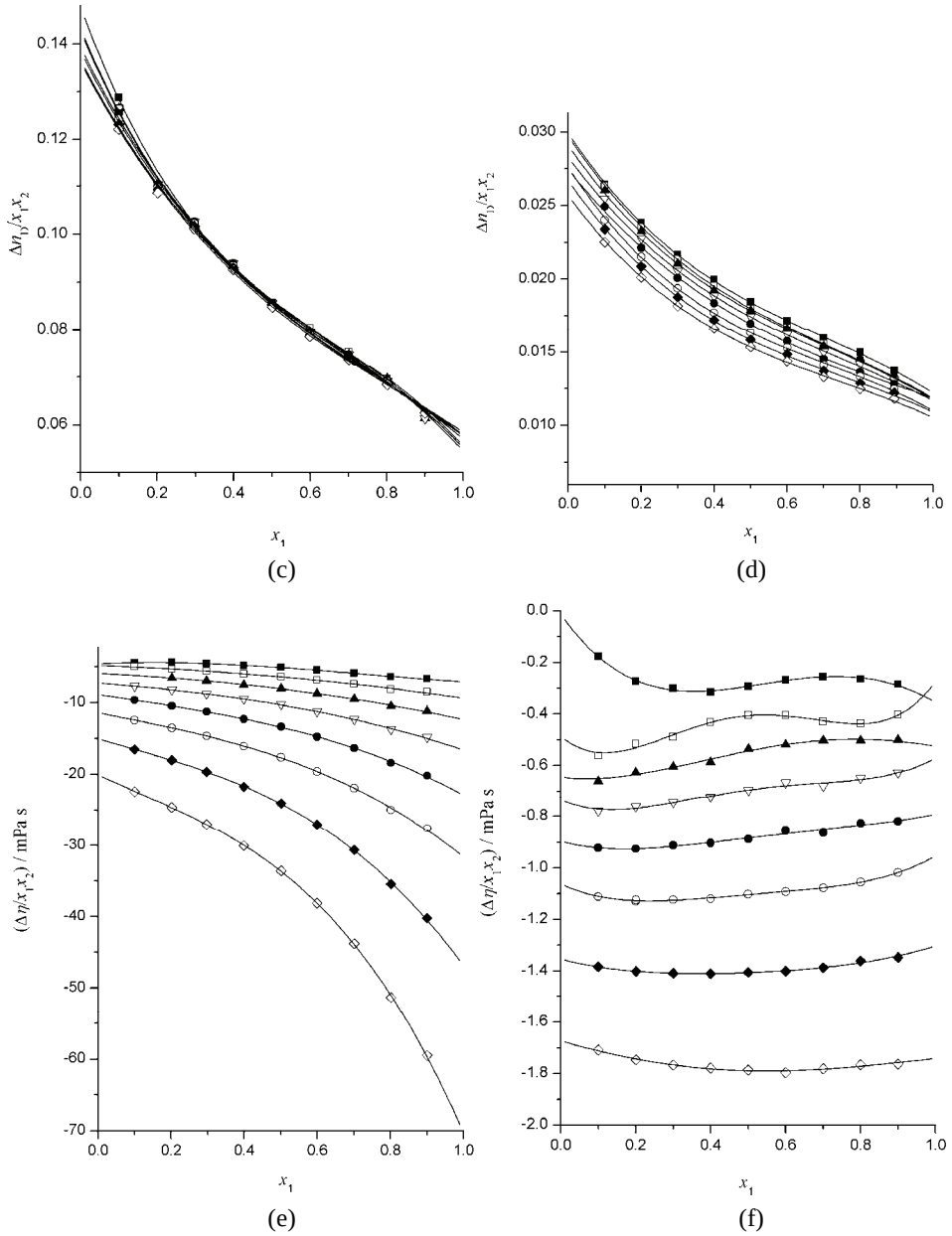

Fig.2. (Continued). c) Values of ($\Delta n_D/x_1x_2$) for dimethyl phthalate (1) + tetrahydrofuran (2), d) values of ($\Delta n_D/x_1x_2$) for dimethyl adipate (1) + tetrahydrofuran (2), e) values of ($\Delta\eta/x_1x_2$) for dimethyl phthalate (1) + tetrahydrofuran (2), and f) values of ($\Delta\eta/x_1x_2$) for dimethyl adipate (1) + tetrahydrofuran (2).

The compounds analyzed herein have good hydrogen bond abilities and polar nature. However, there is no possibility for hydrogen bonds in their mixtures since all analyzed compounds only act as good hydrogen bond acceptors and not proton donors. Tetrahydrofuran[24] has a dipole moment of 5.7×10^{-30} C m, whereas those of dimethyl phthalate[25] and dimethyl adipate[26] are somewhat higher 9.3×10^{-30} and 7.3×10^{-30} C m, respectively. Due to these distinguished polarities of the compounds, association through dipolar forces might be expected. As shown in Fig. 1a, both binaries are characterized by negative V^E values over the entire concentration range. The curve V^E–x_1 for the system dimethyl phthalate + tetrahydrofuran is symmetrical, while that for the system with dimethyl adipate is slightly asymmetrical and shifted towards lower mole fractions of the ester. Tetrahydrofuran is a saturated heterocyclic compound having the characteristics of an aliphatic ether with two free electron pairs on the oxygen atom. In a binary system with an ester, dipole–dipole interactions occur resulting in negative V^E values. The negative sign of V^E also indicates a net packing effect contributed by structural changes arising from interstitial accommodation. It is obvious from Fig. 1 that the contraction in volume for the system with dimethyl phthalate is almost an order of magnitude larger than that for the system with dimethyl adipate. It could be presumed that the dipole–dipole interactions between dimethyl phthalate and tetrahydrofuran are much stronger than the interactions between dimethyl adipate and tetrahydrofuran, due to the higher value of the dipole moment for dimethyl phthalate. With increasing temperature, the V^E values decrease due to the increased molecule activity.

Both binary systems are characterized by a slightly asymmetrical positive Δn_D–x_1 curve, shifted towards lower mole fractions of ester, over the entire concentration range (Fig. 1c and d). The refractive index deviations for the binary containing dimethyl phthalate are an order of magnitude higher than those recorded for the system with dimethyl adipate. The influence of temperature on Δn_D for the system containing dimethyl phthalate is almost negligible, while the Δn_D values increase with increasing temperature for the binary containing dimethyl adipate.

As it is shown in Fig. 1e and f, the $\Delta\eta$–x_1 values are negative for both systems over the entire concentration range, although symmetrical for the system with dimethyl adipate and asymmetrical and shifted towards the higher mole fraction of ester for the system containing dimethyl phthalate. Negative $\Delta\eta$ values mean that a mixture is more viscous than the pure substances. As in the case of the excess molar volumes and changes of refractive indices, deviations in viscosities are much more pronounced for the system with dimethyl phthalate, which confirms that the interactions between dimethyl phthalate and tetrahydrofuran are greatly stronger than those between dimethyl phthalate and tetrahydrofuran. Additionally, the influence of temperature is much more pronounced for

the system containing dimethyl phthalate. In both instances, the $\Delta\eta$ values become less negative with increasing temperature.

CONCLUSIONS

The densities, refractive indices and viscosities for the binary mixtures dimethyl phthalate (or dimethyl adipate) + tetrahydrofuran were measured at eight temperatures (288.15–323.15 K) at atmospheric pressure. The excess molar volumes, refractive index deviations and viscosity deviations were calculated from the experimental data. For both investigated systems, the excess molar volumes and viscosity deviations were negative, while the refractive index deviations were positive.

SUPPLEMENTARY MATERIAL

Densities, excess molar volumes, refractive indices, refractive index deviations, viscosities, and viscosity deviations, for the investigated binary mixtures at different temperatures and atmospheric pressure are available electronically from http://www.shd.org.rs/JSCS/, or from the corresponding author on request.

Acknowledgement. The authors gratefully acknowledge the financial support received from the Research Fund of the Ministry of Education, Science and Technological Development of the Republic of Serbia and the Faculty of Technology and Metallurgy, University of Belgrade (Project No 172063).

И З В О Д

ГУСТИНЕ, ИНДЕКСИ РЕФРАКЦИЈЕ И ВИСКОЗНОСТИ БИНАРНИХ СМЕША ДИМЕТИЛФТАЛАТА ИЛИ ДИМЕТИЛАДИПАТА СА ТЕТРАХИДРОФУРАНОМ

АЊЕЛА Б. КНЕЖЕВИЋ–СТЕВАНОВИЋ, ЈЕЛЕНА Д. СМИЉАНИЋ, СЛОБОДАН П. ШЕРБАНОВИЋ, ИВОНА Р. РАДОВИЋ и МИРЈАНА Љ. КИЈЕВЧАНИН

Технолошко–металуршки факултет, Универзитет у Београду, Карнегијева 4, 11120 Београд

Густине, индекси рефракције и вискозности бинарних смеша диметилфталата (или диметиладипата) + тетрахидрофуран су мерене на осам температура (288,15–323,15 K) и на атмосферском притиску. Сва мерења су извршена на Anton Paar DMA 5000 дигиталном густиномеру, односно Anton Paar RXA 156 рефрактометру и Anton Paar SVM 3000/G2 дигиталном вискозиметру. Из експерименталних вредности густина, индекса рефракције и вискозности израчунате су допунске моларне запремине, односно промене индекса рефракције и вискозности наведених смеша.

(Примљено 7. априла, ревидирано 23. априла 2013)

REFERENCES

1. V. D. Spasojević, S. P. Šerbanović, B. D. Djordjević, M. Lj. Kijevčanin**,** *J. Chem. Eng. Data* **58** (2013) 84
2. A. B. Knežević-Stevanović, S. P. Šerbanović, B. D. Djordjević, D. K. Grozdanić, J. D. Smiljanić, M. Lj. Kijevčanin, *Thermochim. Acta* **533** (2012) 28
3. I. R. Radović, S. P. Šerbanović, B. D. Djordjević, M. Lj. Kijevčanin**,** *J. Chem. Eng. Data* **56** (2011) 344

4. E. M. Živković, M. Lj. Kijevčanin, I. R. Radović, S. P. Šerbanović, B. D. Djordjević, *Fluid Phase Equilib.* **299** (2010) 191
5. I. R. Radović, M. Lj. Kijevčanin, S. P. Šerbanović, B. D. Djordjević, *Fluid Phase Equilib.* **298** (2010) 117
6. J. D. Smiljanić, M. Lj. Kijevčanin, B. D. Djordjević, D. K. Grozdanić, S. P. Šerbanović, *J. Chem. Eng. Data* **53** (2008) 1965
7. I. R. Radović, M. Lj. Kijevčanin, E. M. Djordjević, B. D. Djordjević, S. P. Šerbanović, *Fluid Phase Equilib.* **263** (2008) 205
8. M. Lj. Kijevčanin, M. M. Djuriš, I. R. Radović, B. D. Djordjević, S. P. Šerbanović, *J. Chem. Eng. Data* **52** (2007) 1136
9. M. Lj. Kijevčanin, I. M. Purić, I. R. Radović, B. D. Djordjević, S. P. Šerbanović, *J. Chem. Eng. Data* **52** (2007) 2067
10. S. P. Šerbanović, M. Lj. Kijevčanin, I. R. Radović, B. D. Djordjević, *Fluid Phase Equilib.* **239** (2006) 69
11. A. P. Kudchadker, S. A. Kudchadker, R. C. Wilhoit, *Key Chemicals Data Books – Furan, Dihydrofuran, Tetrahydrofuran*, Thermodynamics Research Center, Texas Engineering Experiment Station, Texas A & M University, College Station, TX, 1984
12. *TRC Thermodynamic Tables – Non-Hydrocarbons*, Thermodynamics Research Centre, The Texas A & M University System, College Station, TX, 1985
13. J. A. Riddick, W. B. Bunger, *Organic Solvents: Physical Properties and Methods of Purification*, 3rd ed., Wiley Interscience, New York, 1970
14. A. A. Rostami, M. J. Chaichi, M. Sharifi, *Monatsh. Chem*. **138** (2007) 967
15. W. J. Svirbely, W. M. Eareckson, K. Matsuda, H. B. Pickard, I. S. Solet, W. B. Tuemmler, *J. Amer. Chem. Soc.* **71** (1949) 507
16. Kirk-Othmer, *Encyclopedia of Chemical Technology*, 3rd ed., Interscience, New York, 1978
17. E. Ince, *Fluid Phase Equilib*. **230** (2005) 58
18. D. R. Lide, *Handbook of Chemistry and Physics*, 83rd ed., Section 3, CRC Press Inc., Boca Raton, FL, 2002
19. M. J. P. Comuñas, J.-P. Bazile, L. Lugo, A. Baylaucq, J. Fernandez, C. Boned, *J. Chem. Eng. Data* **55** (2010) 3697
20. N. Radojković, A. Tasić, B. Djordjević, D. Grozdanić, *J. Chem. Thermodyn.* **8** (1976) 1111
21. A. Ž. Tasić, D. K. Grozdanić, B. D. Djordjević, S. P. Šerbanović, N. Radojković, *J. Chem. Eng. Data* **40** (1995) 586
22. O. Redlich, A. Kister, *Ind. Eng. Chem.* **40** (1948) 345
23. P. R. Bevington, D. K. Robinson, *Data Reduction and Error Analysis for the Physical Sciences*, McGraw-Hill, Singapore, 1994
24. B. E. Poling, J. M. Prausnitz, J. P. O'Connell, *The Properties of Gases and Liquids*, 5th ed., McGraw-Hill, Singapore, 2007, p. A.23
25. C. L. Yaws, *Thermophysical Properties of Chemicals and Hydrocarbons*, William Andrew Inc., Norwich, NY, 2008, p. 678
26. M.-J. Lee, C.-H. Lai, T.-B. Wang, H.-M. Lin, *J. Chem. Eng. Data* **52** (2007) 1291.

Journal of the Serbian Chemical Society
JSCS@tmf.bg.ac.rs • www.shd.org.rs/JSCS
J. Serb. Chem. Soc. 79 (1) S6–S11 (2014) *Supplementary material*

SUPPLEMENTARY MATERIAL TO

Densities, refractive indices and viscosities of the binary mixtures of dimethyl phthalate or dimethyl adipate with tetrahydrofuran

ANDJELA B. KNEŽEVIĆ-STEVANOVIĆ, JELENA D. SMILJANIĆ, SLOBODAN P. ŠERBANOVIĆ, IVONA R. RADOVIĆ[#] and MIRJANA LJ. KIJEVČANIN[*#]

Faculty of Technology and Metallurgy, University of Belgrade, Karnegijeva 4, P. O. Box 35-03, 11120 Belgrade, Serbia

J. Serb. Chem. Soc. 79 (1) (2014) 77–87

TABLE S-I. Densities, ρ, excess molar volumes, V^E, refractive indices, n_D, refractive index deviations, Δn_D, viscosities, η, and viscosity deviations, $\Delta\eta$, for the investigated binary mixtures at different temperatures (288.15 to 323.15 K) and atmospheric pressure

x_1	ρ / 10^3 kg m^{-3}	V^E / 10^{-6} m^3 mol^{-1}	n_D	Δn_D	η / mPa s	$\Delta\eta$ / mPa s
Dimethyl phthalate (1) + tetrahydrofuran (2)						
T = 288.15 K						
0.0000	0.893223	–	1.41035	–	0.52938	–
0.1001	0.951806	–0.2981	1.43213	0.0110	0.78600	–2.0116
0.2019	1.000397	–0.4856	1.44958	0.0175	1.1555	–3.9489
0.2966	1.038220	–0.6014	1.46331	0.0211	1.6460	–5.6042
0.3989	1.072728	–0.6633	1.47543	0.0222	2.4016	–7.1667
0.5009	1.101964	–0.6745	1.48538	0.0212	3.5339	–8.3457
0.5992	1.125852	–0.6028	1.49360	0.0189	5.0064	–9.1006
0.7006	1.147415	–0.5133	1.50114	0.0155	7.2867	–9.1180
0.8013	1.165669	–0.3358	1.50733	0.0109	10.581	–8.1055
0.9004	1.181524	–0.1394	1.51266	0.0056	15.675	–5.2571
1.0000	1.196257	–	1.51779	–	23.189	–
T = 293.15 K						
0.0000	0.887792	–	1.40769	–	0.50849	–
0.1001	0.946485	–0.3080	1.42959	0.0111	0.74260	–1.4794
0.2019	0.995169	–0.5000	1.44709	0.0176	1.0727	–2.8918
0.2966	1.033099	–0.6201	1.46091	0.0212	1.5055	–4.0800
0.3989	1.067701	–0.6834	1.47309	0.0223	2.1555	–5.1812
0.5009	1.097024	–0.6947	1.48303	0.0213	3.1066	–5.9761
0.5992	1.120978	–0.6204	1.49133	0.0189	4.3128	–6.4525
0.7006	1.142600	–0.5274	1.49890	0.0156	6.1205	–6.3805

* Corresponding author. E-mail: mirjana@tmf.bg.ac.rs

TABLE S-I. Continued

x_1	ρ / 10^3 kg m^{-3}	V^E / 10^{-6} m^3 mol^{-1}	n_D	Δn_D	η / mPa s	$\Delta\eta$ / mPa s
Dimethyl phthalate (1) + tetrahydrofuran (2)						
T = 293.15 K						
0.8013	1.160910	–0.3454	1.50512	0.0109	8.6381	–5.5867
0.9004	1.176814	–0.1440	1.51051	0.0056	12.375	–3.5461
1.0000	1.191593	–	1.51565	–	17.626	–
T = 298.15 K						
0.0000	0.882330	–	1.40498	–	0.48821	–
0.1001	0.941143	–0.3188	1.42706	0.0112	0.70282	–1.1175
0.2019	0.989952	–0.5181	1.44459	0.0177	0.99857	–2.1765
0.2966	1.027969	–0.6403	1.45851	0.0213	1.3832	–3.0521
0.3989	1.062668	–0.7050	1.47070	0.0224	1.9472	–3.8495
0.5009	1.092073	–0.7154	1.48069	0.0213	2.7556	–4.3985
0.5992	1.116104	–0.6395	1.48906	0.0190	3.7563	–4.7059
0.7006	1.137790	–0.5429	1.49668	0.0156	5.2137	–4.5979
0.8013	1.156155	–0.3560	1.50295	0.0110	7.1807	–3.9710
0.9004	1.172107	–0.1490	1.50834	0.0056	9.9981	–2.4724
1.0000	1.186933	–	1.51354	–	13.796	–
T = 303.15 K						
0.0000	0.876836	–	1.40227	–	0.46834	–
0.1001	0.935781	–0.3307	1.42451	0.0113	0.66597	–0.8632
0.2019	0.984707	–0.5362	1.44210	0.0178	0.93136	–1.6766
0.2966	1.022833	–0.6625	1.45604	0.0214	1.2760	–2.3356
0.3989	1.057632	–0.7285	1.46832	0.0225	1.7694	–2.9263
0.5009	1.087120	–0.7378	1.47837	0.0214	2.4631	–3.3136
0.5992	1.111228	–0.6598	1.48677	0.0191	3.3033	–3.5152
0.7006	1.132980	–0.5596	1.49444	0.0157	4.4963	–3.3968
0.8013	1.151403	–0.3675	1.50076	0.0110	6.0632	–2.8970
0.9004	1.167407	–0.1550	1.50619	0.0056	8.2385	–1.7720
1.0000	1.182276	–	1.51146	–	11.066	–
T = 308.15 K						
0.0000	0.871306	–	1.39957	–	0.44865	–
0.1001	0.930389	–0.3431	1.42195	0.0114	0.61968	–0.6914
0.2019	0.979440	–0.5555	1.43956	0.0178	0.86978	–1.3183
0.2966	1.017681	–0.6861	1.45353	0.0214	1.1814	–1.8226
0.3989	1.052580	–0.7530	1.46589	0.0225	1.6162	–2.2691
0.5009	1.082165	–0.7622	1.47597	0.0214	2.2168	–2.5473
0.5992	1.106351	–0.6817	1.48450	0.0191	2.9301	–2.6809
0.7006	1.128170	–0.5774	1.49223	0.0157	3.9201	–2.5645
0.8013	1.146650	–0.3796	1.49859	0.0110	5.1889	–2.1632
0.9004	1.162703	–0.1607	1.50400	0.0055	6.9065	–1.2994
1.0000	1.177622	–	1.50943	–	9.0640	–

TABLE S-I. Continued

x_1	ρ / 10^3 kg m^{-3}	V^E / 10^{-6} m^3 mol^{-1}	n_D	Δn_D	η / mPa s	$\Delta\eta$ / mPa s
Dimethyl phthalate (1) + tetrahydrofuran (2)						
T = 313.15 K						
0.0000	0.865736	–	1.39685	–	0.42859	–
0.1001	0.924971	–0.3568	1.41934	0.0114	0.65314	–0.4891
0.2019	0.974157	–0.5767	1.43700	0.0178	0.81357	–1.0544
0.2966	1.012514	–0.7114	1.45096	0.0213	1.0972	–1.4460
0.3989	1.047524	–0.7800	1.46338	0.0224	1.4828	–1.7897
0.5009	1.077208	–0.7890	1.47349	0.0213	2.0074	–1.9923
0.5992	1.101471	–0.7053	1.48220	0.0191	2.6187	–2.0818
0.7006	1.123357	–0.5964	1.49001	0.0157	3.4504	–1.9731
0.8013	1.141900	–0.3931	1.49646	0.0111	4.4942	–1.6472
0.9004	1.158004	–0.1674	1.50189	0.0055	5.8703	–0.9776
1.0000	1.172969	–	1.50736	–	7.5580	–
T = 318.15 K						
0.0000	0.860127	–	1.39417	–	0.40722	–
0.1001	0.919522	–0.3713	1.41669	0.0114	0.55702	–0.4500
0.2019	0.968881	–0.6025	1.43433	0.0177	0.76188	–0.8552
0.2966	1.007333	–0.7388	1.44842	0.0213	1.0212	–1.1634
0.3989	1.042457	–0.8089	1.46096	0.0225	1.3652	–1.4324
0.5009	1.072177	–0.8098	1.47117	0.0214	1.8279	–1.5810
0.5992	1.096585	–0.7305	1.47999	0.0193	2.3566	–1.6413
0.7006	1.118541	–0.6168	1.48780	0.0158	3.0628	–1.5428
0.8013	1.137144	–0.4070	1.49430	0.0111	3.9331	–1.2759
0.9004	1.153304	–0.1745	1.49978	0.0056	5.0561	–0.7467
1.0000	1.168316	–	1.50524	–	6.3997	–
T = 323.15 K						
0.0000	0.854771	–	1.39130	–	0.38401	–
0.1001	0.914043	–0.3608	1.41407	0.0116	0.49574	–0.3977
0.2019	0.963530	–0.6012	1.43151	0.0176	0.71370	–0.7018
0.2966	1.002133	–0.7473	1.44588	0.0214	0.95223	–0.9472
0.3989	1.037375	–0.8218	1.45833	0.0224	1.2606	–1.1615
0.5009	1.067215	–0.8267	1.46865	0.0213	1.6739	–1.2694
0.5992	1.091695	–0.7455	1.47763	0.0193	2.1356	–1.3099
0.7006	1.113723	–0.6295	1.48554	0.0158	2.7388	–1.2248
0.8013	1.132391	–0.4161	1.49210	0.0111	3.4739	–1.0042
0.9004	1.148606	–0.1791	1.49765	0.0056	4.4040	–0.5804
1.0000	1.163668	–	1.50320	–	5.4933	–
Dimethyl adipate (1) + tetrahydrofuran (2)						
T = 288.15 K						
0.0000	0.893293	–	1.40963	–	0.52194	–
0.1000	0.925379	–0.0236	1.41374	0.0020	0.69104	–0.1538
0.2000	0.952013	–0.0457	1.41702	0.0032	0.88883	–0.2790
0.3000	0.974375	–0.0557	1.41970	0.0038	1.1197	–0.3711

TABLE S-I. Continued

x_1	ρ / 10^3 kg m^{-3}	V^E / 10^{-6} m^3 mol^{-1}	n_D	Δn_D	η / mPa s	$\Delta\eta$ / mPa s
Dimethyl adipate (1) + tetrahydrofuran (2)						
T = 288.15 K						
0.3994	0.993294	–0.0551	1.42195	0.0040	1.3843	–0.4275
0.5001	1.009824	–0.0496	1.42390	0.0038	1.6904	–0.4466
0.5909	1.022900	–0.0438	1.42543	0.0035	1.9975	–0.4327
0.5999	1.024112	–0.0430	1.42560	0.0035	2.0280	–0.4313
0.7003	1.036767	–0.0360	1.42703	0.0028	2.4094	–0.3741
0.7999	1.047887	–0.0263	1.42832	0.0020	2.8224	–0.2828
0.8937	1.057253	–0.0138	1.42940	0.0011	3.2410	–0.1671
0.8996	1.057811	–0.0130	1.42945	0.0011	3.2679	–0.1593
1.0000	1.066794	–	1.43050	–	3.7514	–
T = 293.15 K						
0.0000	0.887862	–	1.40698	–	0.50196	–
0.1000	0.920056	–0.0282	1.41123	0.0021	0.65616	–0.1245
0.2000	0.946777	–0.0528	1.41460	0.0033	0.83538	–0.2241
0.3000	0.969213	–0.0642	1.41735	0.0039	1.0425	–0.2957
0.3994	0.988197	–0.0643	1.41967	0.0041	1.2771	–0.3381
0.5001	1.004778	–0.0582	1.42166	0.0040	1.5448	–0.3512
0.5909	1.017898	–0.0517	1.42323	0.0036	1.8108	–0.3382
0.5999	1.019114	–0.0508	1.42341	0.0036	1.8380	–0.3361
0.7003	1.031808	–0.0423	1.42487	0.0029	2.1629	–0.2911
0.7999	1.042963	–0.0308	1.42619	0.0021	2.5137	–0.2179
0.8937	1.052357	–0.0161	1.42731	0.0012	2.8656	–0.1275
0.8996	1.052916	–0.0152	1.42735	0.0011	2.8878	–0.1217
1.0000	1.061928	–	1.42842	–	3.2894	–
T = 298.15 K						
0.0000	0.882402	–	1.40432	–	0.47984	–
0.1000	0.914707	–0.0329	1.40869	0.0022	0.62287	–0.1000
0.2000	0.941520	–0.0605	1.41217	0.0034	0.78522	–0.1807
0.3000	0.964035	–0.0735	1.41500	0.0041	0.97313	–0.2358
0.3994	0.983085	–0.0741	1.41737	0.0043	1.1828	–0.2677
0.5001	0.999728	–0.0683	1.41942	0.0041	1.4199	–0.2753
0.5909	1.012886	–0.0603	1.42105	0.0037	1.6519	–0.2640
0.5999	1.014108	–0.0595	1.42121	0.0037	1.6760	–0.2618
0.7003	1.026843	–0.0494	1.42271	0.0030	1.9557	–0.2261
0.7999	1.038034	–0.0360	1.42408	0.0021	2.2549	–0.1689
0.8937	1.047457	–0.0192	1.42520	0.0012	2.5548	–0.0970
0.8996	1.048018	–0.0181	1.42525	0.0011	2.5742	–0.0919
1.0000	1.057056	–	1.42636	–	2.9101	–
T = 303.15 K						
0.0000	0.876909	–	1.40164	–	0.45948	–
0.1000	0.909335	–0.0382	1.40615	0.0022	0.59091	–0.0830
0.2000	0.936245	–0.0689	1.40971	0.0035	0.74026	–0.1481

TABLE S-I. Continued

x_1	ρ / 10^3 kg m^{-3}	V^E / 10^{-6} m^3 mol^{-1}	n_D	Δn_D	η / mPa s	$\Delta\eta$ / mPa s
Dimethyl adipate (1) + tetrahydrofuran (2)						
T = 303.15 K						
0.3000	0.958844	–0.0837	1.41265	0.0042	0.91111	–0.1916
0.3994	0.977965	–0.0851	1.41510	0.0044	1.0999	–0.2159
0.5001	0.994666	–0.0788	1.41720	0.0042	1.3111	–0.2207
0.5909	1.007872	–0.0701	1.41884	0.0038	1.5168	–0.2097
0.5999	1.009098	–0.0691	1.41901	0.0038	1.5407	–0.2051
0.7003	1.021874	–0.0571	1.42055	0.0031	1.7800	–0.1811
0.7999	1.033101	–0.0414	1.42194	0.0022	2.0420	–0.1326
0.8937	1.042555	–0.0222	1.42310	0.0012	2.2980	–0.0778
0.8996	1.043118	–0.0209	1.42319	0.0012	2.3143	–0.0741
1.0000	1.052185	–	1.42429	–	2.6037	–
T = 308.15 K						
0.0000	0.871379	–	1.39896	–	0.43953	–
0.1000	0.903933	–0.0440	1.40358	0.0023	0.55977	–0.0701
0.2000	0.930947	–0.0781	1.40725	0.0036	0.69823	–0.1219
0.3000	0.953632	–0.0947	1.41025	0.0043	0.85393	–0.1565
0.3994	0.972827	–0.0968	1.41277	0.0045	1.0259	–0.1737
0.5001	0.989586	–0.0895	1.41495	0.0044	1.2174	–0.1738
0.5909	1.002844	–0.0803	1.41664	0.0039	1.3997	–0.1643
0.5999	1.004072	–0.0790	1.41680	0.0039	1.4211	–0.1600
0.7003	1.016894	–0.0652	1.41840	0.0032	1.6296	–0.1426
0.7999	1.028161	–0.0473	1.41984	0.0023	1.8579	–0.1038
0.8937	1.037648	–0.0256	1.42100	0.0013	2.0804	–0.0599
0.8996	1.038212	–0.0242	1.42105	0.0012	2.0947	–0.0567
1.0000	1.047308	–	1.42222	–	2.3425	–
T = 313.15 K						
0.0000	0.865809	–	1.39627	–	0.41845	–
0.1000	0.898500	–0.0504	1.40100	0.0023	0.52938	–0.0594
0.2000	0.925623	–0.0881	1.40477	0.0037	0.65877	–0.1003
0.3000	0.948400	–0.1067	1.40786	0.0044	0.80241	–0.1269
0.3994	0.967674	–0.1097	1.41043	0.0046	0.95798	–0.1406
0.5001	0.984497	–0.1018	1.41269	0.0045	1.1343	–0.1358
0.5909	0.997805	–0.0914	1.41442	0.0040	1.2991	–0.1256
0.5999	0.999039	–0.0900	1.41459	0.0040	1.3155	–0.1245
0.7003	1.011908	–0.0743	1.41624	0.0032	1.5057	–0.1053
0.7999	1.023215	–0.0539	1.41771	0.0023	1.7003	–0.0803
0.8937	1.032733	–0.0291	1.41889	0.0013	1.8924	–0.0479
0.8996	1.033299	–0.0274	1.41895	0.0012	1.9053	–0.0451
1.0000	1.042427	–	1.42017	–	2.1214	–
T = 318.15 K						
0.0000	0.860201	–	1.39357	–	0.39564	–
0.1000	0.893035	–0.0571	1.39841	0.0024	0.49891	–0.0505

TABLE S-I. Continued

x_1	ρ / 10^3 kg m^{-3}	V^E / 10^{-6} m^3 mol^{-1}	n_D	Δn_D	η / mPa s	$\Delta\eta$ / mPa s
Dimethyl adipate (1) + tetrahydrofuran (2)						
T = 318.15 K						
0.2000	0.920275	–0.0990	1.40226	0.0038	0.62048	–0.0827
0.3000	0.943148	–0.1198	1.40544	0.0045	0.75434	–0.1026
0.3994	0.962501	–0.1233	1.40808	0.0047	0.90596	–0.1038
0.5001	0.979394	–0.1151	1.41038	0.0045	1.0630	–0.1016
0.5909	0.992751	–0.1030	1.41217	0.0041	1.2060	–0.0982
0.5999	0.993991	–0.1017	1.41235	0.0040	1.2209	–0.0971
0.7003	1.006909	–0.0838	1.41408	0.0033	1.3824	–0.0900
0.7999	1.018258	–0.0607	1.41557	0.0023	1.5555	–0.0700
0.8937	1.027811	–0.0329	1.41682	0.0013	1.7310	–0.0388
0.8996	1.028379	–0.0310	1.41691	0.0012	1.7425	–0.0363
1.0000	1.037539	–	1.41819	–	1.9332	–
T = 323.15 K						
0.0000	0.854545	–	1.39088	–	0.34173	–
0.1000	0.887537	–0.0650	1.39578	0.0024	0.47056	–0.0160
0.2000	0.914900	–0.1113	1.39974	0.0038	0.58774	–0.0436
0.3000	0.937873	–0.1342	1.40300	0.0046	0.71316	–0.0631
0.3994	0.957311	–0.1385	1.40576	0.0048	0.84589	–0.0743
0.5001	0.974273	–0.1294	1.40812	0.0046	0.99290	–0.0731
0.5909	0.987687	–0.1162	1.40998	0.0042	1.1317	–0.0658
0.5999	0.988931	–0.1147	1.41015	0.0041	1.1464	–0.0641
0.7003	1.001900	–0.0944	1.41191	0.0033	1.3023	–0.0537
0.7999	1.013293	–0.0683	1.41348	0.0024	1.4580	–0.0422
0.8937	1.022881	–0.0370	1.41476	0.0013	1.6088	–0.0273
0.8996	1.023450	–0.0348	1.41483	0.0012	1.6189	–0.0257
1.0000	1.032645	–	1.41614	–	1.7900	–

Journal of the Serbian Chemical Society
JSCS-info@shd.org.rs • www.shd.org.rs/JSCS
J. Serb. Chem. Soc. 79 (1) 89–100 (2014)
JSCS–4567
UDC 547.53–304.9+66.081:556.34:627.157(282.243.74)
Original scientific paper

Sorption of benzothiazoles onto sandy aquifer material under equilibrium and non-equilibrium conditions

MARIJANA M. KRAGULJ*, JELENA S. TRIČKOVIĆ#, BOŽO D. DALMACIJA#, IVANA I. IVANČEV-TUMBAS#, ANITA S. LEOVAC, JELENA J. MOLNAR and DEJAN M. KRČMAR#

University of Novi Sad, Faculty of Sciences, Department of Chemistry, Biochemistry and Environmental Protection, Trg Dositeja Obradovića 3, 21000 Novi Sad, Serbia

(Received 15 January, revised 13 May 2013)

Abstract: In this study, the sorption behaviour of 1,3-benzothiazole (BT) and 2-(methylthio)benzothiazole (MTBT, 2-methylsulphanyl-1,3-benzothiazole) on Danube geosorbent under equilibrium and non-equilibrium conditions was investigated. All sorption isotherms fitted well with the Freundlich model (R^2: 0.932–0.993). The results showed that the organic matter of the Danube geosorbent has a higher sorption affinity for the more hydrophobic MTBT compared to BT. However, sorption-desorption experiments showed that MTBT was more easily desorbed than BT molecules, which indicates the importance of absorption relative to adsorption in the overall sorption mechanism of MTBT. In general, molecules of BT and MTBT were more easily desorbed in the lower concentration range, which resulted in an increase in the hysteresis indices with increasing concentration. Column experiments revealed that the retention of the investigated compounds on the aquifer material followed the hydrophobicity of the compound. BT showed a lower retention, in accordance with its lower sorption affinity obtained in the static experiments, while MTBT showed a greater sorption affinity, and thus had a longer retention time on the column. Thus during transport, BT represent a greater risk for groundwaters than MTBT. These results improved the understanding of the sorption and desorption processes of benzothiazoles, which represent one of the most important factors that influence the behaviour of organic compounds in the environment.

Keywords: geosorbents; sorption; hysteresis; transport; benzothiazoles.

INTRODUCTION

Sorption of hydrophobic organic compounds on sediment organic matter (SOM) is an essential process that controls the transport and fate of these com-

* Corresponding author. E-mail: marijana.kragulj@dh.uns.ac.rs
# Serbian Chemical Society member.
doi: 10.2298/JSC130115063K

pounds in an aquatic environment. Soil, sediments and solid particles suspended in water are called geosorbents. Geosorbents consist of a heterogeneous solid phase consisting of mineral and organic matter, which is the primary sorbent if the content is higher than 0.1 %.[1] There are several mechanisms to explain the sorption behaviour of hydrophobic organic compounds (HOCs) on geosorbent organic matter.[2,3] The most acceptable mechanism is the SOM dual-mode concept. The chemical heterogeneity of SOM affects the rates and equilibrium of sorption and desorption of HOCs in soils and sediments.[4,5] The concept of expanded (flexible, rubbery-like) and condensed (rigid, glassy-like) domains of SOM has been employed to operationally describe the chemical heterogeneity of SOM having two domains with distinctly different degrees of physicochemical condensation and markedly different HOC sorption behaviour.[6–9] The sorption of HOCs in expanded domains of SOM generates linear isotherms due to solid-phase dissolution (absorption), while nonlinear isotherms are observed for the sorption in condensed domains due to a hole-filling (adsorption) process. In a condensed domain, the "holes" are closed internal pores – voids of nanometre dimensions where sorbate molecules undergo an adsorption-like interaction with the polymer strands making up the void walls. Therefore, the total sorption is the sum of sorption in the absorption domain and sorption in the adsorption domain.[10] However, some authors consider that the exact mechanism of the sorption of these compounds on geosorbent has not yet been described.[11,12]

In recent years, great attention has been paid to the identification of specific pollutants in aquatic systems. Monitoring of the water and sediment of the Danube River identified specific organic pollutants, such as compounds from the class of benzothiazoles (BTs).[13]

BTs comprise a group of heterocyclic compounds the molecular structure of which includes benzene condensed with a thiazole ring. Large amounts of BTs are used as vulcanization accelerators in rubber production, where they are added in amounts of over 1 %.[14] Thus, BTs are found in urban run-off, in residential and highway road dust and in urban particulate matter, most probably as a result of vehicle tire wear.[14,15] The daily increase in their use in industrial processes makes them important environmental pollutants listed as emerging pollutants at the European level.[16]

However, data on the behaviour of benzothiazoles in the aquatic environment is scarce, and the results published are not conclusive. One group of authors who investigated the sorption of BTs onto suspended matter and sediments suggested that sorption is the relevant process that affects the fate and behaviour of BTs,[14,17] while the results of other authors suggest that the sorption mechanism is not relevant for BTs.[18] In addition, Ni *et al.*[17] suggest that due to their relatively hydrophilic character (log K_{OW} (partition coefficient) in the range 2.0–3.20),

BTs are pollutants relevant for the water phase. Therefore there is a need for further investigation of the sorption behaviour of this class of compounds.

The key objectives of this work were to investigate: 1) the sorption behaviour of 1,3-benzothiazole (BT) and 2-(methylthio)benzothiazole (MTBT, 2--methylsulphanyl-1,3-benzothiazole) on the Danube River geosorbent under equilibrium conditions; 2) the desorption of benzothiazoles and sorption-desorption hysteresis which might give further insights into the sorption mechanism; 3) the transport of BT and MTBT through a column of Danube sandy aquifer material in order to examine the behaviour of BT and MTBT under non-equilibrium conditions.

EXPERIMENTAL

Sorbates and sorbent

BT and MTBT (96%) were obtained from Sigma-Aldrich. Certain physical–chemical properties of the benzothiazoles are listed in Table I. BT is more polar (log K_{OW} = 2.17) and more soluble in water (S_W = 4300 mg·L^{-1}) than MTBT (log K_{OW} = 3.22; S_W = 125 mg·L^{-1}).

TABLE I. Basic characteristic of the selected benzothiazoles; M – molecular weight; S_w – water solubility;[18] ρ – density;[20] log K_{OW}[18,19] – octanol–water partition coefficient; T_b – boiling point[20]

Compound	M / g mol^{-1}	S_W / mg·L^{-1}	log K_{OW}	ρ / g·cm^{-3}	T_b / °C
BT	135	4300	2.17	1.238	227–228
MTBT	181	125	3.22	1.319	177

The sediment sample was taken from the left bank of the Danube River in the vicinity of the Veliko Ratno Island, which is a drinking water source for the city of Novi Sad. This sediment was used as a sorbent in order to investigate the risk of pollutant infiltration from the Danube into the underground water wells. Danube geosorbent was chosen as it represents a typical sandy aquifer material with a low content of organic carbon (OC). Several samples were taken from different depths ranging from 0 to 30 cm and a composite sample was prepared in order to obtain a representative sample.

The moisture and organic matter contents in the geosorbent sample were determined gravimetrically.[21] The OC content was determined using a total organic carbon (TOC) analyzer (LiquiTOCII, Elementar, Germany) after acid pre-treatment of the geosorbent to remove inorganic carbon. Particle size analysis between 2000 and 63 μm was performed by the wet sieving method (Sieve Shaker mode, PR. 09, CISA), while the analysis articles smaller than 63 μm was performed according to ISO method 13317-2:2001.[22] The precision of the particle size determination expressed as *RSD* was 5 %.

The specific surface area, pore volume and pore size were determined by N_2 adsorption isotherms at 77 K obtained using an Autosorb iQ surface area analyzer (Quantochrome Instruments, USA). The geosorbent sample was out-gassed at 105 °C for 2 h before running the isotherms. The specific surface area was calculated from the N_2 sorption isotherms using the multi-point Brunauer–Emmett–Teller (BET) method. The pore size and pore volume were derived from sorption isotherms using the Barrett–Joyner–Halenda (BJH) model. The micropore volume was calculated using the *t*-test method.

Sorption and desorption experiments

All sorption isotherms were run in duplicate at room temperature (20±2 °C) in 40 mL glass vials with a screw cap with a Teflon-lined silicon septum covered with silver foil. The background solution was 0.01 M $CaCl_2$ in deionised water with 100 mg·L^{-1} NaN_3 as a biocide. Due to the low solubility, before spiking the background solution, stock solutions of BT and MTBT (1000 μg·mL^{-1}) were prepared in MeOH. The initial BT and MTBT concentrations ranged from 50 to 1000 μg·L^{-1}. The volume of the BT and MTBT stock solutions used for background solution spiking was < 0.1% (v/v), which was shown to have no measurable influence on the sorption behaviour of hydrophobic organic compounds.[5]

The amount of geosorbent used in each experiment corresponded to a sample/solution ratio that resulted in 20–80 % uptake of solute. The head space was kept minimal in order to minimize the loss of compounds during the experiment due to evaporation. An equilibration period of 10 days was defined from a preliminary kinetics experiment to determine the time required to reach sorption-desorption equilibrium. The solids were then separated from the aqueous solution by centrifugation at 3000 rpm for 15 min and 30 mL of supernatant was removed using a glass pipette and replaced with the same volume of the fresh solute-free background solution to begin the desorption step by the conventional decant-refill method.[23] The weights of each vial were determined before and after refilling. The vials were further agitated under the same conditions. At the end of the desorption step, the solids were removed by centrifugation under the same conditions and an aliquot of supernatant was withdrawn for BT or MTBT determination. The solid-phase solute concentrations before and after desorption were calculated from a mass balance of the solute between the solid and the aqueous phases.

To determine the initial concentration of BT and MTBT for each point of the sorption isotherm and to account for sorbates losses other than sorption to the sorbent, two control flasks without any sorbent were prepared and treated in the same manner. The recoveries of the initial concentrations of BT and MTBT from the control flasks were in the range of the recoveries for BT and MTBT analysis, indicating no losses of sorbate due to the processes other than sorption to the sorbents (*e.g.*, volatilisation, biodegradation, adsorption on the walls of the glass vials, etc.).

Column experiments

A stainless steel column filled with aquifer material was used and all experiments were realised at room temperature (20±2 °C). The flow direction of the sorbate solution was from bottom to top. Sorbate solutions were prepared in a background solution containing $CaCl_2$ (0.01 M) and NaN_3 (100 mg·L^{-1}) in deionised water. The experiments were performed under sterile conditions as the sorbate solution contained NaN_3 as a biocide. Thiourea, as a non-sorbing solute, was added to the column influent solution to measure tracer breakthrough curves. The column parameters and experimental conditions are given in Table II.

The stainless steel column was packed with aquifer material using the following procedure: a suspension of a specific amount of dried and ground geosorbent and background solution was added to the column from the top, while a peristaltic pump (MasterflexR, Cole-Parmer Instrument Company, USA) connected to the bottom of the column compacted the solid material, giving a homogeneous geosorbent column with minimal entrapped air bubbles and grain size separation. The uniformity of the packing was indirectly reflected by the symmetrical breakthrough curve obtained for the tracer. Accordingly, physical (transport-related) non-equilibrium processes could be excluded.[24]

At the beginning of the experiment, background solution was injected through the column for 24 h at a flow rate of about 2 mL·min^{-1}, in order to have a fully saturated porous

medium.[25] Subsequently, the conservative tracer thiourea was applied at a concentration of about 4 mg·L^{-1}. At certain times, the eluate was collected for determination of thiourea by UV spectrophotometry (UV-1800 spectrophotometer, Shimadzu, Japan) at a wavelength of 235 nm. These tracer assays were stopped when the measured thiourea concentration at the outlet of the column became equal to the injected one. The sorbate solution was then passed through the column at a flow rate of about 2.2 mL·min^{-1}. The initial sorbate concentration in solution was 60 μg·L^{-1}. Eluates were collected at regular intervals over 130 h and analyzed for BT or MTBT as described below.

TABLE II. Characteristics of the packed column

Parameter	Value
Length, cm	20.0
Radius, cm	1.00
Cross section area, cm^2	3.14
Volume of column, cm^3	62.8
Density of packed column, g·cm^{-3}	1.35
Porosity	0.48
Flow rate, cm^3·min^{-1}	2.25

Chemical analysis

Supernatants collected after each of the sorption and desorption steps as well as column eluates were quantitatively analyzed for BT and MTBT after liquid–liquid extraction with toluene, using gas chromatography-mass spectrometry (GC/MS, Agilent 7890A/5975C) on a HP-5MS column (J&W Scientific) and quantified according to internal standard calibration using pentachloronitrobenzene as an internal standard. The results of the analytical method performance, obtained from seven measurements at two concentration levels, are presented in Table III.

TABLE III. Data on the performance of the analytical method

Compound	Measurement range, μg·L^{-1}	Detection limit μg·L^{-1}	Quantification limit μg·L^{-1}	Recovery, %	Precision, %
BT	7.50–120	1.90	10.0	97–107	1.71–10.0
MTBT	7.50–120	1.80	9.00	96–117	2.90–7.80

Recoveries of the liquid–liquid extraction and GC/MS determination, measured over a wide concentration range from 7.5–120 μg·L^{-1} for BT and MTBT, ranged from 97–107 % and 96–117 %, respectively. Accordingly, no corrections were made for the analytically determined BT and MTBT concentrations.

Data analysis

All sets of equilibrium sorption and desorption data were fitted using the Freundlich model:

$$q_e = K_F c_e^n \quad (1)$$

where q_e and c_e are the solid phase and aqueous phase equilibrium concentrations (in μg·g^{-1} and mg·L^{-1}, respectively); K_F and the exponent n are the Freundlich sorption capacity coefficient expressed as (μg·g^{-1})/(mg·L^{-1})^n, and the site energy heterogeneity factor indicating iso-

therm nonlinearity (dimensionless), respectively. K_F and n were obtained from direct nonlinear curve fitting of the sorption and desorption data.

The organic carbon-normalized single point distribution coefficients (K_{OC}) were determined by calculating the q_e values for chosen c_e values from the respective best fit of the Freundlich isotherms according to the following equation:

$$K_{OC} = \frac{q_e / c_e}{f_{oc}} \tag{2}$$

where f_{OC} represents the organic carbon fraction.

Sorption-desorption hysteresis was explored using the Hysteresis Index (*HI*) as proposed by Huang *et al.*:[23]

$$HI = \left. \frac{q_e^d - q_e^s}{q_e^s} \right|_{T,c_e} \tag{3}$$

where q_e^s and q_e^d are solid-phase solute concentrations for single-cycle sorption and desorption experiments, and the subscripts T and c_e specify constant temperature and the residual aqueous phase concentration, respectively.

RESULTS AND DISCUSSION

Geosorbent characterization

The geosorbent consisted mainly of sand (96.2 mass %), in particular with particle sizes over 180 μm (76.1 %). The contents of silt (2–63 μm) and clay (< 2 μm) were 8.17 and 0.78 mass %, respectively. The organic carbon and organic matter contents were 1.21 and 5.61 %, respectively. Based on these results, it could be concluded that the Danube geosorbent represents a typical sandy aquifer material with low organic carbon content. The specific surface area and pore volume of the geosorbent were 3.19 and 0.018 $cm^3 \cdot g^{-1}$, respectively. The geosorbent had an average mesopore radius of about 11.4 nm, while the results of the *t*-test method clearly showed that it did not contain micropores.

Sorption isotherms

The geosorbent exhibited nonlinear isotherms for both BT and MTBT (Fig. 1), meaning that the sorption affinity of the geosorbent decreased as the sorbate concentration increased. The Freundlich model parameters are presented in Table IV.

Slightly higher linearity was obtained for the sorption isotherm of the more hydrophobic MTBT (n = 0.595) compared to BT (n = 0.554). The higher isotherm linearity for MTBT indicates that organic matter of the Danube geosorbent represents a favourable environment for the distribution of this compound. The organic carbon-normalized sorption coefficient (K_FOC) was higher for BT (166) than for MTBT (112.8). However, a direct comparison of K_FOC values could not be made because of their different units as a result of the nonlinearity of the sorption isotherms obtained for the sorbates. The concentration dependent OC-normalized sorption coefficients K_{OC} at three selected equilibrium concentra-

tions (c_e = 1, 5 and 50 % solubility in water) were calculated based on Eq. (2) from the respective best fit Freundlich isotherms, the parameters for which are given in Table IV. In case of both the investigated compounds, the sorption affinity decreased with increasing concentration of sorbate, with log K_{OC} values being higher for MTBT compared to BT, indicating the greater importance of absorption in relation to adsorption in the overall sorption mechanism of MTBT. The obtained log K_{OC} values are in the range of values obtained for the sorption of BT and MTBT on organic matter on suspended particulates.[17]

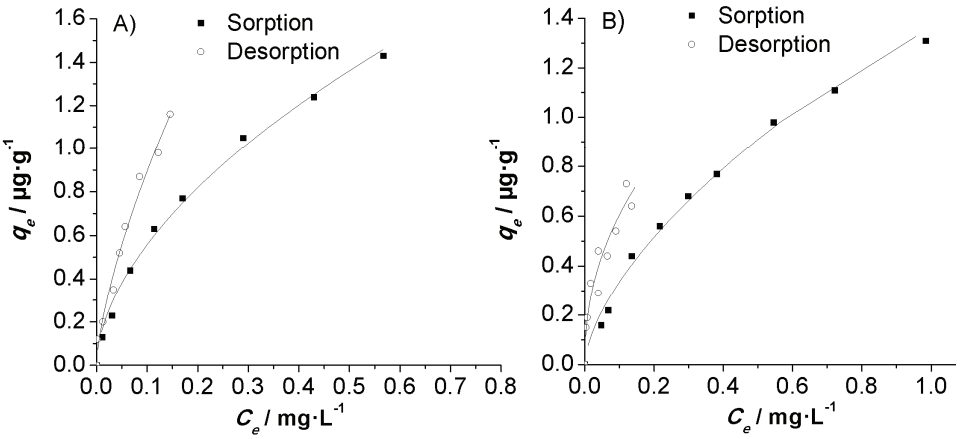

Fig. 1. Sorption and desorption isotherms of A) BT and B) MTBT on the Danube River geosorbent.

TABLE IV. Freundlich sorption and desorption model parameters and hysteresis index

Model	Compd.	R^2	n	K_F (µg·g^{-1})/ /(mg·L^{-1})^n	K_FOC[a]	log K_{OC}			*HI*		
						c_e / mg·L^{-1}					
						0.01 S_w	0.05 S_w	0.5 S_w	0.01 S_w	0.05 S_w	0.5 S_w
Sorp.	BT	0.993	0.554 (±0.018[b])	1.997 (±0.034[b])	166.6	1.49	1.18	0.73	2.50	3.30	4.90
Desorp.		0.979	0.684 (±0.047[b])	4.321 (±0.213[b])	360.0	2.04	1.82	1.50			
Sorp.	MTBT	0.992	0.595 (±0.090[b])	1.354 (±0.356[b])	112.8	2.01	1.73	1.33	0.90	1.40	2.20
Desorp.		0.932	0.721 (±0.095[b])	2.563 (±0.251[b])	213.6	2.30	2.11	1.83			

[a]$K_FOC = K_F/F_{OC}$; [b]standard deviation

Sorption-desorption hysteresis

Sorption reversibility provides an additional insight into the sorption mechanism. The apparent sorption-desorption hysteresis was quantified for each of the

sorption and desorption isotherms using the hysteresis index (Eq. (3)). Hysteresis indices at three sorbate equilibrium concentrations (c_e = 1, 5 and 50 % solubility in water) were calculated using the Freundlich model parameters given in Table IV. The calculated *HI* values are included in Table IV.

Positive values of *HI* indicate that hysteresis exists and is more pronounced as the *HI* value increases. The molecules of BT and MTBT are more easily desorbed in the lower concentration range, which resulted in the hysteresis indices increasing with increasing concentration.

In the case of BT and MTBT, hysteresis could be explained as follows: at low concentrations, sorption may be the result of surface interactions. Surface-bound molecules are probably desorbed much faster. However, as the concentration of sorbate increases, the increased concentration gradient caused the molecules to penetrate deeper into the pores of the geosorbent and organic matter causing pores in which they are trapped to be created, resulting in the pronounced hysteresis. Since the geosorbent has mesopores with an average radius of about 114 Å, the pore volume can be calculated and is equal to 6.20×10^6 Å^3. The volume of one BT molecule is 181 Å^3 and of one MTBT molecule 228 Å^3, which means that "irreversible entrapment" could be the cause of the observed sorption-desorption hysteresis.

In accordance with the dual-mode concept, Sander *et al.*[26] indicated that desorption hysteresis was widely reported for organic contaminants from soils/ /sediments, and was attributed to irreversible pore deformation of the sorbent by the sorbate and the formation of meta-stable states of sorbate in fixed mesopores. The porous structure becomes swollen during sorption and collapses during desorption. Therefore, desorption occurs by a different pathway from that of sorption.

Additionally, it is interesting to note that the organic matter of the Danube geosorbent had a higher sorption affinity for the more hydrophobic compound MTBT compared to BT, with the MTBT molecules more easily desorbed than the BT molecules, which indicates the greater importance of absorption in relation to adsorption in the overall sorption mechanism.

Non-equilibrium sorption of benzothiazoles

Dynamic (column) experiments were used in order to investigate the non-equilibrium sorption of BT and MTBT on the sandy aquifer material. Samples were taken from the column outlet and the measured concentrations plotted *versus* time to obtain a breakthrough curve, which is the basis for estimating the sorption coefficient. The breakthrough curves of the non-sorbing tracer and the selected benzothiazoles are presented in Fig. 2.

The results presented in the Fig. 2 show that in the case of thiourea, the breakthrough curve was a symmetrical S-shaped curve, which indicates the

absence of physical non-equilibrium processes in the porous media. Other authors made the same observations.[27]

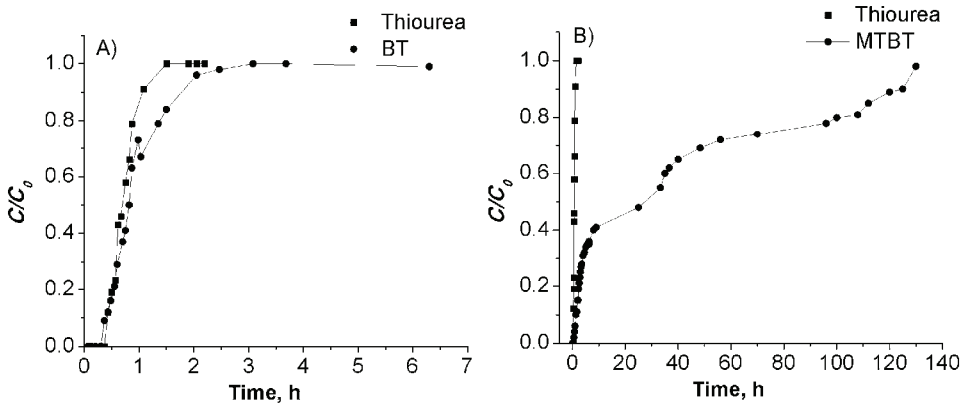

Fig. 2. Breakthrough curves of A) BT and thiourea and B) MTBT and thiourea.

Comparison of the breakthrough curve of thiourea with the breakthrough curve of BT shows a slight asymmetry (Fig. 2A). The breakthrough curve obtained for BT was not fully identical with the breakthrough curve of thiourea, indicating slightly non-equilibrium sorption.

In the case of MTBT, under the same conditions as those applied for BT, as much as 130 h passed before 99 % of the initial concentration was detected in the eluate. It can be seen that the resulting breakthrough curve exhibited a significantly higher asymmetry, which showed a higher degree of non-linear sorption in relation to BT (Fig. 2B).

In order to compare the breakthrough curves of BT and MTBT, c/c_0 = 0.5, the midpoint of the breakthrough curve, was calculated (Table V). The time required to achieve c/c_0 = 0.5 for BT and MTBT was 0.70 and 27.5 h, respectively.

TABLE V. Parameters of transport for BT and MTBT

Compound	Compound in effluent, %	Time (at c/c_0 = 0.5), h
Thiourea	100	0.70
BT	99	0.82
MTBT	99	27.5

If the obtained values for c/c_0 = 0.5 are compared with the log K_{OW} for the two investigated compounds, it could be observed that with increasing molecular hydrophobicity, the time to reach c/c_0 = 0.5 increases. In fact, the polar BT molecule had a relatively short times to c/c_0 = 0.5, whereas the hydrophobic

MTBT molecule reached c/c_0 = 0.5 after 28 h, indicating non-equilibrium sorption during the transport (Table V).

Other authors who examined the transport of various phenolic compounds as relatively polar compounds and phenanthrene as a non-polar compound came to similar conclusions.[27]

Comparing the parameters obtained from the column experiments and the parameters of the Freudlich model for the same compounds and the same geosorbent, the following could be concluded: the shorter time to c/c_0 = 0.5 for BT is in accordance with the lower sorption affinities obtained from the static experiments for BT compared with MTBT, which shows a greater affinity for sorption on the geosorbent and thus has a longer retention time on the column.

These similarities in the sorption behaviour obtained from static and dynamic experiments have been discussed by other authors.[25] However, a number of authors point to a disparity in their results,[28-30] and suggested explanations, such as the limited availability of sites for sorption in the columns due to the compression of the geosorbent, loss of the sorbent during column conditioning or differences in the experimental conditions.

CONCLUSIONS

In this study, the sorption behaviour of two compounds from the group of the benzothiazoles onto Danube River geosorbent was investigated. The organic matter of the Danube geosorbent had a higher sorption affinity for the hydrophobic compound MTBT compared to BT, which indicates the greater importance of absorption in relation to adsorption in the overall sorption mechanism. Sorption-desorption hysteresis existed for both benzothiazoles. In both cases, the existence of hysteresis may be due to irreversible pore deformation of the geosorbent, which results in the formation of meta-stable states in the mesopores of the sorbate. The obtained transport parameters indicate that with increasing molecular hydrophobicity, the retention time on the column increased, which is consistent with the higher sorption affinity of the hydrophobic MTBT for the Danube geosorbent. Further research should be focused on a more detailed characterization of the organic matter in the geosorbent to better define the sorption behaviour. Understanding these results could be useful for exposure and risk assessment of benzothiazoles in aquifer materials and groundwater.

Acknowledgment. This research was supported under the funding scheme of the Ministry of Education, Science and Technological Development of the Republic of Serbia (Projects No. III43005 and OI172028).

ИЗВОД

СОРПЦИЈА БЕНЗОТИАЗОЛА НА ПЕШЧАНОМ МАТЕРИЈАЛУ АКВИФЕРА У РАВНОТЕЖНИМ И НЕРАВНОТЕЖНИМ УСЛОВИМА

МАРИЈАНА М. КРАГУЉ, ЈЕЛЕНА С. ТРИЧКОВИЋ, БОЖО Д. ДАЛМАЦИЈА, ИВАНА И. ИВАНЧЕВ-ТУМБАС, АНИТА С. ЛЕОВАЦ, ЈЕЛЕНА Ј. МОЛНАР и ДЕЈАН М. КРЧМАР

Универзитет у Новом Саду, Природно-математички факултет, Департман за хемију, биохемију и заштиту животне средине, Трг Доситеја Обрадовића 3, 21 000 Нови Сад

У овом раду испитано је сорпционо понашање 1,3-бензотиазола (BT) и 2-(метилтио)бензотиазола (MTBT) на геосорбенту Дунава. Сорпционо понашање је испитано применом статичких и динамичких експеримената. Све сорпционе изотерме дале су задовољавајуће коефицијенте корелације применом Фројндлиховог модела (R^2: 0,932–0,993). Органска материја геосорбента Дунава има већи афинитет за сорпцију хидрофобнијег једињења MTBT у поређењу са BT. Интересантно је уочити да с молекули MTBT били лакше десорбовани у односу на молекуле BT, што указује на већи значај апсорпције у односу на адсорпцију у укупном механизму сорпције. Додатно, молекули BT и MTBT су лакше били десорбовани при нижим концентрацијама, што указује да су индекси хистерезе расли са повећањем концетрације сорбата. Уколико се добијене c/c_0 = 0,5 вредности упореде са коефицијентом хидрофобности испитиваних молекула (log K_{OW}), може се уочити да са порастом хидрофобности молекула расту и вредности за c/c_0 = 0,5. Ниже c/c_0 = 0,5 вредности добијене за BT у складу са мањим афинитетом за сорпцију добијеним из статичких експеримената, док MTBT показује већи афинитет за сорпцију и тиме и дуже време задржавања на колони. Током транспорта, BT представља већи ризик за подземне воде у односу на MTBT. Добијени резултати доприносе бољем разумевању процеса сорпције и десорпције бензотиазола с обзиром на то да ови процеси представљају један од најзначајнијих фактора који утичу на понашање органских једињења у животној средини.

(Примљено 15. јануара, ревидирано 13. маја 2013)

REFERENCES

1. R. P. Schwarzenbach, J. Westall, *Environ. Sci. Technol.* **15** (1981) 1360
2. W. J. J. Weber, H. Huang, E. J. LeBoeuf, *Colloids Surfaces, A* **151** (1999) 167
3. B. Xing, J. J. Pignatello, B. Gigliotti, *Environ. Sci. Technol.* **30** (1996) 2432
4. J. J. Pignatello, B. Xing, *Environ. Sci. Technol.* **30** (1996) 1
5. W. J. J. Weber, H. Huang, *Environ. Sci. Technol.* **30** (1996) 881
6. W. J. J. Weber, P. M. McGinley, L. E. Katz, *Environ. Sci. Technol.* **26** (1992) 1955
7. P. M. McGinely, L. E. Katz, W. J. J. Weber, *Environ. Sci. Technol.* **27** (1993) 1524
8. T. M. Young, W. J. J. Weber, *Environ. Sci. Technol.* **29** (1995) 92
9. B. Xing, J. J. Pignatello, *Environ. Sci. Technol.* **31** (1997) 792
10. J. J. Pignatello, *Adv. Colloid Interface Sci.* **76-77** (1998) 445
11. M. J. Salloum, B. Chefetz, P. G. Hatcher, *Environ. Sci. Technol.* **36** (2002) 1953
12. L. Luo, S. Zhang, Y. Ma, *Chemosphere* **72** (2008) 891
13. I. Liška, F. Wagner, J. Slobodník, *Joint Danube Survey 2*, ICPDR – International Commission for the Protection of the Danube River, Vienna, Austria, 2008, p. 242
14. H. Kumata, J. Yamada, K. Masuda, H. Takada, Y. Sato, T. Sakurai, K. Fujiwara, *Environ. Sci. Technol.* **36** (2002) 702
15. H. G. Ni, R. L. Shen, H. Zeng, E. Y. Zeng, *Environ. Pollut.* **157** (2009) 3502

16. Network of reference laboratories, research centres and related organisations for monitoring of emerging environmental substances http://www.norman-network.net/ /index_php.php?module=public/about_us/emerging&menu2=public/about_us/about_us#substances (accessed on 29.09.2012)
17. H. G. Ni, F. H. Lu, X. L. Luo, H. Y. Tian, E. Zeng, *Environ. Sci. Technol.* **42** (2008) 1892
18. B. Brownlee, J. H. Carey, G. A. MacInnis, I. T. Pellizzari, *Environ. Toxicol. Chem.* **11** (1992) 1153
19. R. F. Platford, *Chemosphere* **12** (1983) 1107
20. H. Kirouani-Harani, *Microbial and photolytic degradation of benzothiazoles in water and wastewater*, Technical University of Berlin, Berlin, 2003, p. 123
21. The weight of solid material combustible at 550°C http://water.epa.gov/scitech/methods/ /cwa/bioindicators/upload/2007_07_10_methods_method_160_4.pdf (accessed on 29.09.2012)
22. EN ISO 13317-2:2001, *Determination of particle size distribution by gravitational liquid sedimentation methods*, 2001
23. W. Huang, H. Yu, W. J. Weber, *J. Contam. Hydrol.* **31** (1998) 129
24. F. Amiri, M. Rahman, H. Bornick, E. Worch, *Acta Hydrochim. Hydrobiol.* **32** (2004) 214
25. S. Jellali, E. Diamantopoulos, H. Kallali, S. Bennaceur, M. Anane, N. Jedidi, *J. Environ. Manage*. 91 (2010) 897
26. M. Sander, Y. F. Lu, J. J. Pignatello, *J. Environ. Qual.* **34** (2005)1063
27. E. Worch, *J. Contam. Hydrol.* **68** (2004) 97
28. M. A. Maraqa, *J. Environ. Geol.* **41** (2001) 219
29. M. Maraqa, X. Zhao, R. B. Wallace, T. C. Voice, *Soil Sci. Sol. Am. J.* **62** (1998) 142
30. M. A. Maraqa, X. Zhao, J. Lee, F. Allan, T. Voice, *J. Contam. Hydrol.* **125** (2011) 57.

Journal of the Serbian Chemical Society
JSCS-info@shd.org.rs • www.shd.org.rs/JSCS
J. Serb. Chem. Soc. *79* (1) 101–112 (2014) UDC 631.004.12:712.25:631.4:546.56'47'711
JSCS–4568 *Original scientific paper*

Effects of agricultural practices on properties and metal content in urban garden soils in a tropical metropolitan area

JEAN AUBIN ONDO[1,2]*, PASCALE PRUDENT[1], CATHERINE MASSIANI[1], PATRICK HÖHENER[1] and PIERRE RENAULT[3]

[1]Aix-Marseille Université, CNRS, LCE, FRE 3416, 13331 Marseille, France, [2]Laboratoire Pluridisciplinaire des Sciences, Ecole Normale Supérieure – B.P. 17009 Libreville, Gabon and [3]INRA, Unité "Climat, Sol et Environnement", Domaine Saint-Paul, Site Agroparc, 84914 Avignon Cedex 9, France

(Received 21 January, revised 19 June 2013)

Abstract: The appearance of agriculture in urban areas improved the healthiness of the diet of people by enabling their consumption of fresh vegetables and fruits. This study assessed the level of fertility, and the impact of the cropping system and of the exploitation time on the physicochemical properties and the pseudo-total and EDTA-extractable metals contents of the vegetable soils of urban garden of in Libreville (Gabon). The results indicated a low fertility of the cultivated soils. The metal contents in the open field cultured soils were generally different from the soils cultured under shelters. Except Al that could be toxic for cultivated vegetables, the soil properties and metal element concentrations decreased significantly with time in the open field soil, while they did not vary in open shade cultured soils. The pseudo-total cadmium concentration was below the detection limit in all soils. Multivariate analysis showed that Al, Fe and Pb were of lithogenic origin, while Cu, Zn and Mn were of anthropogenic origin.

Keywords: soil fertility; metal mobility; multivariate statistical analysis; Libreville.

INTRODUCTION

Rapid urbanization in developing countries is accompanied by a growing demand for food, which raises the problem of securing urban food and nutritional supplies.[1] This demand relies in part on agriculture inside or close to cities.[2] Thus, it is often observed that market-gardening farming systems, including leafy vegetables, have recently increased within or near expanding cities.[3] Urban farmers concerned with maintaining soil productivity must consider the impacts of agricultural practices upon the features of the production sites.

* Corresponding author. E-mail: laplus_ens@yahoo.fr
doi: 10.2298/JSC130121068O

Conventional open field farming has played a significant role in improving food and fiber productivity to meet human consumption demands, but has led to soil erosion, soil nutrient depletion and excessive fertilizer use.[4] The problems arising from conventional agricultural open field management have led to the development and promotion of other farming practices with regard to the improvement of soil fertility and quality.[5]

Farming in protected environments, such a greenhouses or under shelters, is a frequently utilized technique by horticultural producers. It allows plant protection against the action of external agents, such as high and low temperature, intense precipitation and strong winds.[6] Greenhouses or shelters promote rationalization of the production factors, result in less pesticide use and minimize the incidence of pathogens and insects.[7] They also promote increased production of fresh and dry matter, and foliar areas and leaf numbers.[6] The main advantage of protected farming is that the yield and quality of vegetables are higher.[8]

Temporal changes in physicochemical properties and heavy metal levels of cultivated soils according to the exploitation time or to agricultural practices, *i.e.*, in open fields or under shelters, have been already reported.[9–11] However, few studies dealt with the effects of both cultural practices and exploitation time. The present study was aimed at assessing the effects of agricultural practices and farming time on the properties and metal concentrations in soils of urban gardens located at different sites in the City of Libreville (Gabon).

EXPERIMENTAL

This study was realized in 2008 and 2009 in urban garden areas of Libreville (Fig. 1). The city is situated in West Gabon (9°25′ E and 0°27′ N). The climate is hot and humid with two rain seasons and two dry seasons. It is characterized by an average rate of annual rainfall that varies from 1,600 to 1,800 mm. Hygrometry is usually above 80 % and reaches 100 % during the rain seasons. Monthly-averaged temperatures oscillate between 25 and 28 °C, with daily minima (18 °C) in July and maxima (35 °C) in April.

The population of the urban area of Libreville is estimated at about 648,000 inhabitants, which represents nearly half the total population of the country. Farmers grow vegetables on plots of 100 to 10,000 m^2 within the city and its surroundings. They use both techniques open field (OF) and under a protection structure (under shelters) (PS), as other market gardening crops producers in the World.[6]

Nine sites were selected for this study (Fig. 1). The major distinctions between the plots were the exploitation periods (between 2 and 38 years) and the cultural practices (OF or PS). The study plots were separated in four groups: urban gardens cultivated in open fields for less than ten years (OF1), in open fields but for more than ten years (OF2), urban gardens cultivated under shelters for less than ten years (PS1) and under shelters for more than ten years (PS2). Two sites presented two plots belonging to different groups; hence, this study concerned eleven urban garden plots (Fig. 1).

Surface soils (0–10 cm) were collected using the technique of systematic random sampling with 3 replicates.[12] The soil samples were air dried, then crushed in a mortar, passed through a 2 mm sieve and stored in polyethylene bags. The fraction > 2 mm was discarded.[13]

A part of the fraction < 2 mm was crushed with a tungsten carbide blade grinder and subsequently sieved through a 0.2 mm titanium mesh.

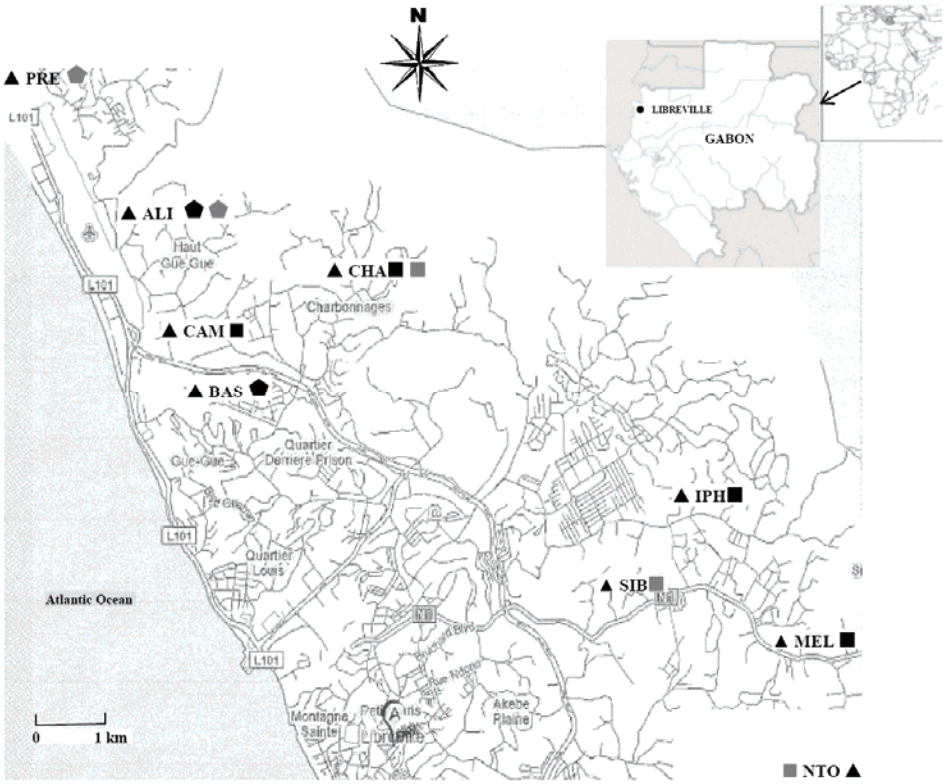

Fig. 1. Location of studied urban gardens in Libreville with sampling sites: (▲) gardens under shelters (PS) = ⬟: exploited for less than10 years (PS1) and exploited for more than 10 years (PS2); gardens in open fields (OF) = ■: exploited for less than 10 years (OF1) and exploited for more than 10 years (OF2).

The physicochemical properties of the soil were assessed according to the ISO standard.[14] They included: particle size (three fractions), pH, conductivity (*EC*), cation exchange capacity (*CEC*), total Kjeldahl nitrogen (*TKN*) and total organic carbon (*TOC*). Considering that the average content of carbon in soil organic matter was 58 %, the conversion factor 1.724 was used to calculate the percentage of organic matter (*OM*) from the content of organic carbon.[15]

Soil samples were mineralized in microwave mineralizer using *aqua regia* (1/3 HNO_3+2/3 HCl, ultra grade purity) according to the AFNOR NF X31-151 standard.[14] The mineralization products were filtered through a 0.45 μm mesh and the concentrations of the metals in the filtrates were determined by ICP-AES (Jobin Yvon Horiba, Spectra 2000). Quality assurance–quality controls and accuracy were checked using standard soil reference materials (CRM-SS1, EPA-3050A) with accuracies within 100±10 %. In order to determine the mobile or "potentially available" fraction of metals in the studied soils, the 0.05 M EDTA extraction procedure at pH 7, proposed by Quevauviller, was used.[16]

The mean, standard error and mean comparison test were performed. A correlation matrix was used to identify the relationship between heavy metal contents and soil properties. Multivariate analysis methods, such as Principal Component Analysis (PCA), cluster analysis and two-way analysis of variance (ANOVA) were used to extract information from the physicochemical and metallic analysis of the soils. PCA and cluster analysis were interpreted in accordance with the hypothetical source of heavy metals (lithogenic, anthropogenic or mixed). The statistical analyses were performed using XLSTAT 2010 software, version 6.04.

RESULTS AND DISCUSSION

The mean values of analyzed parameters are presented in Table I. A comparison of the fertility parameters (pH, *TNK*, *CEC* and *OM*) was performed between the present data and those proposed by Landon as mean ranges of tropical soil fertility.[17] The soils were acidic with pH values in the range proposed

TABLE I. Physicochemical properties and concentrations of pseudo-total metal (subscript: tot) and EDTA-extracted metal (subscript: mob), expressed in mg kg^{-1} of dry weight, of cultivated soils; and variance analysis results (ANOVA); N: number of samples; ns: non-significant; *: $p < 0.05$; **: $p < 0.01$; the means in same line followed by same letter do not differ at the stated significance level of 0.05

Parameter	Groups of cultivated gardens				Two-way ANOVA (Tukey HSD) *F* (variance and probability)		
	PS1 (*N* = 6)	PS2 (*N* = 6)	OF1 (*N* = 12)	OF2 (*N* = 9)	Agricultural system	Time of exploitation	System *x* Time
EC / µS cm^{-1}	312^{a}	235^{ab}	247^{ab}	100^{b}	4.366*	5.011*	0.233 ns
pH_{water}	6.17^{a}	6.00^{a}	6.49^{a}	4.98^{b}	14.212**	1.216 ns	9.526**
pH_{KCl}	5.71^{a}	5.49^{a}	5.65^{a}	4.44^{b}	6.594*	3.172 ns	3.926 ns
ΔpH	0.5^{a}	0.5^{a}	0.8^{a}	1.2^{a}	1.412 ns	3.928 ns	2.853 ns
TKN / mg g^{-1}	1.27^{b}	1.17^{b}	2.06^{a}	1.23^{b}	12.851**	13.473**	10.092**
MO / g g^{-1}	18.9^{b}	22.3^{b}	33.9^{a}	23.3^{b}	1.772 ns	11.218**	8.781**
Sands, g kg^{-1}	833^{a}	848^{a}	435^{c}	633^{b}	3.600 ns	35.734**	3.065 ns
Loams, g kg^{-1}	99^{b}	86^{b}	319^{a}	226^{a}	1.944 ns	23.807**	0.852 ns
Clays, g kg^{-1}	69^{c}	66^{c}	250^{a}	141^{b}	6.273*	38.911**	6.259*
CEC / meq 100 g^{-1}	4.4^{b}	3.8^{b}	13^{a}	3.8^{b}	6.063*	5.229*	5.031*
Al_{tot}	9135^{c}	9144^{c}	28269^{a}	19863^{b}	2.271 ns	36.878**	2.542 ns
Cd_{tot}	<1.85	<1.85	<1.85	<1.85	<1.85	<1.85	<1.85
Cu_{tot}	24^{a}	30.3^{a}	19.5^{a}	17.3^{a}	0.108 ns	7.461**	0.759 ns
Fe_{tot}	14206^{b}	16002^{b}	29030^{a}	13641^{b}	13.703**	11.639**	22.873**
Mn_{tot}	214^{b}	324^{ab}	640^{a}	250^{b}	2.393 ns	3.679 ns	7.405**
Pb_{tot}	7.2^{b}	3.2^{b}	17.3^{a}	6.7^{b}	19.42**	22.266**	6.648*
Zn_{tot}	44.5^{a}	55.1^{a}	44.8^{a}	23.6^{b}	4.089 ns	28.643**	30.975**
Al_{mob}	143 ^{a}	177 ^{a}	125 ^{a}	202 ^{a}	4.378*	0.056 ns	0.426 ns
Cd_{mob}	< 0.30	< 0.30	< 0.30	< 0.30	< 0.30	< 0.30	< 0.30
Cu_{mob}	2.15^{ab}	2.57^{ab}	3.29^{a}	1.03^{b}	5.345 ns	0.542*	9.973**
Fe_{mob}	313^{a}	196^{ab}	120^{b}	127^{b}	1.841 ns	22.21**	5.643*
Mn_{mob}	26.9^{b}	33.8^{b}	99.7^{a}	30.8^{b}	8.408*	8.218*	8.003**
Pb_{mob}	1.32^{b}	0.65^{b}	3.2^{a}	0.47^{b}	8.112**	3.375 ns	4.597*
Zn_{mob}	10.8^{b}	17.7^{a}	4.4^{c}	2.6^{c}	3.976 ns	78.624**	11.865**

by Landon (5.5–7.0), except OF2 soils with average pH<5. The *TNK*, *CEC* and *OM* in all soils were below the standards of tropical soil fertility, *i.e.*, 2–4 g kg^{-1}, 15–25 meq kg^{-1} and 40–100 g kg^{-1}, respectively.[17]

Analysis of variance (ANOVA) showed that the conductivity was higher in the PS gardens and recent gardens (influence of exploitation time). The results indicated that salts were more strongly accumulated in the PS1 soils than in the others soils. The time of exploitation seemed to play an important role in the evolution of all soil properties, except pH. A significant increase of sand content and a significant decrease in *EC*, *TKN*, *MO*, silt, clay and *CEC* were found with increasing exploitation time. This could be linked to low intakes of organic fertilizers for vegetable production, indeed it should be noted that for studied urban gardens as well as in other Africa small sub-Saharan farms, only low quantities of fertilizers were applied.[18] Urban gardens are generally far away from poultry farms and neither solid wastes nor waste water for intakes are used.[19]

The values of the physicochemical properties with time were not significantly different in the PS soils, with most of them decreasing with time in open field soils. It was estimated that more than 50 % of the world's potentially arable lands are acidic and up to 60 % of the acid soils in the world occur in developing countries in South America, Central Africa and Southeast Asia, where food production is critical. Soil acidity is a natural occurrence in tropical and subtropical zones.[20] The decrease of pH in OF soils led to a decrease in soil fertility and may cause aluminum toxicity and lots of micronutrients.[21]

Low fertility is a characteristic of many tropical soils, mainly because of the significant and rapid degradation of organic matter, but also because of leaching, weathering of minerals and low-input agricultural practices.[23] A chronosequence study by Moebius-Clune *et al.*[10] showed that most soil quality indicators followed exponential decay trends under continuous low-input for maize, and that organic matter and quality indicators (P, Zn and K possibly) were preserved under kitchen garden polyculture with organic inputs.[10] These results suggested that regular organic inputs could significantly reduce degradation of soils, especially with regards to nutrient retention and soil structure. Organic matter is essential for soil life by allowing a soil to perform efficiently its primary function of supporting plant growth. Its endemic deficiency in tropical soils is a major factor contributing to their low productivity.[24] Organic matter facilitates two essential categories of soil processes: organic matter stabilization and decomposition. Loss of stable organic matter results in destabilization of aggregates over time and thus in a decrease of cation retention (as represented by *CEC*), buffering of pH, and soil structure, which in turn decreases water storage, infiltration, root proliferation and physical access to nutrients, with increased likelihood of surface crusting, runoff and erosion.[10] A non-appropriate amendment of mineral fertilizers could sometimes lead to low yields, depending on the physical and biolo-

gical characteristics of the soil.[25] Organic matter and pH are the most important factors that control the availability of metals in soil. Increase content of soil organic matter could improve soil *CEC*, a parameter that could affect the concentrations of total and exchangeable metals.[26]

The low inputs of organic–matter and crop residues could be the major reasons for the low soil fertility of gardens in the area of Libreville. A survey among urban gardeners of Libreville indicated that the mineral fertilizer NPK and urea were the most used. However, to improve soil quality, the use of lime could increase the soil pH, and the employment of organic fertilizers, such as manure or compost, could increase the organic matter contents. These types of organic fertilizers are widely used by urban gardeners in other African countries because they are readily available. In Senegal, for example, nitrogen fertilizer (poultry manure, cow dung and garbage) are available locally at low cost. Hence, farmers prefer to settle near garbage dumps because of their important resources in organic matter at low cost.[22] It is therefore necessary to add organic matter to improve agricultural soil quality in the region of Libreville.

In all the analyzed soil samples, the Cd concentrations were below the detection limits of the ICP-AES analysis (1.85 mg kg^{-1}).

The Al, Cu, Fe, Mn, Pb and Zn pseudo-total concentrations in the studied soils are presented in Table I. They were below or within the ranges reported in the literature for uncontaminated soils.[27] However, the coefficients of variation (*CV*) showed considerable heterogeneities for Al, Cu, Mn and Pb (58.3, 51.1, 83.7 and 76.2 %, respectively). The heterogeneities of Fe and Zn were relatively lower (*CV* <50 %). According to Kabata-Pendias and Pendias,[27] the allowable or tolerable concentration of a metal element in soil is the limit concentration of this element over which the plants produced are considered dangerous for human or animal health. However, it is not advisable to interpret some results based only on pseudo-total concentrations. The determination of the total concentrations of metals in soils may be useful in predicting their potential risk to the environment, but it is not a good indicator of the metal mobility to plants, which depends on the physicochemical properties of soils.[28] Therefore, the mobility of a metal element is important in the evaluation of the effect of metal uptake by plants.

The levels of EDTA-extractable metals found in the soils are presented in Table I. The mean concentrations of metals were all within the ranges of concentrations of mobile metals in agricultural soils proposed by Berrow and Burridge.[29] Among all metals, the more readily available pool was particularly important for Zn (around 27 % of pseudo-total metal), indicating that Zn was potentially bioavailable and/or may leach through the soil. The mobility potential of the other studied metals was less important (12 % for Mn and < 10 % for Al, Cu and Fe, relative to the pseudo-total contents). A correlation analysis was performed between the physicochemical properties (*EC*, pH, *TKN*, *MO*, clay and

CEC) and the EDTA-extractable metals (Table II). Cu was the only metal presenting significant positive correlation coefficients with all soil parameters. The correlations between Mn and Pb and the soil parameters were also all positives, but not always significant. Significant negatives correlations were observed with Al, Fe and Zn. Thus, according to these correlation analysis results, the physicochemical properties seemed to play a crucial role in metal bioavailability.

TABLE II. Correlation coefficient (Pearson) matrices between the physicochemical soil parameters and the EDTA-extractable metal concentrations in soils from Libreville, Gabon

Metal	*EC*	pH_{water}	*TKN*	*OM*	Clay	*CEC*
Al	–0.331	–0.589	–0.236	–0.356	0.089	–0.149
Cu	0.497	0.430	0.608	0.522	0.515	0.658
Fe	0.353	0.010	–0.308	–0.370	–0.420	–0.129
Mn	0.301	0.131	0.721	0.680	0.758	0.787
Pb	0.134	0.464	0.275	0.359	0.182	0.185
Zn	0.209	0.298	–0.326	–0.285	–0.483	–0.228

In general, urban garden soils cultivated under shelters and in open field soils presented different metal pseudo-total concentrations, except for Mn. In open fields, the average Al, Fe and Pb concentrations in the soils were, respectively, 2.66, 1.41 and 2.46 times higher than those of soils under shelters were, whereas the average soil concentrations of Cu and Zn were, respectively, 1.48 and 1.41 lower. In both agricultural practices, the soils presented different metal concentrations for EDTA-extractable Fe, Mn and Zn. The Fe and Zn concentrations were higher (2.24 and 3.99 times, respectively) and the Mn concentrations were lower (2.09) in PS than in OF. No significant differences were found in the mobile Zn values between PS1 and PS2. For soils in open fields, the Al, Fe, Mn, Pb and Zn pseudo-total and mobile Cu, Mn and Pb concentrations were significantly higher on recent than on former cultivated soils. The mean ratios PS1/PS2 of these parameters were, respectively, 1.42, 2.13, 2.56, 2.58, 1.90, 3.19, 3.24 and 6.81. These differences could be attributed to leaching of the former open field soils that were more exposed to weather than the young soils. Soil degradation is a major agricultural and environmental problem, particularly in tropical soils. Soil erosion *via* water appears to be the most widespread process of soil degradation. Water erosion is a primary cause for the loss of nutrients and organic matter, and certainly also plays a role in acidification, pollution, and sometimes compaction and subsidence.[30,31]

The exploitation time of cultivated soils influenced the pseudo-total Mn, Fe, and Pb contents, which were higher in recently cultivated soils. The loss of organic matter in PS2 soils led to a *CEC* decrease. It could be hypothesized that losses of OM and fine mineral constituents were the main causes for the loss of nutrients and metals, and the remaining organic matter in soil had become more

inert with time, and therefore unable to retain cations and make them available for plants.[10]

The mobile Al content in soil could allow the risks of plant poisoning to assessed by application of the relation proposed by Boyer: Al×100/(sum of exchangeable base cations + Al).[32] In Brazil, this relationship allowed a threshold value of 45–50 to be proposed above which crops are generally not viable. The exchangeable bases of the studied soils were determined by Ondo.[33] The results showed that for OF2 soils, the threshold of 45–50 was generally exceeded (up to 74), raising fears of low crop yields on these soils.

The "cropping practices" factor showed that the pseudo-total Al, Fe and Pb contents and the mobile Mn contents were significantly highest in open field soils, and the pseudo-total Cu and Zn, and mobile Cu, Fe and Zn concentrations were significantly higher in soils under shelters. The trends showed that soils in open field were more exposed to erosion than soils under shelters. This led to leaching of Cu and Zn and increases in the Al, Fe and Pb contents. A study on the effects of erosion by Oguz *et al*. showed a decrease in Cu content and an increase in Fe, Mn and Zn concentrations in the surface soil.[34]

In general, correlation analysis is useful to investigate associations between parameters.[11] The results of the Pearson coefficients in the correlation analysis for heavy metal concentrations in the studied soils are shown in Table III. Most of the metal concentrations were positively correlated with each other and correlations were significant and positive between Al and Fe ($p < 0.001$), Al and Mn ($p < 0.01$), Al and Pb ($p < 0.01$), Fe and Mn ($p < 0.001$), Fe and Pb ($p < 0.001$), and Fe and Zn ($p < 0.05$). The significantly positive correlations of Mn, Pb and Zn with Fe and Al suggested their strong associations with Fe and Mn oxides in the soils, which could be important products of parent rock weathering.[35] Cu was negatively correlated with Al ($p < 0.01$) and Pb ($p < 0.01$). The origin of Cu could be anthropogenic, as applied organic fertilizers and pesticides, which have been extensively investigated in other studies.[11,33,36]

TABLE III. Correlation coefficient (Pearson) matrices between pseudo-total metal concentrations in urban gardens soils from Libreville, Gabon; *$p < 0.05$; **$p < 0.01$; ***$p < 0.001$

	Al	Cu	Fe	Mn	Pb	Zn
Al	1					
Cu	–0.439**	1				
Fe	0.730***	–0.014	1			
Mn	0.468**	0.244	0.668***	1		
Pb	0.442**	–0,436**	0.507***	0.087	1	
Zn	–0.130	0.245	0.332*	0.230	0.232	1

In this study, an agglomerative hierarchical cluster analysis (HCA) was performed to identify different geochemical groups. This clustering divided the

metals into groups with significant correlations within the groups. The dendrogram (Fig. 2) showed two distinct groups of elements. Cu and Zn formed a distinct group (Group I). Al and Fe formed another one (Group II), and Mn and Pb joined this last group. Based on these groups, the origin of the metals in the studied soils in Libreville could be ascribed to two different origins.

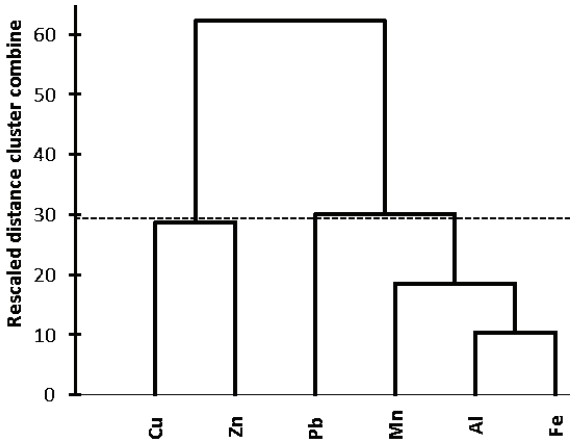

Fig. 2. Dendrogram of hierarchical cluster analysis of the metal concentrations in the studied soils.

The results of Principal Component Analysis to determine the origin of metals in the studied soils are presented in Table IV. Metals were correlated with a two-component model representing 70.8 % of the variability.

TABLE IV. Principal component analysis in 2-D loading plots for the 6 metals in the urban garden soils of Libreville, Gabon

Parameter	PC1	PC2
Eigenvalue	2.61	1.63
Variability, %	43.58	27.18
Cumulated, %	43.58	70.77
Al	0.848	–0.301
Cu	–0.279	0.867
Fe	0.925	0.231
Mn	0.661	0.526
Pb	0.672	–0.334
Zn	0.270	0.590

The first two principal components (PC1 and PC2) had eigenvalues >1 and accounted for 70.8 % of the total variance. The first principal component PC1 explained 43.6 % of the total variance, and had high positive loadings of Al and Fe (> 0.85), Mn and Pb (> 0.66). Al and Fe are included in the chemical composition of major minerals in soils. Both metals and Mn sometimes occur espe-

cially in lateritic soils as oxides, hydroxides or oxyhydroxides.[37] Reactivity and generally high surface areas of Mn and Fe oxides make them proficient sorbents of many inorganic cations, such as Pb among others. In particular, Mn (III/IV) and Fe (III) oxide/hydroxide mineral particles and coatings in soils seem to have a strong affinity for Pb.[38] These results suggested that the PC1 component could be linked to soil minerals and contents of Al, Fe, Mn and Pb. PC1 could thus be considered as a lithogenic component.

The second principal component (PC2) explained 27.2 % of the total variance, and had high positive loadings of Cu and Zn (> 0.8 and > 0.6, respectively). This component could be considered as an anthropogenic component. This factor is likely due to human activities, particularly application of fertilizer and pesticides in agriculture. Zhang indicated that metals such as Cu and Zn in urban soils may also be linked to pollution from traffic: wear of brake discs and motor vehicle exhausts.[39] In agricultural soils, the concentrations of these metals may also stem from pesticides and fertilizers.[36] The correlation between Mn and OF2 (0.526) indicated that, in addition to a lithogenic origin, Mn could also stem from an anthropogenic source.[40]

CONCLUSIONS

Poverty in Libreville, as in cities in developing countries, has contributed to the development of urban agriculture. This has increased vegetable production on urban soils, both in open fields and under shelters, which has contributed to an improvement in the quality of food in the region. Agricultural practices adopted by market gardeners involved use of small quantities of organic matter or fertilizer. These practices maintained low fertility and nutrient levels, and metal contents below the averages of tropical soils. Significant differences were found between cultivated soils under shelters and in open fields. There was no significant difference between soils under shelters with time of exploitation. In contrast, in open field soils, significant acidification, losses of nutrients and metals, and aluminum mobility were observed. Multivariate statistical analysis identified the origin of metals in agricultural soils of Libreville. Hence, a management program of soil quality should be performed to protect soils against the effects of climate, and to improve significantly soil fertility and yields of crops. The Gabonese authorities should encourage the research and formulation of agricultural policies at the national level, to develop a database on cultivated soils characteristics and to improve extension services of agricultural practices and environmentally friendly production. Such research, including Geographic Information System (GIS), could confirm the results of this study.

Acknowledgements. The authors thank the Government of Gabon for the scholarship given to Jean Aubin Ondo to achieve his Ph.D. They also thank Carine Demelas, Laurent Vassalo and Jean Felix Ndzime for their active participation during the analysis, and Dimitra

Ondo and Claude Obame for their involvement in the surveys. We express special thanks to urban gardeners of Libreville who participated in this study.

ИЗВОД

УТИЦАЈ ПОЉОПРИВРЕДНЕ ПРАКСЕ НА СВОЈСТВА И САДРЖАЈ МЕТАЛА У ГРАДСКИМ БАШТАМА ТРОПСКОГ ПОДРУЧЈА

JEAN AUBIN ONDO[1,2], PASCALE PRUDENT[1], CATHERINE MASSIANI[1], PATRICK HÖHENER[1] и PIERRE RENAULT[3]

[1]Aix-Marseille Université, CNRS, LCE, FRE 3416, 13331 Marseille, France, [2]Laboratoire Pluridisciplinaire des Sciences, Ecole Normale Supérieure – B.P. 17009 Libreville, Gabon и [3]INRA, Unité "Climat, Sol et Environnement", Domaine Saint-Paul, Site Agroparc, 84914 Avignon Cedex 9, France

Обрада земље у урбаним подручјима побољшала је здраву исхрану људи, због конзумирања свежег воћа и поврћа. Ова студија процењује ниво плодности, утицај система узгајања и времена експлоатације на физичкохемијска својства и псеудо-тотални и EDTA-екстрактабилни садржај метала у земљишту градских башта за узгајање поврћа у Либревилу (Габон). Добијени резултати указују на ниску плодност обрађеног земљишта. Садржај метала је био генерално различит између отвореног и заклоњеног земљишта. Осим Al, који би могао бити токсичан за узгајано поврће, концентрације метала су значајно временом опадале у отвореном земљишту, а нису варирале у заклоњеном земљишту. Псеудо-тотални садржај кадмијума био је испод границе детекције у свим земљиштима. Мултиваријантна анализа показала је да су Al, Fe и Pb били литогеног порекла, док су Cu, Zn и Mn били антропогеног.

(Примљено 21. јануара, ревидирано 19. јуна 2013)

REFERENCES

1. M. Mawois, C. Aubry, M. Le Bail, *Land Use Policy* **28 (**2011) 434
2. N. Bricas, P.A. Seck, *Cah. Agric.* **13** (2004) 10
3. H. De Bon, L. Parrot, P. Moustier, *Agron. Sustain. Dev.* **30** (2010) 21
4. T. Ge, S. Nie, J. Wu, J. Shen, H. Xiao, C. Tong, D. Huang, Y. Hong, K. Iwasaki, *J. Soil. Sediment* **11** (2011) 25
5. E. A. Stockdale, M. A. Shepherd, S. Fortune, S. P. Cuttle, *Soil Use Manage.* **18** (2006) 301
6. B. G. Santos Filho, A. K. S. Lobato, R. B. Silva, D. Schmidt, R. C. L. Costa, G. A. R. Alves C. F. Oliveira Neto, *J. Appl. Sci. Res.* **5** (2009) 529
7. J. L. Andriolo, *Rev. Hort. Bras.* **18** (2000) 26
8. H. Gubbuk, M. Pekmezci, *New Zeal. J. Crop Hort.* **32** (2004) 375
9. X. G. Lin, R. Yin, H. Y. Zhang, J. F. Huang, R. R. Chen, Z. H. Cao, *Environ. Geochem. Health* **26** (2004) 119
10. B. N. Moebius-Clune, H. M. van Es, O. J. Idowu, R. R. Schindelbeck, J. M. Kimetu, S. Ngoze, J. Lehmann, J. M. Kinyangi, *Agr. Ecosyst. Environ.* **141** (2011) 86
11. J. Wang, X. Chen, Y. Shi, M. Zhao, F. Meng, *Evaluation of heavy metal accumulation in open shade structure soils in Shenyang, Northeast China*, in *Proceedings of SPIE 7491, 749101*, 2009
12. M. Tabari, A. Salehi, *J. Environ. Sci.* **21** (2009) 1438
13. P. Quevauviller, *Methodologies for Soil and Sediment Fractionation Studies Single and Sequential Extraction Procedures*, Royal Society of Chemistry, Cambridge, 2002

14. AFNOR (Association Française de Normalisation), *Qualité des sols. Recueil de normes françaises*, Vol. I and II, 4th ed., AFNOR, Paris-La Défense, Paris, 1999
15. O. Abollino, M. Aceto, M. Malandrino, E. Mentasti, C. Sarzanini, F. Petrella, *Chemosphere* **49** (2002) 545
16. P. Quevauviller, *Trends Anal. Chem.* **17** (1998) 289
17. J. R. Landon, *Booker tropical soil manual: a handbook for soil survey and agricultural land evaluation in the tropics and subtropics*, 2nd ed., Longman Scientific & Technical, Harlow, 1991
18. S. S. Snapp, P. L. Mafongoya, S. Waddington, *Agr. Ecosyst. Environ.* **71** (1998) 185
19. S. Zingore, H. K. Murwira, R. J. Delve, K. E. Giller, *Agr. Ecosyst. Environ.* **119** (2007) 112
20. F. Vardar, M. Ünal, *Adv. Mol. Biol.* **1** (2007) 1
21. J. A. C. Rodriguez, M. M. Hanafi, S. R. S. Omar, Y. M. Rafii, *Malays. J. Soil Sci.* **13** (2009) 13
22. T. Sposito, *Ph.D. Thesis*, Universita Degli Studi di Milano, Milan, 2010
23. U. D. Mansur, K. A. Garba, *Bayero J. Pure Appl. Sci.* **3** (2010) 255
24. J. C. Katyal, N. H. Rao, M. N. Reddy, *Nutr. Cycl. Agroecosys.* **61** (2001) 77
25. P. P. Marenya, C. B. Barrett, *Am. J. Agr. Econ.* **91** (2009) 991
26. A. K. Gupta, S. Sinha, *Chemosphere* **64** (2006) 161
27. A. Kabata-Pendias, H. Pendias, *Trace Elements in Soils and Plants*, 3rd ed., CRC Press, Boca Raton, FL, 1984
28. M. Imperato, P. Adamo, D. Naimo, M. Arienzo, D. Stanzione, P. Violante, *Environ. Pollut.* **124** (2003) 247
29. M. L. Berrow, J. C. Burridge, in *Inorganic pollution and Agriculture Series*, J. C. Maff, Ed., Ministry of Agriculture, Fisheries and Food Reference Book, HMSO, London, 1980
30. V. B. Asio, R. Jahn, F. O. Perez, I. A. Navarrete, S. M. Abit Jr., *Ann. Trop. Res.* **31** (2009) 69
31. O. A. Oghenero, *J. Geol. Min. Res.* **4** (2012) 13
32. J. Boyer, *Cah. ORSTOM, série Pédol.* **14** (1976) 259
33. J. A. Ondo, *Ph.D. Thesis*, Université de Provence, Marseille, 2011
34. I. Oguz, K. Cagatay, A. Durak, M. Kilic, *J. Agron.* **5** (2006) 5
35. C. Tao, L. Xingmei, L. Xia, Z. Keli, Z. Jiabao, X. Jianming, S. Jiachun, A. D. Randy, *Environ. Pollut.* **157** (2009) 1003
36. P. Liu, H. J. Zhao, L. L. Wang, Z. H. Liu, J. L. Wei, Y. Q. Wang, L. H. Jiang, L. Dong, Y. F. Zhang, *Agr. Sci. China* **10** (2011) 109
37. C. Mico, L. Recatala, M. Peris, J. Sanchez, *Chemosphere* **65** (2006) 863
38. S. E. O'Reilly, M. F. Hochella Jr., *Geochim. Cosmochim. Acta* **67** (2003) 4471
39. C. Zhang, *Environ. Pollut.* **142** (2006) 501
40. N. S. Duzgoren-Aydin, C. S. C. Wong, A. Aydin, Z. Song, M. You, X. D. Li, *Environ. Geochem. Health* **28** (2006) 375.

Journal of the Serbian Chemical Society
JSCS-info@shd.org.rs • www.shd.org.rs/JSCS
J. Serb. Chem. Soc. 79 (1) 113 (2014)

Errata (printed version only)

Issue No. 12 (2013), Vol. 78, paper No. *JSCS-4536*:

– page 1847, line 6 from above: instead of „SINA BAVARI[5]“, it should be „SINA BAVARI[5]*“

Issue No. 12 (2013), Vol. 78, paper No. *JSCS-4549*:

– page 2043, line 9 from the bottom: instead of „CoPc“, it should be „16C(F)CoPc“;

– page 2047, line 7 from the bottom: instead of „1.2“, it should be „0.94“;

– page 2047, line 6 from the bottom: instead of „0.58“, it should be „0.53“;

– page 2050, line 6 from the top and line 3 from the bottom: instead of „0.120“, it should be „0.1“;

– page 2050, line 1 from the bottom: instead of „Nucleo Milenio de Ingenieria Molecular“, it should be „Millenium Nucleus of Molecular Engineering for Catalysis and Biosensors“.

Issue No. 12 (2013), Vol. 78, paper No. *JSCS-4550*:

– pages 2053–2067, line 1 from above on odd pages: instead of „KINETICS OF HYDROGEN CHLORIDE OXIDATION“, it should be „PASSIVE FILM ON N-STEEL“

Issue No. 12 (2013), Vol. 78, paper No. *JSCS-4557*:

– page 2165, line 3 from the bottom: instead of „shj@tmf.edu.mk“, it should be „shj@tmf.ukim.edu.mk“